Peripheral Nerve Regeneration through Tubular Devices: A Comparison of Assays of Device Effectiveness

by

Mark H. Spilker

S.M., Mechanical Engineering
Massachusetts Institute of Technology, 1997

B.S., Mechanical Engineering
University of Utah, 1994

Submitted to the Department of Mechanical Engineering
in Partial Fulfillment of the Requirements for the
Degree of

Doctor of Philosophy in Mechanical Engineering

at the
Massachusetts Institute of Technology
June, 2000

Signature of Author_____
Department of Mechanical Engineering
May 8, 2000

Certified by_____
Ioannis V. Yannas
Professor of Polymer Science
Thesis Supervisor, Thesis Committee Chair

Accepted by_____
Ain A. Sonin
Professor of Mechanical Engineering
Chariman, Department Committee

Peripheral Nerve Regeneration through Tubular Devices: A Comparison of Assays of Device Effectiveness

by

Mark H. Spilker

Submitted to the Department of Mechanical Engineering
on May 8, 2000, in Partial Fulfillment of the
Requirements for the Degree of
Doctor of Philosophy in Mechanical Engineering

Abstract

Peripheral nerve injury affects nearly 200,000 patients annually in the United States and unless treated results in paralysis of skeletal muscle and loss of sensation. Previous studies in this laboratory have focused on comparing the effectiveness of various tubular devices in repairing experimental nerve injuries in an animal model. The devices were rank-ordered based on clinically relevant assays of regeneration such as number regenerated nerve fibers and electrophysiological conduction properties of the regenerated nerves. Such assays provide a useful measure of the clinical efficacy of devices but require long-term (up to 60-week) studies in order to obtain meaningful results. There exists a need for a short-term (less than 12-week) assay with which nerve repair devices can be compared. The overall goal of this thesis was to establish an experimental assay that can be used to detect statistically significant differences among nerve repair devices in short-term studies.

In this thesis, four different assays of nerve regeneration were compared on the basis of their appropriateness to quantify the regeneration promoted by nerve repair devices in studies less than 12 weeks in duration. An acceptable assay must reach a plateau with time during short-term studies and must yield a quantitative metric with which nerve devices can be compared. The results of this thesis suggest that an assay based on ability of a nerve repair device to promote reinnervation across nerve gaps of various lengths meets the criteria for an acceptable assay. The data also indicate that the characteristic gap length (L_c), which is derived from curve-fitting the experimental data for reinnervation versus gap length, can be used as a quantitative metric of nerve regeneration. The experimental data indicate that for the silicone tube device, the value of L_c reached a plateau with time before 9 weeks, and the standard error in L_c was less than 5 percent of the value in two different nerve repair models (single-leg and cross-anastomosis). The data also suggest that statistically significant differences between the silicone tube device and a collagen-based device (the CG device) are obtainable during short-term (12-week) studies.

Thesis Supervisor: Ioannis V. Yannas, Professor of Polymer Science
Thesis Committee: Myron Spector, Senior Lecturer of Mechanical Engineering
Peter So, Professor of Mechanical Engineering

Acknowledgments

At the conclusion of yet another degree and another thesis, I am grateful for the opportunity that I have to pursue an education. I realize how fortunate I am. I feel forever indebted to God for blessing me so richly with a family and friends that support me in my efforts. I only hope that I can use my education to improve the lives of others.

For Professor Yannas, I have the deepest respect and admiration. I have learned so much during my education in your lab. You have provided me with the freedom and responsibility to learn how to perform careful research. At the end of six years, I truly feel like a capable scientist. I thank Dr. Spector for motivation and energy. Your enthusiasm and excitement have always impressed me.

I would like to thank my parents, who instilled in me a drive to learn. I am becoming keenly aware of the value of hard work and the perfectionist ethic that was taught to me as a child by you and by my siblings. As always, I am grateful for the support of my parents and family, especially during the times when it seemed that I would be working on my degree "forever".

I owe a special thanks to Hu-Ping Hsu. You have become a true friend over the years. I will never be able to pay back the countless hours spent in the operating room or the honest and wise advice that you have given me. As always, you were willing to fit the extra days of surgery into your schedule. We have been quite a team, and a large part of this thesis belongs to you.

I would also like to thank everyone in the Yannas Lab including Toby, Ken, Cyndi, Lila, Libby, Susan, and Gema. And thanks to Chris, Matt, Neil, and Nate, the people who did their best to fill my spare time with good times.

Table of Contents

Abstract 2
Acknowledgments 3
Table of Contents 4
List of Tables 6
List of Figures 7

CHAPTER 1: INTRODUCTION 9

1.1 CLINICAL PROBLEM 9
1.2 PERIPHERAL NERVE STRUCTURE AND FUNCTION 11
1.3 PERIPHERAL NERVE REGENERATION 14
1.4 EXPERIMENTAL MODELS OF NERVE INJURY 15
1.4.1 Choice of Animal Species 16
1.4.2 Choice of Injury Mode 16
1.4.3 Choice of Anatomical Site 18
1.4.4 Assays of nerve regeneration 20
1.5 EXPERIMENTAL APPROACHES TO NERVE REGENERATION 24
1.5.1 Tubes 24
1.5.2 Substrates 26
1.6 OBJECTIVES 28

CHAPTER 2: COMPARISON OF ASSAYS OF NERVE REGENERATION 31

2.1 INTRODUCTION 31
2.1.1 Regeneration and Gap Length 31
2.1.2 Specific Aims 34
2.2 MATERIALS AND METHODS 35
2.2.1 Experimental Configuration 35
2.2.2 Silicone Tubes 37
2.2.3 Animal Model: Single-leg Nerve Repair 37
2.2.4 Tissue Allocation and Histological Processing 40
2.2.5 Morphometric Evaluation 42
2.2.6 Statistical Analysis 43
2.2.7 Mathematical Relationship: Regeneration and Gap Length 44
2.3 RESULTS 48
2.3.1 General Observations 48
2.3.2 Assay #1: Percent Reinnervation at Gap Midpoint 48
2.3.3 Assay #2: Reinnervation at the Distal Nerve Stump 53
2.3.4 Assay #3: Number of Myelinated Axons at Gap Midpoint 57
2.3.5 Assay #4: Number of Myelinated Axons in Distal Nerve Stump 59
2.4 DISCUSSION 60
2.4.1 Relationship between Regeneration and Gap Length: Sigmoidal Equation 61
2.4.2 Alternative to the Sigmoidal Equation: Step Function 61
2.4.3 Changes with Time: Time Independence 63
2.4.4 The Characteristic Gap Length 64
2.4.5 Comparison of Assays 65
2.4.6 Significance of Findings 66

CHAPTER 3: COMPARISON OF SINGLE-LEG AND CROSS-ANASTOMOSIS MODELS 69

3.1 INTRODUCTION 69
3.1.1 Single-leg and Cross-anastomosis Models of Nerve Repair 69
3.1.2 Specific Aims 70
3.2 MATERIALS AND METHODS 71
3.2.1 Experimental Configuration 72
3.2.2 Animal Model: Cross-anastomosis Repair 73

3.2.3 Tissue Allocation, Histological Processing, and Morphometric Evaluation 75
3.2.4 Statistical Analysis and Sigmoidal Curve Fit 75
3.3 RESULTS 75
3.3.1 General Observations 75
3.3.2 Assay #1: Percent Reinnervation at Gap Midpoint 76
3.3.3 Assay #2: Reinnervation at the Distal Nerve Stump 81
3.3.4 Assay #3: Number of Myelinated Axons at Gap Midpoint 82
3.3.5 Assay #4: Number of Myelinated Axons in Distal Nerve Stump 83
3.4 DISCUSSION 85
3.4.1 Comparison of Assays: Validation of the Characteristic Gap Length Assay 85
3.4.2 Comparison of Single-leg and Cross-anastomosis Models 87
3.4.4 Significance of Findings 88

CHAPTER 4: COMPARISON OF THE SILICONE TUBE AND THE CG DEVICE 91

4.1 INTRODUCTION 91
4.1.1 Previous studies of the Silicone Tube and the CG Device 91
4.1.2 Specific Aims 92
4.2 MATERIALS AND METHODS 94
4.2.1 Experimental Configuration 94
4.2.2 Preparation of the collagen-GAG (CG) Devices 95
4.2.3 Animal Model: Cross-anastomosis Repair 100
4.2.4 Tissue Allocation, Histological Processing, and Morphometric Evaluation 100
4.2.5 Statistical Analysis and Sigmoidal Curve Fit 100
4.3 RESULTS 100
4.3.1 General Observations 100
4.3.2 Assay #1: Percent Reinnervation at Gap Midpoint 101
4.3.3 Assay #2: Reinnervation at the Distal Nerve Stump 103
4.3.4 Assay #3: Number of Myelinated Axons at Gap Midpoint 107
4.3.5 Assay #4: Number of Myelinated Axons in Distal Nerve Stump 108
4.4 DISCUSSION 110
4.4.1 Comparison of Assays 110
4.4.2 Comparison of the Silicone Tube and the CG Device 112
4.4.3 Significance of Findings 114

CHAPTER 5: CONCLUSIONS 116

5.1 THE CHARACTERISTIC GAP LENGTH ASSAY 116
5.2 FUTURE WORK 117

APPENDIX A: PROTOCOLS 119

A.1 Collagen-Glycosaminoglycan (CG) Slurry Protocol 119
A.2 CG Matrix Manufacture Protocol 120
A.3 Sterile Procedure and Implant Assembly Protocols 124
A.4 Surgical Protocol 126
A.5 Animal Sacrifice and Tissue Processing Protocols 129
A.6 Epon Embedding Protocol 131
A.7 Toluidine Blue Staining Protocol 133
A.8 Image Capture and Analysis Protocol 134
A.9 Sample Input Code and Output from Mathematica Software 139

REFERENCES 143

List of Tables

Table 2.1 Experimental groups: silicone tube, single leg 36

Table 2.2 Percent reinnervation at gap midpoint: silicone tube, single leg 49

Table 2.3 Percent reinnervation at distal nerve stump: silicone tube, single leg 53

Table 3.1 Experimental groups: silicone tube, cross-anastomosis 72

Table 3.2 Percent reinnervation at gap midpoint: silicone tube, cross-anastomosis 77

Table 3.3 Percent reinnervation at distal nerve stump: silicone tube, cross-anastomosis 81

Table 4.1 Experimental groups: CG device, cross-anastomosis 94

Table 4.2 Percent reinnervation at gap midpoint: CG device, cross-anastomosis 102

Table 4.3 Percent reinnervation at distal nerve stump: CG device, cross-anastomosis 104

Table 4.4 Comparison of curve-fit parameters for silicone tube and CG device 113

List of Figures

Figure 1.1 Schematic of central and peripheral nervous systems..... 12

Figure 1.2 Schematic of myelinated axon structure..... 13

Figure 1.3 Illustration of single-leg and cross-anastomosis models of nerve repair..... 19

Figure 2.1 Musculature and nerve structure of the rat hind limb..... 38

Figure 2.2 Schematic diagram of a silicone tube device bridging a peripheral nerve gap..... 39

Figure 2.3 Diagram showing allocation of nerve tissue for histological processing..... 41

Figure 2.4 Representative step function fit to experimental data for percent reinnervation versus gap length..... 47

Figure 2.5 Sigmoidal curve fits to the gap midpoint reinnervation data: silicone tube, single-leg..... 50

Figure 2.6 Changes with time in the curve fit parameters (K and L_c): gap midpoint, silicone tube, single-leg..... 51

Figure 2.7 Sigmoidal curve fit and experimental data for percent reinnervation versus gap length: gap midpoint, silicone tube, single-leg..... 52

Figure 2.8 Sigmoidal curve fits to the distal stump reinnervation data: silicone tube, single-leg..... 54

Figure 2.9 Changes with time in the curve fit parameters (K and L_c): distal stump, silicone tube, single-leg..... 55

Figure 2.10 Sigmoidal curve fit and experimental data for percent reinnervation versus gap length: distal stump, silicone tube, single-leg..... 56

Figure 2.11 Number of myelinated axons at gap midpoint: silicone tube, single-leg..... 58

Figure 2.12 Number of myelinated axons at distal stump: silicone tube, single-leg..... 59

Figure 3.1 Sigmoidal curve fits to the gap midpoint reinnervation data: silicone tube, cross-anastomosis..... 78

Figure 3.2 Changes with time in the curve fit parameters (K and L_c): gap midpoint, silicone tube, cross-anastomosis..... 79

Figure 3.3 Sigmoidal curve fit and experimental data for percent reinnervation versus gap length: gap midpoint, silicone tube, cross-anastomosis..... 80

Figure 3.4 Number of myelinated axons at gap midpoint: silicone tube, cross-anastomosis..... 82

Figure 3.5 Number of myelinated axons at distal stump: silicone tube, cross-anastomosis..... 84

Figure 4.1 Scanning electron micrograph (SEM) of collagen tube..... 97

Figure 4.2 Scanning electron micrograph (SEM) of collagen-GAG matrix..... 99

Figure 4.3 Experimental data and sigmoidal curve fit to 9-week reinnervation data from the distal stump: CG device, cross-anastomosis..... 106

List of Figures (continued)

Figure 4.4 Number of myelinated axons at gap midpoint: CG device, cross-anastomosis..... 107

Figure 4.5 Number of myelinated axons at distal stump: CG device, cross-anastomosis..... 109

Chapter 1: Introduction

1.1 Clinical Problem

The clinical outcome of severe peripheral nerve injury is the loss of function and sensation in the affected limb or organ. Peripheral nerve injuries necessitate approximately 200,000 surgical repair procedures each year in the United States alone (Madison et al., 1992). Injuries to peripheral nerves may be the result of disease, trauma, or intentional nerve transection during certain surgical procedures. Traumatic injuries to peripheral nerves may be the result of violence, industrial accidents, or sports-related injuries. An example of intentional peripheral nerve transection is the procedure used for oncological surgery to remove tumors from the cranial base, in which the facial nerve is transected to provide access to the tumor site (Janecka et al., 1990).

Regardless of the cause of peripheral nerve injury, the result is loss of function of the denervated organ. The most common clinical treatments for peripheral nerve damage are direct suture of the nerve stumps or interposition of a segment of autograft nerve tissue. The direct suture technique is most often used when the two nerve stumps can be directly apposed without the introduction of mechanical tension at the suture line (Madison et al., 1992). Clinical studies of direct suturing of the median nerve in humans demonstrated that only 25% of patients recovered full motor function and 3% recovered full sensory function (Mackinnon and Dellon, 1988). Autografting is the current clinical treatment for damaged peripheral nerves in which the gap separating the two nerve stumps is too large to allow direct suture without tension. This procedure requires that a segment of nerve tissue be harvested from a donor site, commonly the sural nerve. The autograft tissue is then sutured to bridge the initial nerve injury. Clinical studies of

autograft repair of the median nerve in humans demonstrated that only 20% of patients recovered full motor function and none of the patients recovered full sensory function (Mackinnon and Dellon, 1988). The unsatisfactory results obtained with both the direct suture and the autograft techniques clearly demonstrate the need for a more effective therapy for the treatment of peripheral nerve injury.

A third approach to peripheral nerve repair is to bridge the nerve defect with a tubular implant device. A number of research efforts have been dedicated to the goal of developing an artificial tubular implant for nerve repair that will achieve a level of performance equivalent to or even superior to that of the autograft. This notion is supported by studies that have demonstrated that bioengineered tubular devices promoted peripheral nerve regeneration equivalent to the autograft in the rat animal model (Kim et al., 1994, Chamberlain, 1998, Chamberlain et al., 1998). Bioengineered devices for nerve repair also have the advantage over the autograft in that the characteristics of an engineered device can be systematically modified in order to improve performance. A review of engineering strategies for peripheral nerve repair can be found in section 1.5 later in this chapter.

Although a wide range of nerve gap injuries (1 mm to several centimeters in length) are common in the clinic, a comprehensive study of tubulation repair of nerve gaps of various lengths has not been performed. Two experimental studies, performed by Buti et al. (Buti et al., 1996) and Lundborg et al. (Lundborg et al., 1982), have initially examined the effects of gap length on nerve regeneration. The Buti study examined the return of electrophysiological function in the mouse sciatic nerve following repair with a silicone tube. The results indicated a general decreasing trend in the quality of

regeneration with increasing gap length. The Lundborg study was performed in the sciatic nerve of the adult rat. Nerve gaps 6, 10, 15, and 20 mm in length were repaired with silicone tubes. Nerve fiber regeneration into the gap was qualitatively examined at 4 weeks following implantation. It was observed that nerve fibers had successfully regenerated to the gap midpoint in all animals with small gap lengths (6 and 10 mm) but did not successfully bridge the gap in any animals with larger gaps (15 and 20 mm). This study provides the initial points that describe the relationship between successful axon bridging and gap length.

1.2 Peripheral Nerve Structure and Function

The nervous system consist of a network of cell bodies (neurons) and cellular processes (nerve fibers or axons) throughout the body responsible for conducting electrical impulses from the brain to distal endpoints (skeletal muscle and organs) and from sensory endpoints back to the brain. The cell bodies of motor neurons are located in the gray matter of the spinal cord, and the cell bodies of sensory neurons are located in the peripheral nerve roots (dorsal root ganglia). The central nervous system consists of the nerve cell bodies and processes located in the brain and spinal cord, and the peripheral nervous system consists of the cell processes outside the brain and spinal cord. Figure 1.1 shows a schematic diagram illustrating the distinction between the central and peripheral nervous systems in a simple motor communication network.

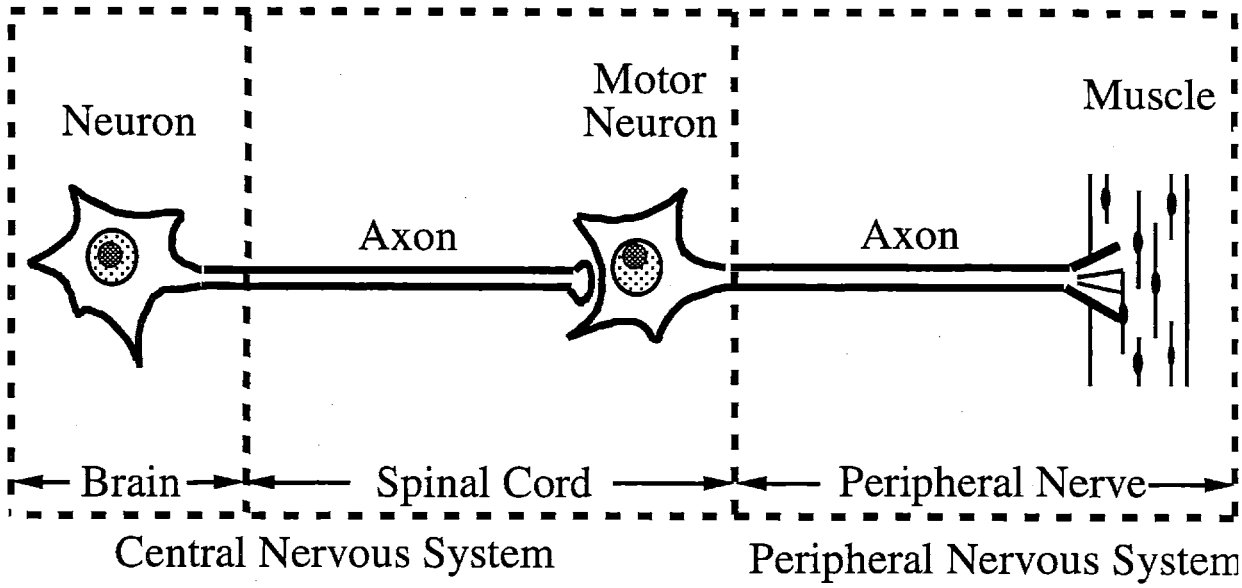

Figure 1.1 Schematic diagram of a simple motor circuit. The central nervous system contains the neurons and axons within the brain and spinal cord. The peripheral nervous system contains the nerve fibers located in the body extremities, outside the brain and spinal cord.

Peripheral nerves conduct electrical impulses to and from the central nervous system using a complex organization of conducting and non-conducting components. The conducting elements of peripheral nerves are axons, which are long cell processes of the nerve cells (neurons). Axons of the peripheral nervous system are organized into bundles which comprise the peripheral nerve trunks (peripheral nerves) located throughout the limbs and body. The axons connect each neuron cell body to the distal target organ without interruption. A single axon may be as long as 1 meter in the human.

Each peripheral nerve contains axons, support cells (mainly fibroblasts and Schwann cells), connective tissue, and a vascular supply. The Schwann cell is the most numerous support cell type in the peripheral nervous system. Schwann cells provide trophic support for the axons and ensheathe or myelinate axons to improve their electrical conduction properties. The myelin sheath consists of multiple layers of Schwann cell

cytoplasm wrapped tightly around the axon (Figure 1.2). Myelination enhances the velocity of the signal conducted by an axon by electrically insulating the axon at periodic segments along its length. The thickness of the myelin sheath varies between axons and depends to some extent on axon diameter.

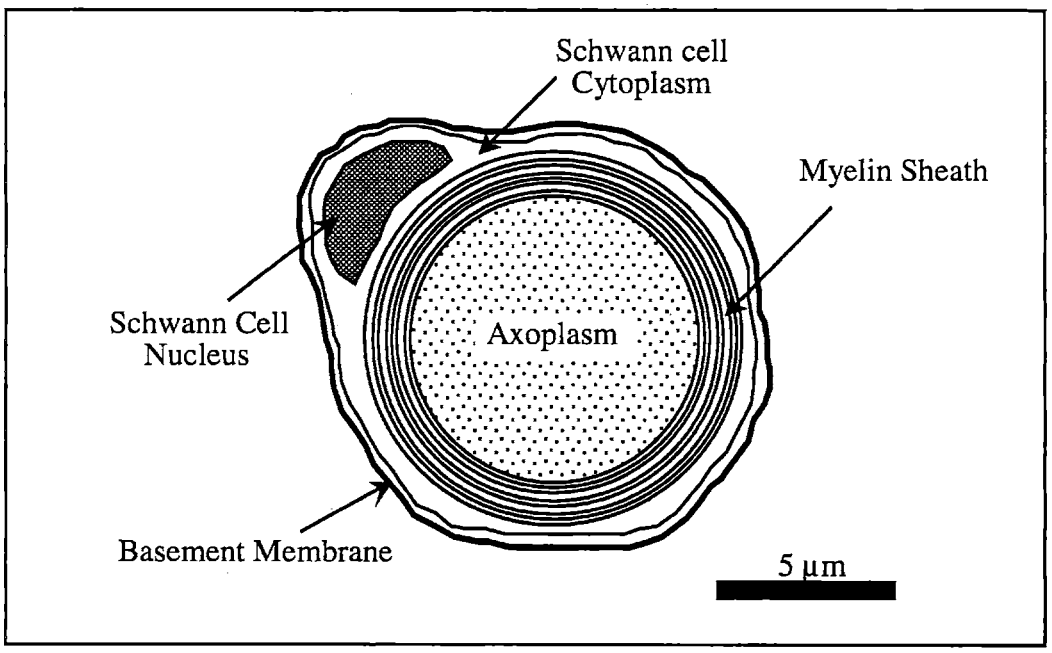

FIGURE 1.2 Schematic showing the cross section of a normal myelinated axon. Adapted from Chamberlain (Chamberlain, 1998).

Peripheral nerve trunks contain a number of small bundles of axons that may be organized into one or more fascicles. Each fascicle contains the axons, supporting Schwann cells, interspersed connective tissue (endoneurium), and endoneurial fibroblasts. Each fascicle is surrounded by a layer of flattened cells and ECM known as the perineurium. The diameter of a typical nerve trunk can vary greatly between less than one millimeter and greater than 10 mm in the human. The sciatic nerve of the rat which is a popular experimental model for nerve repair, is typically 1.0-1.5 mm in diameter.

1.3 Peripheral Nerve Regeneration

There have been many comprehensive reviews of the physiological processes involved in peripheral nerve regeneration (Fields et al., 1989, Fawcett and Keynes, 1990, Fu and Gordon, 1997). A brief review will be presented below to introduce useful concepts for interpreting the results of this thesis.

Transection injury to a peripheral nerve disrupts all sensory and motor axons. The distal portion of each axon has been separated from its neuron and undergoes Wallerian degeneration. The debris of degrading axons is phagocytosed by macrophages and activated Schwann cells within the first few days following injury. The remaining myelin sheaths may persist up to 30 or 40 days before being similarly phagocytosed (Ramon y Cajal, 1928). Schwann cells in the distal nerve stump detach from the degenerating axons and begin to proliferate. Schwann cells and fibroblasts in the proximal nerve stump also become active and undergo mitosis.

In cases when the nerve stumps are bridged with a tubular implant, the lumen of the tube becomes filled with wound fluid within one day after injury (Williams et al., 1983). Fibrinogen from the blood plasma polymerizes to form a continuous clot of fibrin and fibronectin between the nerve stumps (Williams et al., 1983). Cells from both the proximal and distal stumps migrate into the fibrin scaffold during the first week following injury. Initial cell migration into the gap consists mainly of cells of apparent endothelial origin as well as cells resembling fibroblasts and macrophages (Scaravilli, 1984). Other studies suggest that fibroblasts and Schwann cells are the first to migrate, entering the gap during the first week (Williams et al., 1983). These cells are followed by vascular cells during the second week.

The sprouting and elongation of severed axons in the proximal stump begins within hours after transection (Fawcett and Keynes, 1990). Nonmyelinated axons first enter the gap after a delay of 7-14 days(Williams et al., 1983). Initial axon growth was observed in close association with Schwann cells in the gap. The rate at which the leading elongating axons traverse the gap remains an item of debate. Investigators have estimated the velocity of elongation to be 1 to 3 mm per day depending on the age and species of the experimental animal. Studies by Williams et al. indicated that unmyelinated axons traversed a 10-mm gap within 3 weeks with a one-week period of delay (Williams et al., 1983), yielding an elongation velocity of less than 1 mm per day after the delay period. Based on the elongation velocity estimates above, it is possible that regenerating axons may reach distal muscle and sensory targets within 5 weeks after injury. However, electrophysioloigcal impulses are not conducted across a 10-mm gap in rat sciatic nerves until 8 weeks after injury and tubulation (Chang et al., 1990). The time delay before the nerves are able to conduct a signal may be explained by the additional time required for the axons to reach maturity. Once the regenerated axons have reached the distal targets, they typically grow in diameter and may undergo an increase in myelin thickness (Chamberlain, 1998).

1.4 Experimental Models of Nerve Injury

A number of different models have been developed for the study peripheral nerve regeneration. The various models differ in the animal species, the choice of injury mode, choice of anatomical site, and the assays with which regeneration is evaluated. Each topic is discussed below.

1.4.1 Choice of Animal Species

A number of different animal species have been used for experimental models of peripheral nerve injury including the rabbit (Fawcett and Keynes, 1986, Whitworth et al., 1995), the cat (Noback et al., 1958, Rosen et al., 1983), the non-human primate (Dellon and Mackinnon, 1988, Archibald et al., 1995), the mouse (Navarro et al., 1995, Buti et al., 1996), and the rat (Fields et al., 1989). The rat is the most commonly used species, probably due to its high resistant to infection and relatively simple procedures for anesthesia, surgery, and post-operative care. Although many of the same benefits are available in using the mouse, the surgical procedure can more difficult due to the small size of the nerve.

Within the rat species, there exist differences among the different strains in the animals' response to nerve trauma. A study of sciatic nerve repair in several strains of rat revealed that the various strains differed in the incidence of autotomy (self-mutilation) of the affected limb (Carr et al., 1992). In the study by Carr et al., 100% of Sprague-Dawley rats exhibited autotomy following nerve transection without repair, and 71% exhibited autotomy following transection and direct suture. In the same study, no rats of the Lewis rat strain exhibited autotomy following transection with or without repair. In the most severe cases, autotomous behavior can lead to pain and infection of the limb and exclusion of the animal from analysis (Wall et al., 1979, Landstrom, 1993). For this reason, the Lewis rat strain was used for studies in this thesis.

1.4.2 Choice of Injury Mode

The two main modes of injury used by investigators include compression of the nerve tissue and complete transection of the nerve. The compression injury mode

resembles a class of clinical situations in which the continuity of the connective and support tissue remains grossly intact while the nerve fibers themselves are damaged or interrupted by the crushing force. This mode of injury has been used in a number of studies in various laboratories (Haftek and Thomas, 1968, Devor and Govrin-Lippman, 1979, Walker et al., 1994, Danielsson et al., 1996, Hoffman and O'Shea, 1999, Korompilias et al., 1999). The compression injury mode does not easily lend itself to the study of implantable devices since the nerve trunk remains intact, but is more appropriate for pharmacological studies. Nerve compression is also not well suited for morphological studies of nerve regeneration since nerve fibers found in the injury site may be either regenerated nerve fibers or intact nerve fibers that were not damaged by the initial injury. For these reasons, compression injury was not appropriate for the study of nerve repair devices in this thesis.

The transection mode of injury resembles a class of clinical situations in which the continuity of the nerve trunk has been interrupted and the two nerve stumps are separated by a gap. For experimental studies of nerve regeneration, the transection mode of injury provides less ambiguous results than compression injury. Complete transection of the nerve trunk ensures that all nerve fibers have been severed, and all axons that are found in the gap are definitively identified as regenerated axons. Nerve transection is the most common injury used by experimental investigators (Fields et al., 1989, Fu and Gordon, 1997). In the present study, the sciatic nerve transection model was chosen for the ability to create a reproducible wound and for potential comparison to the well-established baseline of data from other investigators.

1.4.3 Choice of Anatomical Site

Studies of nerve transection in the rat are usually performed on the sciatic nerve since it is easily accessible surgically and has a well-defined pattern of innervation. With the transection mode of injury, most investigators transect the sciatic nerve in either the right or left hind limb, creating a gap between the nerve stumps (single-leg injury). The repair therapy (i.e. tubulation) is then applied to the gap injury. The finite length of the sciatic nerve trunk and the length of the femur along which it runs impose geometric constraints on the size of the nerve gap that can be reasonably created. Investigators have studied a number of different gap lengths ranging between 2 and 15 mm using the single-leg sciatic nerve injury model (Fields et al., 1989). From previous experiments in this laboratory, it has been determined that the geometric limit for the length of a nerve gap in the rat sciatic nerve is 15 mm (Chamberlain, Landstrom, personal communication).

When a gap length of larger than 15 mm is required for experimental reasons, it is necessary to use a nerve-repair model that allows for such gap lengths. One such model, the cross-anastomosis model, was first used by Lundborg et al. (Lundborg et al., 1982), and has also been used in this laboratory (Yannas et al., 1987). Figure 1.3 illustrates the cross-anastomosis model in which the proximal sciatic nerve in one leg is bridged over the back of the animal to the distal right nerve. The bridging over the back creates the additional range in gap length between the stumps.

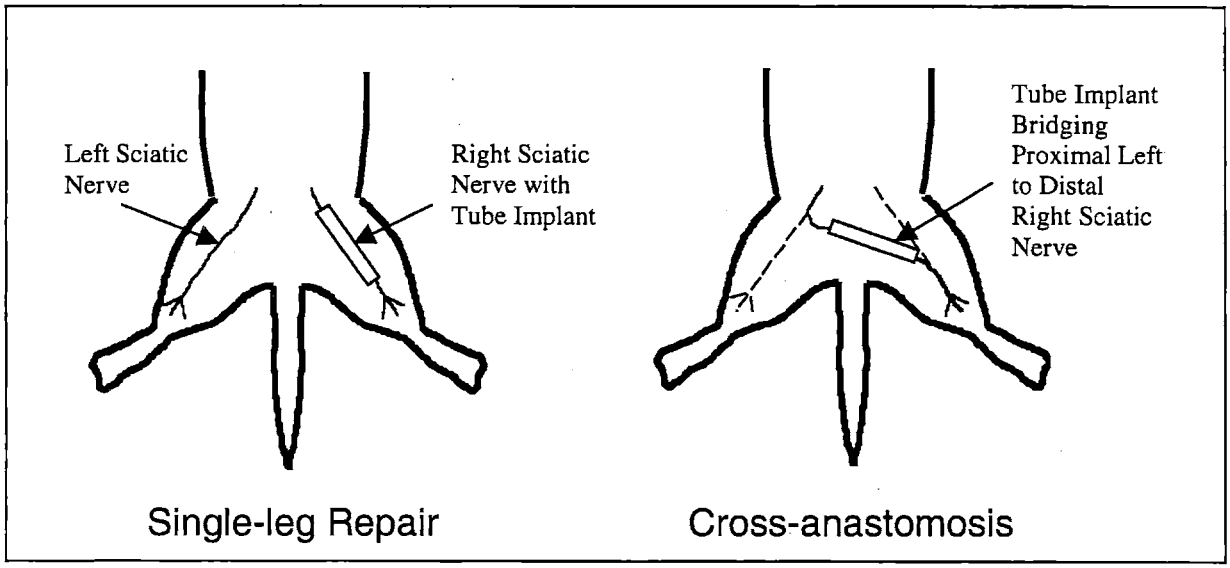

Figure 1.3 Schematic diagram showing the hind limbs of the rat with tubulation repair of the sciatic nerve using the single-leg and cross-anastomosis models.

The purpose of the Lundborg study (Lundborg et al., 1982) was to examine axon regeneration across nerve gaps of various lengths repaired with silicone tubes. The cross-anastomosis model was apparently used to accommodate the larger 15- and 20-mm gaps. Yannas et al. (Yannas et al., 1987) employed the cross-anastomosis model to study nerve regeneration across 15-mm gaps bridged with either saline-filled silicone tubes or silicone tubes filled with collagen-glycosaminoglycan matrix. Although the cross-anastomosis model permits the study of larger gap lengths, it has been less widely utilized due to the additional difficulty of the surgical procedure and the potential ambiguity in interpreting the results in terms of functional recovery.

One goal of the experiments in this thesis was to examine nerve regeneration across gaps of different lengths. The first group of experiments (chapter 2) were performed using the single-leg model of nerve repair since it is a well-established model

and provides a large pool of data from other investigators for comparison. In chapters 3 and 4, the cross-anastomosis model was used to accommodate larger gap lengths (up to 22 mm).

1.4.4 Assays of nerve regeneration

In studies of peripheral nerve regeneration, the quality of regeneration following injury is generally characterized based on the ability of the regenerated nerve to conduct and electrical impulse (electrophysiology), on the return of function to the denervated organ, or on the anatomical structure (morphology) of the regenerated nerve. Each type of assay has been commonly used in experimental studies. One purpose of the work presented in this thesis was to compare a number of experimental assays in order to identify a single assay that can be used in short-term studies to quantify the quality of nerve regeneration.

Electrophysiological studies provide a gross measure of the electrical conduction properties of the entire regenerated nerve trunk. Commonly measured parameters of nerve conduction include the amplitude and the velocity of the electrical impulse. Conduction can be measured across the injury gap or across the entire length of the nerve to the distal endpoint or target. One advantage of an electrophysiological assay is that the functional property (electrical conduction) of the nerve fibers is being directly measured. Another advantage is that electrophysioloigcal measurements can be performed at multiple time points without sacrificing the animal (Archibald et al., 1995). Electrophysiological assays also have disadvantages. In order for a measurement to be taken, nerve fibers must elongate across the across the designated distance and mature to a level at which a signal can be conducted. This concept is illustrated by the fact that no

electrical signal travels across a repaired 10-mm nerve defect during the first 8 weeks after injury (Chang et al., 1990). After the first signals are detected, additional time is typically required for the data to reach a steady state. Studies in this laboratory and others indicate that the recovery of electrophysiological properties does not reach a plateau with time until 30 to 100 weeks after injury (Chang et al., 1990, Archibald et al., 1995). Although electrophysiological assays may yield functionally relevant data for regeneration, due to the long time required to reach a steady state these assays are not well suited for short-term studies.

Assays of functional recovery include measurements of both motor function and sensory function. Motor function has been most commonly assessed in the rat sciatic nerve model by the analysis of the walking gait of the animal based on measurements of footprints made on a walking track (deMedinaceli et al., 1982, Bain et al., 1989, deMedinaceli, 1990). Simple linear measurements such as footprint length and toe spread are combined by a weighted equation into a single index of nerve function, the sciatic functional index. Based on this index, repaired nerves can be compared with normal nerves or with nerves repaired with an alternative therapy. Although the sciatic functional index is reasonably simple and repeatable, it cannot be applied when heel ulceration or chronic toe contracture occur (Dellon and Mackinnon, 1989, Chamberlain, 1996). Experiments performed in this laboratory indicated that the sciatic functional index may not be adequately sensitive to distinguish among different nerve repair devices, even at 30 weeks after injury (Chamberlain, 1996). Sensory function is most commonly measured by recording a response to a painful or uncomfortable stimulus or the return of a reflex (Frykman et al., 1988, Buti et al., 1996). These tests can be difficult to interpret,

and being semi-quantitative often yield ambiguous false positive results. Tests of both motor and sensory function also require sufficient time for nerve fibers to elongate the target muscle or sensory organ, reconnect, and mature to a functional state. For the purposes of identifying a short-term assay to distinguish among nerve repair devices, it is apparent that neither motor nor sensory functional tests are appropriate.

Morphological assays generally consist of the measurement of the number and diameter of regenerated nerve fibers following injury. The analysis is usually performed on plastic-embedded semi-thin sections for light microscopy or thin sections for electron microscopy. One disadvantage of a morphological assay is that the results do not directly assess the conducting function of the nerve. However, a number of studies have demonstrated a correlation between regenerated nerve fiber number and diameter and electrophysiological conduction properties (Cragg and Thomas, 1964, Dellon and Mackinnon, 1989, Chamberlain, 1998). An additional disadvantage is that serial measurements on a single animal with time are not possible since the animal must be sacrificed in order to gather histological data. An advantage of a morphological assay is that it can be applied at earlier times than the electrophysiological or functional assays. Regenerating nerve fibers can be analyzed as they pass through the injury site rather than waiting for them to elongate and mature. One goal of this thesis was to examine peripheral nerve regeneration during the early (less than 12 weeks) period following injury, and morphological assays were chosen for this purpose. It was hypothesized that morphological assays could be applied in an appropriately designed short-term experiment to quantify the quality of regeneration following nerve repair.

Previous studies in this laboratory have focussed on comparing the effectiveness of various nerve repair devices in repairing a standard 10-mm gap in the rat sciatic nerve. Devices were compared on the basis of well-established assays such as number and diameter of regenerated nerve fibers and electrophysiological conduction properties of the regenerated nerves. In these studies, statistically relevant differences among implant devices were not detectable at 6 or 30 weeks following implantation, but became detectable only after 60 weeks (Landstrom, 1993, Chamberlain, 1996, Chamberlain, 1998). There exists a definite need for a short-term (less than 12 week) assay that can be used to identify statistically significant differences among devices and to rank-order the devices based on effectiveness.

A number of investigators have evaluated the quality of nerve regeneration by measuring the proportion or percentage of animals in a given experimental group in which regenerated nerve fibers were able to enter or cross the defect (percent reinnervation). The data for percent reinnervation depend on morphology of the regenerated nerve, but provide an alternative metric to the number and diameter of regenerated nerve fibers. Percent reinnervation has been used in a number of different studies to evaluate regneration in the rat sciatic nerve model (Lundborg et al., 1982, Seckel et al., 1984, Williams et al., 1984, Williams, 1987, Chang et al., 1990, Navarro et al., 1996). Since the presence of axons is measured in the defect or in the distal nerve stump, it is not necessary to wait for the axons to reach the distal targets or to reach maturity. In this thesis, it was hypothesized that the percent reinnervation assay could be used to identify statistically significant differences among nerve repair devices in short-term studies.

1.5 Experimental Approaches to Nerve Regeneration

Although nerve repair using autograft tissue is the standard therapy for severe nerve injury in the clinic, the autograft procedure is far from optimal. Clinical studies have demonstrated that autografting rarely results in complete return of motor or sensory function (Mackinnon and Dellon, 1988). Harvesting nerve tissue from a donor site also requires an additional surgical procedure that results in pain, the formation of a dermal scar, and the loss of nerve function at that site. A number of researchers have examined alternative approaches to nerve repair. The majority of alternative approaches involve bridging of the nerve stumps with a tubular implant in conjunction with filling the tube lumen with elements (i.e. biomaterials, cells, soluble factors) that may promote axon regeneration. A number of these approaches are briefly reviewed below.

1.5.1 Tubes

Tubes have been used to repair transected nerves for over 100 years (Fields et al., 1989). It has been suggested that the tubulation nerve repair procedure serves to facilitate regeneration by a number of mechanisms: allowing regulatory factors and cells from the proximal and distal stumps to accumulate in the wound site, providing direction for cells and axons elongating across the gap, and isolating the wound site from pathological processes in the neighboring connective tissues (Madison et al., 1992). The earliest tubes for peripheral nerve repair were generally composed of naturally occurring materials derived from tissues such as bone, dura, epineurium, perineurium, and vein. More recently, tubes have been synthesized from nondegradable synthetic materials (magnesium, rayon, silicone, stainless steel, and tantalum) as well as degradable

materials, both synthetic (polyester, polyglactin, and polylactate) and natural (collagen, laminin, fibronectin) (Fields et al., 1989).

Silicone tubes were among the first devices used for experimental nerve repair, and a substantial amount of data is available concerning nerve regeneration through silicone tubes (Ducker and Hayes, 1968, Lundborg et al., 1982, Williams et al., 1983, Jenq and Coggeshall, 1984, Williams and Varon, 1985, Fields and Ellisman, 1986, Fields and Ellisman, 1986, LeBeau et al., 1988, Williams et al., 1993, Buti et al., 1996). Promising experimental results in animal models prompted the use of silicone tubes for nerve repair in human patients (Lundborg et al., 1991, Janecka et al., 1993). Experimental researchers studying the basic science of nerve regeneration have used silicone tubes to create a controlled environment (wound chamber) in which the physiological processes of nerve regeneration were examined (Lundborg et al., 1982, Williams et al., 1983, Jenq and Coggeshall, 1984, Jenq and Coggeshall, 1985, Williams and Varon, 1985, Williams, 1987). Nerve regeneration following implantation of a silicone tube has been well-characterized, and many investigators have treated the silicone tube as an experimental standard to which alternative devices or therapies may be compared. Previous studies in this laboratory have used the silicone tube as a baseline for the evaluation of the performance of other devices (Landstrom, 1993, Chamberlain, 1996, Chamberlain, 1998).

Peripheral nerve repair using collagen tubes has been studied by a number of different groups (Colin and Donoff, 1984, Li et al., 1990, Archibald et al., 1991, Li et al., 1992, Archibald et al., 1995, Chamberlain, 1996, Navarro et al., 1996, Chamberlain, 1998, Chamberlain et al., 1998, Chamberlain et al., 2000). Collagen is an attractive

alternative to silicone since it is ultimately resorbable when implanted into the body. Collagen is also a natural component of the extracellular matrix and contains inherent binding sites for attachment and migration of various cell types. Studies in this laboratory demonstrated that unfilled collagen tubes performed better than the unfilled silicone tube standard in a long-term (60-week) evaluation of sciatic nerve repair in the rat (Chamberlain, 1998). Evaluation of performance was based on both the number of regenerated large-diameter nerve fibers and on electrophysiological conduction properties. Collagen tubes may also be manufactured in such a fashion that the tube walls contain small pores that allow the passage of certain soluble agents such as small molecules and proteins. A study by Li and colleagues demonstrated that collagen tubes that were permeable to proteins with molecular weight of 540 kDa or less promoted nerve regeneration across a 5-mm gap in the primate median nerve (Li et al., 1990, Li et al., 1992).

In this thesis, silicone tubes were used as a well-established baseline for nerve repair. Use of the silicone tube makes available a large pool of data from other investigators for comparison and validation of the current data. Collagen tubes were used in this thesis and compared to silicone tubes. For the current studies, the collagen tubes were implanted containing a collagen-glycosaminoglycan matrix. Filling of nerve repair tubes with substrates is described below.

1.5.2 Substrates

When transected nerve stumps are bridged by a tubular device, the lumen of the tube between the stumps becomes filled with exudate after one day. Within one week, plasma precursors from the exudate form a bridge of fibrin that connects the nerve

stumps (Williams et al., 1983). The fibrin matrix serves as a provisional scaffold for the migration of fibroblasts and Schwann cells into the gap. Axons begin to elongate into the gap after the initial migration of support cells (Williams et al., 1983). Eventually, the provisional fibrin matrix is degraded and replaced by a more durable network of collagen and other ECM elements. Based on these observations, a number of investigators have attempted to favorably alter the environment within the tube lumen by pre-filling the tube with a number of different materials. The motivating hypothesis is that axon growth can be promoted by providing a substrate that enhances the migration of support cells and axons into and across the gap.

Axon elongation has been shown to be dependent to a large extent on signals provided to the advancing axon tip (the growth cone) by molecules residing in the ECM or by molecules located on cell surfaces (Fu and Gordon, 1997). Numerous investigators have studied the effect of exogenous substrate materials on axon elongation following nerve injury. Certain components of the extracellular matrix, including collagen, laminin and fibronectin, have been shown capable of enhancing the regeneration of axons across tubulated nerve gaps (Madison et al., 1985, Glasby et al., 1986, Yoshii et al., 1987, Gulati, 1988, Madison et al., 1988, Rosen et al., 1990, Bailey et al., 1993, Bryan et al., 1993, Ohbayashi et al., 1996). Aside from increasing the number of axons crossing the gap, substrates have increased the maximum gap distance that can be bridged by axonal tissue from 10-mm to at least 15-mm (Yannas et al., 1987, Madison et al., 1988) as well as increasing the rate of axonal elongation (Madison et al., 1988, Ohbayashi et al., 1996). In preliminary studies, a collagen-glycosaminoglycan (CG) matrix, ensheathed by a

silicone tube, facilitated regeneration of axons across a 15-mm gap in the rat sciatic nerve (Yannas et al., 1985, Yannas et al., 1987).

For the experiments described in this thesis, two nerve repair devices were studied. The first device was the unfilled silicone tube. This device was chosen since it is an experimental standard and a baseline for comparison with other devices. A second device, a collagen tube filled with collagen-glycosaminoglycan matrix, was used since it is the most effective device that has been tested in this laboratory to date (Chamberlain, 1998). One purpose of the experiments in this thesis was to compare the regeneration through unfilled silicone tubes to the regeneration through a superior device, the matrix-filled collagen tube (the CG device).

1.6 Objectives

The overall objective of this thesis was to establish an assay by which the effectiveness of nerve repair devices can be compared in short-term studies. Using this assay, the silicone tube and the CG device were compared based on the ability to promote nerve regeneration across nerve gaps of various lengths. Previous studies in this laboratory have demonstrated that statistically significant differences among nerve repair devices were not detectable in short-term (6- or 30-week) studies using traditional metrics such as the total number of nerve fibers in a standard 10-mm gap in the rat sciatic nerve (Landstrom, 1993, Chamberlain, 1996, Chamberlain, 1998). However, statistically significant differences among devices were observed in long-term (60-week) studies (Chamberlain, 1998). For the purpose of screening nerve repair devices based on effectiveness, short-term studies are preferable since they require less time and resources. It is hypothesized that differences among devices may be detectable in short-term studies

if an assay of effectiveness other than the number of regenerated nerve fibers is used. In this thesis, an assay of device effectiveness based on the ability of a device to promote nerve regeneration across gaps of different lengths was established. This assay was used to compare the silicone tube and the CG device in a short-term (less than 12-week) study.

In the experiments described in chapter 2, nerve regeneration through silicone tubes was examined using the single-leg model in the rat. The relationship among regeneration, gap length, and time was examined. Four assays of nerve regeneration were used: 1. the percentage of animals in which myelinated axons regenerated to the gap midpoint (percent reinnervation at midpoint), 2. the percentage of animals in which myelinated axons regenerated to the distal stump (percent reinnervation at distal stump), 3. the numbers of myelinated axons at the gap midpoint, and 4. the number of myelinated axons in the distal stump. The goal of these experiments was to compare the four regeneration assays in order to identify an assay that can be used to evaluate the effectiveness of a nerve repair device in short-term studies.

In chapter 3, nerve regeneration through silicone tubes was examined using the cross-anastomosis model of nerve repair. The cross-anastomosis model is necessary for the study of long gap lengths (greater than 15 mm) in the rat sciatic nerve. The four assays described in chapter 2 were used. The goal of these experiments was to compare and validate the assays in a different injury model with the same device. An additional goal was to identify differences in outcome between the single-leg and cross-anastomosis models. Information concerning the differences in outcome between the single-leg and cross-anastomosis models will be used to compare and interpret regeneration outcomes in both models and to compare these data with previous studies.

In chapter 4, nerve regeneration was examined following repair with the CG device in the cross-anastomosis model. The goal of chapter 4 was to evaluate the CG device using the four assays and to compare the results with those using the silicone tube. When taken together, the results of chapters 2, 3, and 4 were used to identify an assay for the evaluation of nerve repair devices, validate this assay in two nerve repair models (single-leg and cross-anastomosis), and compare two devices (the silicone tube and the CG device) on the basis of the assay.

Screening of nerve repair devices based on effectiveness is a time-consuming task. Previous studies indicate that the end-state of regeneration does not reach a plateau until between 30 and 100 weeks after injury based on regeneration assays such as electrophysiology (Chang et al., 1990, Archibald et al., 1995) and axon morphology (Chamberlain, 1998). Therefore, comparisons among competing devices on the basis of such assays may not be appropriate. There exists a definite need for a standardized test that can be used to quantitatively measure the effectiveness of nerve repair devices. Experimental researchers studying nerve repair will benefit from the establishment of a short-term assay with which nerve repair devices may be rank-ordered based on effectiveness. A reduction in time of initial screening studies will allow scientists to more rapidly develop, evaluate, and select devices for nerve repair. The results of this thesis will also be useful for surgeons in the clinic. Clinicians may use these concepts and data when determining the appropriateness of a particular nerve repair device for the repair of a nerve gap of a particular length.

Chapter 2: Comparison of Assays of Nerve Regeneration

2.1 Introduction

2.1.1 Regeneration and Gap Length

Although a wide range of nerve gap injuries (1 mm to several centimeters in length) are common in the clinic, a comprehensive study of tubulation repair of nerve gaps of various lengths has not been performed. Only a handful of investigators have studied tubulation repair of nerve gaps of different lengths. Buti and colleagues (Buti et al., 1996) examined bridging of mouse sciatic nerves with silicone tubes. Only one study of gap length has been performed in the rat model. This study by the Lundborg group (Lundborg et al., 1982) provides initial information describing silicone tube repair of nerve gaps of different lengths in the rat. These investigators performed silicone tubulation repair of transected sciatic nerves of adult rats with inter-stump nerve gaps of 6, 10, 15, and 20 mm in length. Nerve fiber regeneration into the gap was qualitatively examined at 4 weeks following implantation. It was discovered that nerve fibers had successfully regenerated to the gap midpoint in all animals with small gap lengths (6 and 10 mm) but did not successfully bridge the gap in any animals with larger gaps (15 and 20 mm). This study provides the initial data that describe the relationship between successful axon regeneration and gap length.

It is important to recognize that the study by Lundborg et al. (Lundborg et al., 1982) was performed using the cross-anastomosis model of nerve repair in which the proximal left sciatic nerve was bridged over the back of the rat to the right distal sciatic nerve stump. The cross-anastomosis procedure was used by the investigators to

accommodate large gap lengths (20 mm) that are geometrically not feasible with single-leg nerve repair in the rat. While the studies by Lundborg et al. were performed using the cross-anastomosis procedure, the studies presented in this chapter were performed using the single-leg procedure. It is not known whether the different nerve repair models will yield identical results. It is assumed that the general processes of nerve repair will remain common to cross-anastomosis or single-leg nerve repair models, and therefore, the general results will be comparable. Differences between the cross-anastomosis and single leg nerve repair models will be addressed in detail in chapter three. In the present chapter, the Lundborg results will be used as a general baseline with which the results will be compared.

In the Lundborg study (Lundborg et al., 1982), the number of regenerated nerve fibers was not measured. Rather, the proportion of animals with any given gap length in which axons had regenerated to the gap midpoint (reinnervation at midpoint) was measured. When examined as a function of gap length, the Lundborg data for percent reinnervation at the gap midpoint outline the shape of a decreasing curve that varies between 100 percent reinnervation at small gap lengths (less than 10 mm) and zero percent reinnervation at large gap lengths (greater than 15 mm). The data undergo a transition from 100 percent to zero percent reinnervation in the region between 10 and 15 mm. The data also suggest that, for the silicone tube, the curve must pass through a "characteristic" gap length (between 10 and 15 mm) at which reinnervation occurs in 50 percent of the cases. One goal of the work described in this chapter was to identify a mathematical relationship that accurately describes the experimental data for percent reinnervation versus gap length. This mathematical relationship will be used to determine

the characteristic gap length for the silicone tube. The characteristic gap length may be useful as a quantitative parameter that describes the effectiveness of a given device in promoting nerve regeneration.

Lundborg and co-workers (Lundborg et al., 1982) examined nerve regeneration only at 4 weeks following injury. It is unclear from the data whether or not an increase in successful axon regeneration may have occured if a time period longer than 4 weeks had been allowed. It is possible that the Lundborg data may or may not have reached a plateau or a time-independent state by 4 weeks. Previous experiments performed in this laboratory suggest that a plateau in percent reinnervation was reached by 6 weeks after injury (Landstrom, 1993, Chamberlain, 1998). In these studies, the differences in percent reinnervation between 6, 30, and 60 weeks were not statistically significant, and it is apparent that a time-independent state had been reached. These data demonstrated that successful bridging does not necessarily occur in every animal if simply allowed sufficient time and also suggested that, for a given device and gap length, the percent successful bridging will reach a plateau with time. The data described in this chapter will expand upon the results of Lunborg et al. by obtaining a time-independent description of nerve regeneration versus gap length.

Investigators of nerve regeneration have used a number of assays to quantify nerve regeneration. In the Lundborg study, nerve regeneration was quantified by determining the percent of animals with a given gap length in which axons regenerated to the midpoint of the gap or to the distal stump. In previous studies in this laboratory nerve regeneration has been assayed by measuring the number of myelinated nerve fibers at the gap midpoint or in the distal stump (Landstrom, 1993, Chamberlain, 1996, Chamberlain,

1998). One goal of the work described in this chapter was to compare a number of different assays of nerve regeneration. The data in this chapter describe the relationship between regeneration and gap length as measured by four assays: 1. the percentage of animals in which myelinated axons regenerated to the gap midpoint (percent reinnervation at midpoint), 2. the percentage of animals in which myelinated axons regenerated to the distal stump (percent reinnervation at distal stump), 3. the numbers of myelinated axons at the gap midpoint, and 4. the number of myelinated axons in the distal stump. These four assays were selected since they have been commonly used by other investigators and yield quantitative data. Other common assays such as functional evaluation and electrophysiology were not appropriate for the present study since they require long post-operative intervals and are unlikely to yield meaningful data in a short-term study. The specific goal of this study was to identify an assay that can be used in short-term experiments to rank-order nerve repair devices.

2.1.2 Specific Aims

The specific aims of the experiments described in this chapter were: 1. to characterize the relationship between nerve regeneration and gap length for rat sciatic nerves repaired with saline-filled silicone tubes, 2. to determine the dependence of regeneration on time in order to obtain time-independent data if possible, and 3. to compare different assays of regeneration in order to identify an assay that can be used in short-term experiments to rank-order nerve repair devices. For these purposes, groups of animals were implanted with saline-filled silicone tubes connecting the proximal and distal sciatic nerve stumps in the left hind limb (single-leg nerve repair model). At 4, 6, and 9 weeks after injury, nerve regeneration for each gap length was evaluated based on

the four metrics described above. The dependence of regeneration on gap length and time was determined. The regenerative outcome was measured by each of the four assays. The data from the experiment were interpreted based on the predictions and hypotheses below.

Based on the findings of Lundborg et al. (Lundborg et al., 1982), it was expected that the quality of regeneration would decrease with increasing gap length. Although Lundborg and colleagues gathered data for reinnervation at various gap lengths, they did not characterize the relationship between reinnervation and gap length. In the present study, it was anticipated that the data for percent reinnervation (at either the gap midpoint or the distal stump) versus gap length may be described by a sigmoidal curve between 100% and 0%. It was demonstrated by Lundborg et al. (Lundborg et al., 1982) that for the silicone tube there exists a characteristic gap length above which reinnervation would occur in a minority of cases. The characteristic length may be determined from the mathematical relationship that describes the sigmoidal curve.

It was anticipated that the quality of regeneration would increase with increasing time. Based on previous studies (Landstrom, 1993, Chamberlain, 1996, Chamberlain, 1998), it was hypothesized that the percent reinnervation data would increase and reach a plateau, while the data for axon number would increase without a plateau up to 9 weeks.

2.2 Materials and Methods

2.2.1 Experimental Configuration

The purpose of work described in this chapter was to compare four different assays in their ability to measure nerve regeneration across various gap lengths for rat

sciatic nerves repaired with silicone tubes (single-leg model). Table 2.1 below shows the various gap lengths and time points that were studied. Each cell of the table indicates the number of animals that were included in each experimental group.

Gap Length (mm)	4 weeks	6 weeks	9 weeks
6-7 mm	n=6	n=5	
8-9 mm	n=7	n=6	
10-11 mm	n=5	n=6	n=7
12-13 mm	n=5	n=6	n=8
14-15 mm	n=6	n=5	n=3
16-17 mm		n=6	n=4

Table 2.1 Experimental groups for silicone tube nerve repair in the single-leg model

The range of gap lengths was chosen based on the results of previous studies by Lundborg et al. (Lundborg et al., 1982) that provided an initial description of nerve regeneration across gap lengths of 6, 10, 15, and 20 mm repaired with silicone tubes. Nerve regeneration occurred with smaller gap lengths (6 and 10 mm) but did not occur with large gap lengths (15 or 20 mm). For the present experiment, gap lengths were chosen in 2-mm increments that spanned the gap length range of Lundborg over which the decline in regeneration occurred.

Lundborg et al. evaluated regeneration at only 4 weeks after injury. In the present study, time points of 6 and 9 weeks were also included in addition to the 4-week time point in order to characterize any changes in regeneration with time beyond the results of Lundborg et al.

2.2.2 Silicone Tubes

Silicone tubes were obtained from a commercial manufacturer (Helix Medical, Carpentiera, California, Catalog 60-011-06). These tubes were composed of Dow Corning medical grade Silastic and had an internal diameter of 0.058 inches (1.47 mm) and an outside diameter of 0.077 inches (1.96 mm), leaving a wall thickness of 0.019 inches (0.25 mm). The walls of the silicone tubes were assumed to be completely impermeable to transport except to certain gas molecules. Prior to surgery, all silicone tubes were cut to the appropriate length, placed into foil packets open at one end, and sterilized by autoclave. The packets were removed from the autoclave and immediately sealed.

2.2.3 Animal Model: Single-leg Nerve Repair

Adult female Lewis rats (Taconic, Germantown, NY), 175-225 grams, were housed at the Thorn building animal facility, Brigham & Women's Hospital, Boston, MA. All surgical procedures were performed in the Thorn surgical facility by Dr. Hu-Ping Hsu, an orthopedic surgeon who had prior experience with this procedure. A detailed protocol can be found in Appendix A. Anesthesia was achieved by intraperitoneal injection of sodium pentobarbital (Nembutal Sodium Solution, Abbot Laboratories, North Chicago IL) with the dosage of 50 mg of drug per kilogram of animal body weight. Once the animal was fully anesthetized, the entire back and legs were shaved using animal clippers and cleaned using an iodine sponge. The animal was placed in the prone position on a surgical board, arms and legs secured, with the legs in 30° abduction.

For the single-leg nerve repair procedures, all surgeries were performed in the left hind leg. A 4-cm incision was made through the skin parallel to and just posterior of the femur. The subcutaneous tissue was cut away to release the underlying muscle tissue from the skin. The superficial *biceps femoris* was separated carefully using surgical scissors until the sciatic nerve was visible. Once the nerve was visible, the muscle incision was extended along the femur to expose the entire sciatic nerve. Paperclip retractors were used to keep the wound open for surgical access. A schematic of the sciatic nerve and the surrounding musculature and bones is shown in Figure 2.1 below.

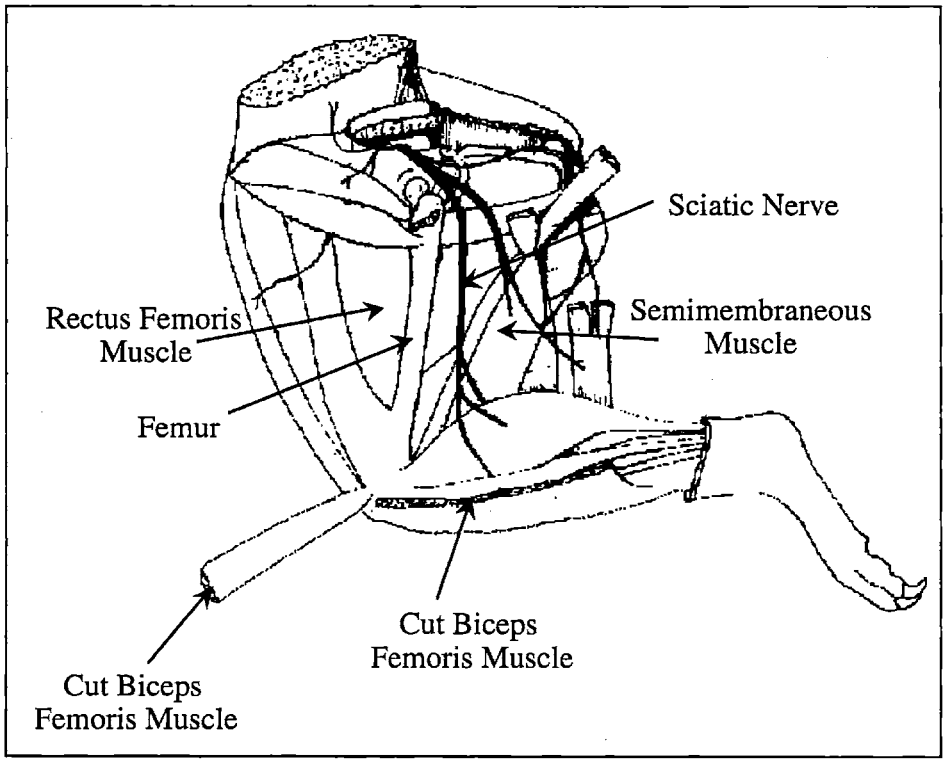

FIGURE 2.1 Anatomical schematic of the musculature of the rat hind leg (adapted from Chamberlain 1998).

Prior to transection, the nerve was locally anesthetized using a few drops of 1% Lidocaine (Abbot Laboratories, North Chicago, IL) dripped directly on the nerve. The

flattened end of a sterile wooden rod was used to elevate the nerve out of the wound. Each nerve was transected using a new #15 scalpel blade. The scalpel blade was drawn in a single motion through the nerve using the flat wooden rod as a cutting surface. Following transection, each nerve stump was marked with a surgical pen at a distance of 4 mm from the transection. This was done to ensure a 4-mm nerve insertion length into each end of the tube.

The silicone tube was placed in the gap and the proximal and distal nerve stumps inserted 4 mm into each end, with a gap between the stumps of the desired length. For the silicone tube in the single-leg model, gap lengths between 6 mm and 16 mm were studied. The error in the gap length at the time of surgery was estimated to be approximately ±1 mm. The nerve was secured to the tube using two 10-0 sutures (Ethicon, Sommerville, NJ) at each end. To the extent possible, the surgeon attempted to place the sutures through the nerve epineurium. Subsequent histological observations indicated that in nearly half of the cases, the sutures penetrated the nerve fascicles and the endoneurium. Each suture was tied with three single knots. Figure 2.2 shows a diagram of a silicone tube with the nerve stumps inserted.

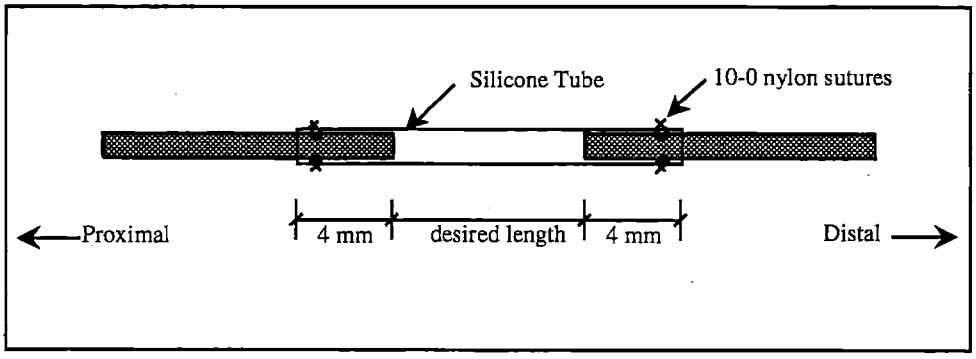

FIGURE 2.2 Diagram showing silicone tube prosthesis after surgical implantation in the rat sciatic nerve.

Following placement of the device, the surgical wound was closed in layers. The musculature was closed using resorbable 4-0 Vicryl sutures (Ethicon, Sommerville, NJ), and the skin wound was closed with steel wound clips (Roboz Surgical, Rockville, MD). Each animal was given a single subcutaneous injection of lactated Ringer's solution (McGaw Inc., Irvine, CA) to compensate for blood volume loss. A numbered ear tag was placed in the left ear of each rat for identification purposes.

Animals were placed in separate cages with warmth provided by a heating pad placed under the cage for the first 24 hours. Thereafter, animals were housed two per cage with wood chip bedding and food and water *ad libitum.* The animals were monitored daily during the first week for the appearance of any abnormal behavior, such as insufficient grooming, lack of appetite and aggressive behavior. Animals were checked twice per week thereafter.

2.2.4 Tissue Allocation and Histological Processing

After 4, 6, 9, or 12 weeks post-operation, rats were sacrificed by carbon dioxide inhalation. The wound site was opened, and the implant device was located. The entire sciatic nerve was removed, including the implant, the proximal stump, and the distal stump with tibial and peroneal branches. Nerve tissue was placed in Yannof's fixative for 24 hours followed by 10 percent formalin for an additional 24 hours before embedding and histological processing. For silicone devices, the tube was cut away from the nerve following fixation and prior to embedding. Nerves were rinsed in 70 percent ethanol, and the gap length of each regenerated nerve was measured as the distance between the nerve

stumps. The nerve stumps were identified by the point at which the diameter of the tissue began to neck down (Figure 2.3).

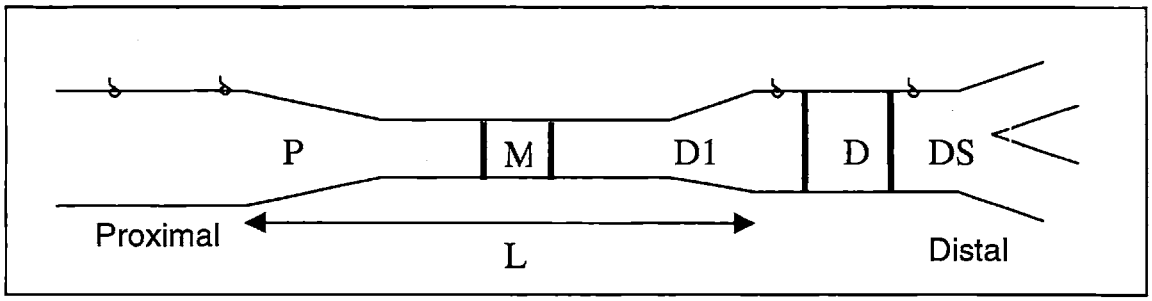

Figure 2.3 Diagram showing the allocation of tissue for Epon embedding and for ethanol storage. Gap length was measured as the distance between the nerve stumps (as identified by reduction in diameter). The sciatic nerve was divided into 5 segments: proximal (P), gap midpoint (M), distal transition (D1), distal (D), and distal stump (DS). Tissues designated M and D were embedded in Epon, sectioned, and stained for myelinated axons. Other tissues (P, D1, and DS) were stored in 70% ethanol for possible future analysis.

Segments of the nerve tissue were allocated for histological processing and ethanol storage as shown in Figure 2.3. A 2-mm segment of tissue from the midpoint of the gap and a 2-mm segment of tissue from the distal nerve stump were allocated for Epon embedding and histological analysis for myelinated axons. The remaining tissue was stored in 70 percent ethanol for possible future histological analysis.

A detailed protocol for toluidine blue staining for myelinated axons can be found in Appendix A. Briefly, to label myelinated axons, tissue segments from the midpoint of the gap and from the distal stump were post-fixed in 1 percent osmium tetroxide (Sigma, St. Louis, MO). The tissue was then dehydrated through graded alcohols and embedded in Epon resin (PolyBed 812, Polysciences Inc., Warrington, PA). Transverse sections were cut at 1 μm and captured on glass microscope slides. Sections were stained with 1

percent toluidine blue solution (toluidine blue O, Fisher Biotech, Boston, MA) and coverslipped with Cytoseal (Stephens Scientific, Riverdale, NJ).

Initial examination of tissue sections was performed with a light microscope (Optiphot, Nikon, Tokyo, Japan). Myelinated axons were identified by examination with 100X objective lens using immersion oil. Initial examination was performed to verify the presence or absence of myelinated axons in the cross section and to examine the general morphology and composition of the tissue. Detailed quantitative analysis of the number of myelinated axons at the gap midpoint and in the distal stump was performed as described below.

2.2.5 Morphometric Evaluation

Quantitative measurement of the number of axons at the gap midpoint and in the distal stump was performed via computerized image analysis of Epon sections. A detailed protocol is located in Appendix A. Digital images (TIFF format) were obtained using a light microscope (Olympus Vanox-T, Olympus, Japan) equipped with a video camera (Hamamatsu CCD Video Camera, Hamamatsu, Japan) and video box (Hamamatsu CCD Camera Control, Hamamatsu, Japan). Images were captured at low magnification (4X objective) to measure the cross-sectional areas of the tissue cables. High magnification images (100X objective), representing 10 percent of the total tissue area, were selected randomly from the nerve cross-section and captured for axon counting.

Computerized stereology software (Scion Image, Scion Corporation, Frederick, MD) was used to analyze digitized images. Scion Image is public domain software and is available for download at http://www.scioncorp.com/pages/scion_image_windows.htm. Myelinated axons in any given image were counted by marking with a single tick mark

from the mouse cursor. Scion Image software contains an automated routine that counts the number of marked axons per digitized image. The density of axons per unit area of each image was calculated, and using this density, the total number of myelinated axons in each nerve was calculated.

2.2.6 Statistical Analysis

In this experiment, the independent variables were nerve gap length and time. The experiment outcome was assessed in terms of 4 measured quantities: 1. percent reinnervation at the gap midpoint, 2. percent reinnervation in the distal nerve stump, 3. number of myelinated axons at the gap midpoint, and 4. number of myelinated axons in the distal nerve stump. Percent reinnervation at the gap midpoint (assay #1) and distal stump (assay #2) were determined as the percentage of animals in a given experimental group in which myelinated axons (more than zero) were identified at the midpoint or distal stump. The number of myelinated axons (assays #3 and #4) was determined by counting the total number of myelinated axons observed at gap midpoint or distal stump.

Two types of data were gathered in this chapter: proportional data and continuous data. Data for percent reinnervation at the gap midpoint or in the distal stump represent proportional data, expressed as the percentage of animals in a given group in which reinnervation was observed. Proportional data were thus bounded between zero and 100 percent. Data for the number of myelinated axons at the gap midpoint or in the distal sump represent continuous data, being quantified for each group as the mean value of a continuous variable, the number of myelinated axons.

Continuous data for any given experimental group were expressed as the arithmetic mean ± standard error of mean (SEM), where the standard error of mean was calculated using the following equation (Daniel, 1995):

$$SEM = \sqrt{\frac{\sum_{i=1}^{n}(X_{mean} - X_i)^2}{n(n-1)}}$$

where X_{mean} is the arithmetic mean of the data set, X_i are the individual data points, and n is the sample size for the group.

Proportional data were expressed as the value of the proportion (usually as a percentage) ± standard error, where the standard error (σ_p) was calculated using the following equation (Daniel, 1995):

$$\sigma_p = \sqrt{\frac{p(1-p)}{n}}$$

where p is the decimal value of the proportion and n is the sample size for the group. The equation above is valid when the sample size is sufficiently large (the quantities np and n(1-p) are both greater than 5). In this thesis, the data did not always meet these criteria, but the equation was still applied as a quantitative estimate of the standard error.

2.2.7 Mathematical Relationship: Regeneration and Gap Length

With the purpose of identifying a mathematical relationship that fits the data for reinnervation and gap length, the proportional data for percent reinnervation at the gap midpoint and in the distal stump were plotted versus gap length and fit to a sigmoidal curve of the form:

$$\%\,\mathrm{Re}innervation = \frac{100}{1+e^{K(L-L_c)}}$$

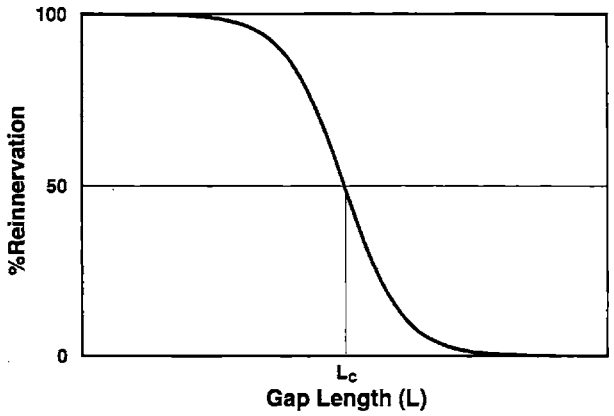

where the percent reinnervation (%Reinnervation) and gap length (L) are experimental data. Nonlinear least-squares regression was used to determine the values of the parameters (K and L_c) of the sigmoidal equation that yielded the best fit to the experimental data. The experimental data were input into Mathematica Software (Wolfram Research Inc., Champaign, IL, www.wolfram.com), and the resulting output included the regression value and standard error for the curve fit parameters (K and L_c) as well as the data necessary to calculate the correlation coefficient (R^2). The slope factor, K, describes the steepness of the decline from 100 to 0 percent reinnervation, and the characteristic length, L_c, describes the gap length at which the curve passes through 50 percent reinnervation. Based on the sigmoidal equation, the parameters K and L_c define the relationship between reinnervation and gap length and may be used as descriptive parameters in evaluating device effectiveness. The nonlinear least squares regression procedure also yielded standard error values associated with the values of K and L_c. In this thesis, K and L_c were expressed as the value resulting from the regression analysis ± standard error.

As a possible alternative to the sigmoidal equation, the proportional data were also fit to a step function between 100% and 0%. The step function was used since, similar to the sigmoidal equation, it would provide a quantitative parameter analogous to the characteristic gap length that would describe the effectiveness of the device. In fitting the experimental data for the silicone tube to the step function, it was noticed that the percent reinnervation data were not well suited for fitting with the step function. In most cases, the experimental data for a given device included only two or three points with values between 0 and 100 percent. With too few intermediate data values between 0 and 100 percent, the step function can be shifted along the gap length axis without changing the quality of the fit to the data (see Figure 2.4). As a result of this ambiguity, fitting the experimental data with the step function does not yield a single quantitative parameter that describes the effectiveness of the device. For the reasons described above, the step function was abandoned as a mathematical model to describe the relationship between reinnervation and gap length and as a means of obtaining values for a quantitative assay.

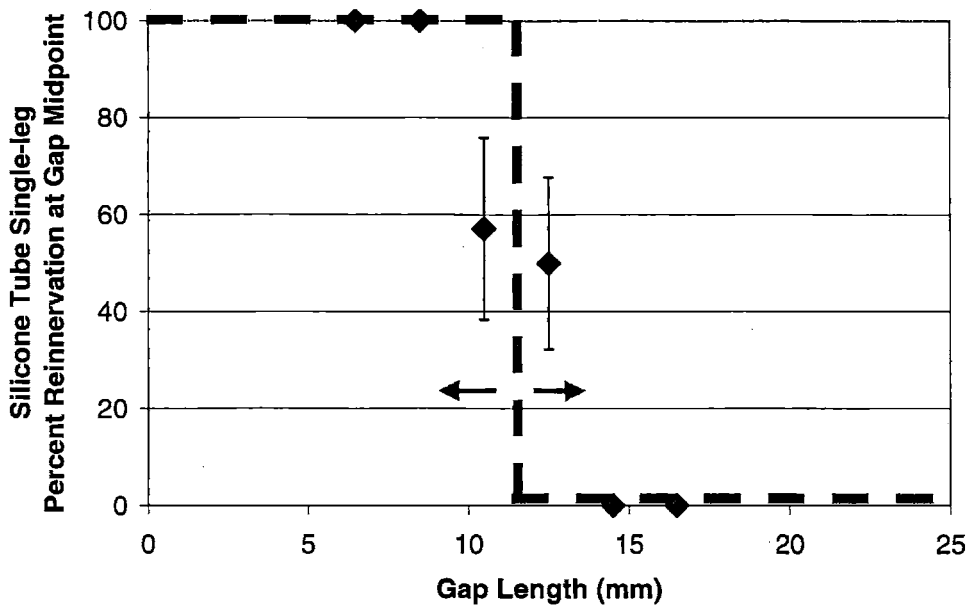

Figure 2.4 Chart showing representative data (♦) for percent reinnervation versus gap length. Also shown is a step function fit to the experimental data (dashed line). The position of the step function along the gap length axis is ambiguous. Since only two of the data points lie between 0 and 100 percent, the step may be positioned anywhere between the two experimental data points without changing the accuracy of the fit. Fitting the data with a step function is therefore non-deterministic and does not yield a single quantitative parameter to describe the effectiveness of a given nerve repair device.

The student's t-test was used in this chapter as well as in chapters 3 and 4 to determine the significance of differences in curve fit parameters (K and L_c) between devices, between nerve repair models, and with time for a given device and model. The criterion for significance was $p<0.05$.

For continuous data (number of myelinated axons at gap midpoint and distal stump), the data were plotted as a function of gap length and time. Two-way ANOVA was performed in order to determine the statistical significant of the effects of gap length and time on myelinated axon number at the gap midpoint and in the distal stump. The

criterion for significance was $p<0.05$. Two-way ANOVA was performed using StatView software (Version 5.0, SAS Institute Inc.).

2.3 Results

2.3.1 General Observations

All animal experimentation protocols described in this thesis were approved by the MIT Committee on Animal Care and the Harvard Medical Area Standing Committee on Animals. A total of 95 rats were implanted with silicone tubes. Two animals died from unknown causes before the scheduled sacrifice. In eight animals, one of the nerve stumps was found at time of sacrifice to have pulled out of the end of the tube. It was apparent that the nerve tissue had pulled through the sutures. These animals were excluded from the study. The total number of animals included in the experiments in this chapter was 85 as indicated in Table 2.1. The rats generally remained in good condition following surgery and throughout the duration of the experiment. The animals maintained the ability to move about the cage and access food and water. The gait of the animals was only slightly impaired.

2.3.2 Assay #1: Percent Reinnervation at Gap Midpoint

The data for reinnervation at the gap midpoint are expressed as the percent of animals in any group in which myelinated axons were identified at the midpoint of the gap. Table 2.2 below shows the data for percent reinnervation at the gap midpoint for all gap lengths and time points included in this chapter.

Gap Length (mm)	4 weeks	6 weeks	9 weeks
6-7 mm	67 ± 19% (4/6)	100 ± 0% (5/5)	
8-9 mm	57 ± 19% (4/7)	100 ± 0% (6/6)	
10-11 mm	20 ± 18% (1/5)	67 ± 19% (4/6)	57 ± 19% (4/7)
12-13 mm	20 ± 18% (1/5)	67 ± 19% (4/6)	50 ± 18% (4/8)
14-15 mm	17 ± 15% (1/6)	0 ± 0% (0/5)	0 ± 0% (0/3)
16-17 mm		0 ± 0% (0/6)	0 ± 0% (0/4)

Table 2.2 Percent of animals in which myelinated axons successfully reached the gap midpoint (silicone tube, single-leg model). Data are given for groups of animals with gap lengths between 6 and 17 mm and time points of 4, 6, and 9 weeks following tube implantation. Data expressed as percent ± standard error. Actual proportion for each group is given in parentheses.

The general trends of the data indicate a decrease in percent reinnervation with increasing gap length. For a given gap length, percent reinnervation tended to increase between 4 and 6 weeks (average 31 percent increase over all gap lengths) with little change between 6 and 9 weeks (average 7 percent decrease over all gap lengths). At smaller gap lengths (less than 10 mm), the percent reinnervation approached or reached saturation at 100% by six weeks. At larger gap lengths (14 mm or greater), the percent reinnervation was at or very near 0% even at 9 weeks after tube implantation. Due to the proportional nature of these data, the values were bounded by a maximum of 100% and a minimum of zero.

In order to define a mathematical relationship between regeneration and gap length, the experimental data were fit to a sigmoidal equation as described in section 2.2.7. Figure 2.5 below shows the results of nonlinear regression fitting of the 4-, 6-, and 9-week experimental data to the sigmoidal equation.

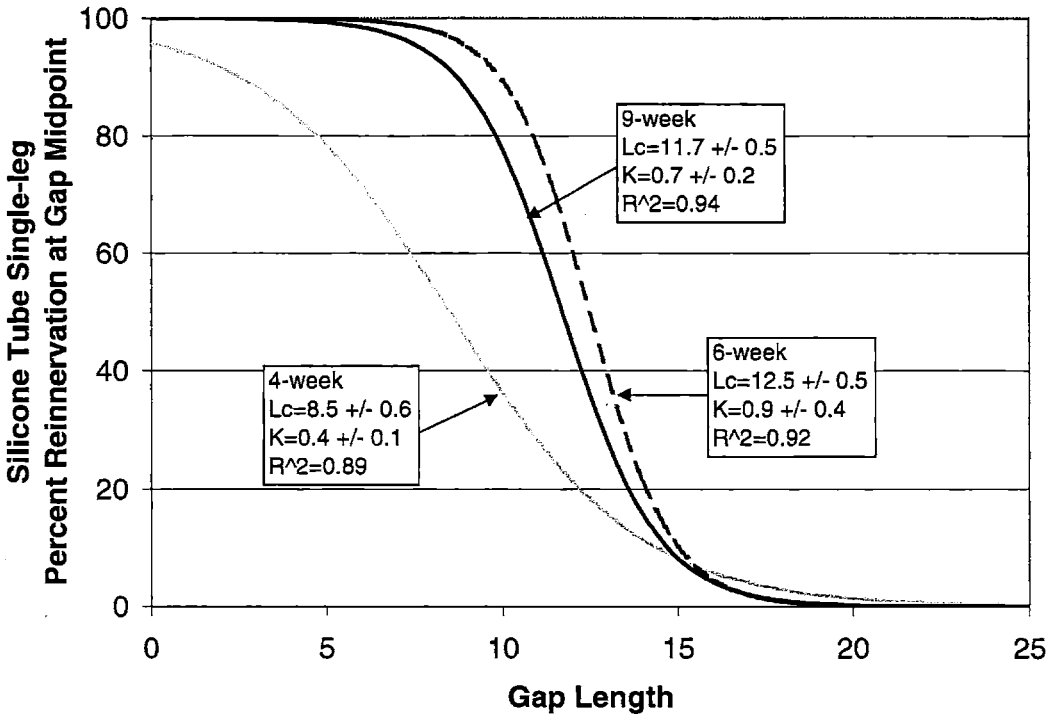

Figure 2.5 Chart showing the nonlinear regression sigmoidal curve fits to the experimental data for percent reinnervation at gap midpoint versus gap length (silicone tube, single-leg model). Curve fitting was performed for the 4-, 6-, and 9-week data separately. For each curve, the values for the curve fit parameters (K and L_c) are indicated along with their associated standard error. The correlation coefficient is also given for each curve.

The experimental data show a high degree of correlation with the sigmoidal model. The smallest correlation coefficient was observed for the 4-week data (R^2=0.89), and the highest correlation coefficient was observed for the 9-week data (R^2=0.94). Changes in the percent reinnervation data with time are apparent as changes in the slope of the sigmoidal curves and their position along the gap length axis. The 6- and 9-week curves had higher slopes and tended to be located further to the right along the gap length axis than the 4-week curve. The most substantial changes were evident between the 4-

and 6-week curves, with comparatively smaller changes between 6 and 9 weeks. Figure 2.6 below plots the changes in the values of L_c and K with time.

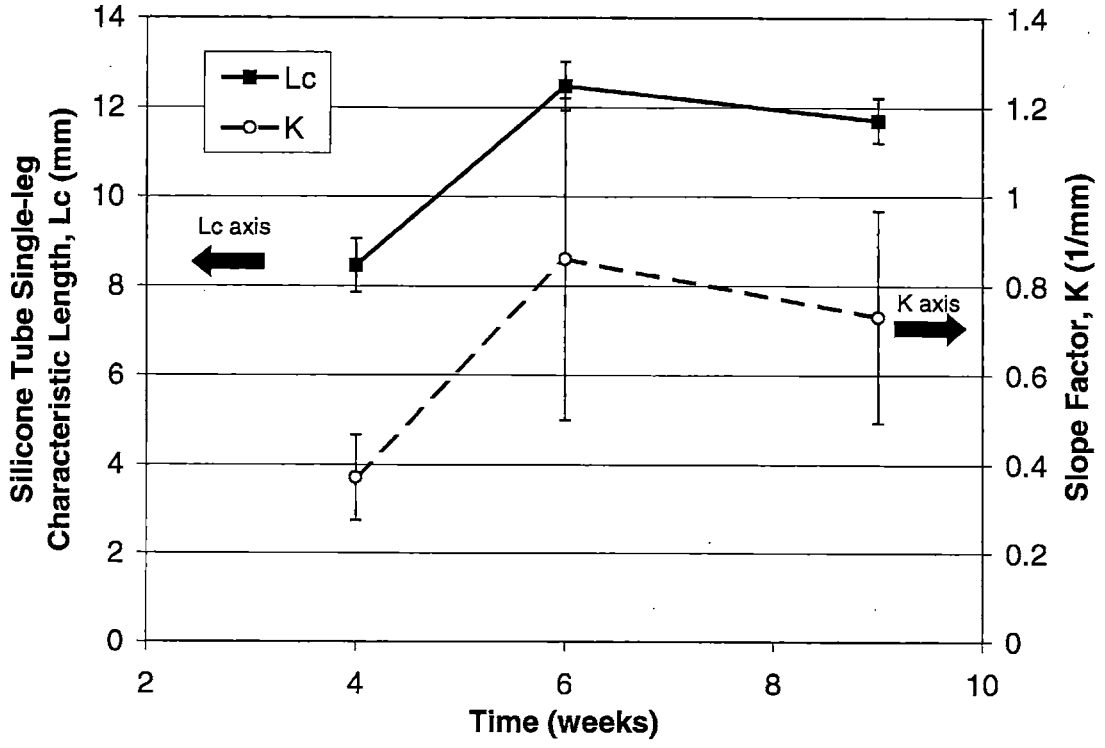

Figure 2.6 Chart showing the changes in characteristic length (L_c) and slope factor (K) between 4, 6, and 9 weeks for the sigmoidal curve fit to data for percent reinnervation at the gap midpoint (silicone tube, single-leg model). Data expressed as the resulting value from nonlinear least squares regression ± standard error.

The data from the sigmoidal curve fit revealed a 47% increase in L_c (statistically significant, $p<0.001$, student's t-test) and a 110% increase in K (not significant, $p>0.05$, student's t-test) between 4 and 6 weeks. Changes between 6 and 9 weeks were comparatively smaller and not statistically significant, with a 6% decrease in L_c (not significant, $p>0.2$) and a 22% decrease in K (not significant, $p>0.5$). The data suggest that the value of L_c has reached an apparent plateau by 6 weeks, with no significant changes

between 6 and 9 weeks. Due to the large uncertainty in the curve fit values for K, differences with time were not statistically significant.

Figure 2.7 below shows the experimental data and the regression curve for the longest-time data gathered in this study. 9-week data were not available at smaller gap lengths (6-7 and 8-9 mm, see Table 2.2). Therefore, 6-week data were included since the percentage values had already reached saturation at 100% by 6 weeks. It was assumed for these two shorter gap lengths that the percent reinnervation values would also be 100% at 9 weeks.

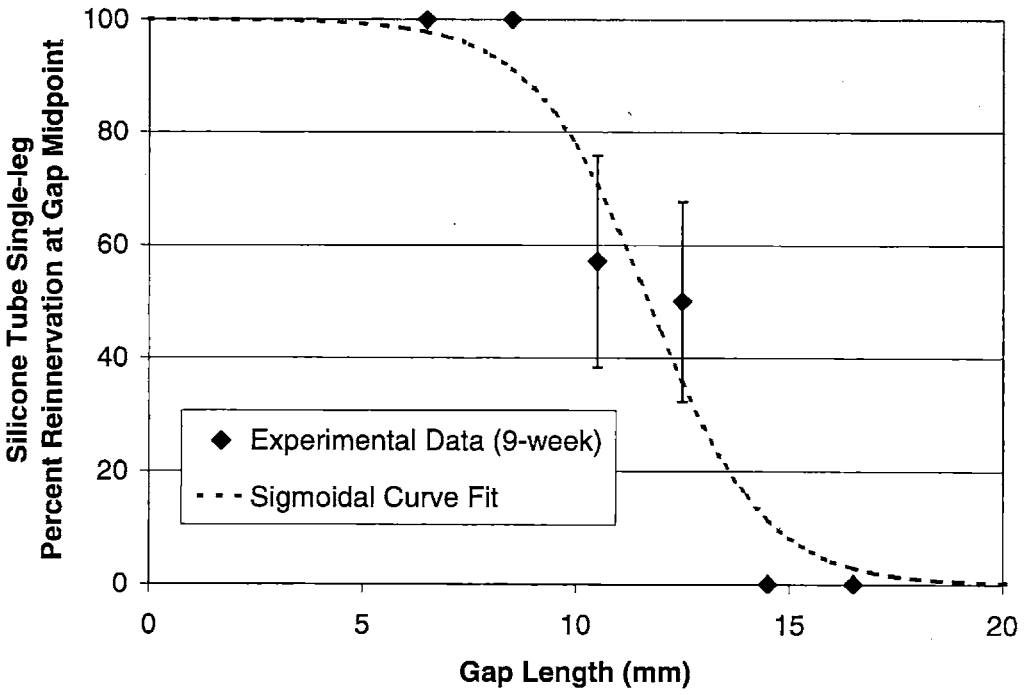

Figure 2.7 Chart showing the longest-time (including both 6- and 9-week) experimental data points for percent reinnervation at the gap midpoint versus gap length and the sigmoidal curve fit (silicone tube, single-leg model). Experimental data expressed as value ± standard error.

The data in Figure 2.7 represent the longest-time data available from this study for reinnervation at the gap midpoint for silicone tube nerve repair in the single-leg model.

The curve closely approximates the experimental data points with a correlation value R^2=0.94. The parameters of the sigmoidal equation that describes the relationship between percent reinnervation and gap length were L_c=11.7 ± 0.5 mm and K=0.7 ± 0.2 mm^{-1}. As discussed in section 2.2.7, the value for the characteristic gap length (L_c) for the silicone tube indicates that the sigmoidal reinnervation curve passes through the 50 percent success level at a gap length of 11.7 mm.

2.3.3 Assay #2: Reinnervation at the Distal Nerve Stump

In addition to measuring reinnervation at the gap midpoint (section 2.3.2 above), reinnervation was also measured in the distal nerve stump. The data for reinnervation in the distal stump are expressed as the percent of animals in any group in which myelinated axons (a non-zero number) were identified in the distal stump. Table 2.3 below shows the data for percent reinnervation at the distal nerve stump for all gap lengths and time points.

Gap Length (mm)	4 weeks	6 weeks	9 weeks
6-7 mm	50 ± 19%	100 ± 0%	
8-9 mm	43 ± 19%	83 ± 15%	
10-11 mm	20 ± 18%	50 ± 20%	57 ± 19%
12-13 mm	0 ± 0%	50 ± 20%	38 ± 17%
14-15 mm	0 ± 0%	0 ± 0%	0 ± 0%
16-17 mm		0 ± 0%	0 ± 0%

Table 2.3 Percent of animals in which any myelinated axons successfully reached the distal nerve stump (silicone tube, single-leg model). Data are given for groups of animals with gap lengths between 6 and 17 mm and time points of 4, 6, and 9 weeks following tube implantation. Data expressed as percent ± standard error. Actual proportion for each group is given in parentheses.

In general, the data for percent reinnervation at the distal nerve stump were similar to those for percent reinnervation at the gap midpoint, showing a decrease in percent reinnervation with increasing gap length and an increase in percent reinnervation with increasing time. For a given gap length, percent reinnervation tended to increase between 4 and 6 weeks (average 34 percent increase) with little change between 6 and 9 weeks (average 1 percent decrease). Percent reinnervation at the distal stump tended to be slightly lower than the percent reinnervation at the gap midpoint (compare Tables 2.2 and 2.3). In the distal stump, only one group (6-week, 6-7 mm gap) showed saturation at the 100% level, while six groups showed 0% reinnervation. Figure 2.8 below shows the results of nonlinear regression fitting of the distal stump experimental data to the sigmoidal curve at 4, 6, and 9 weeks.

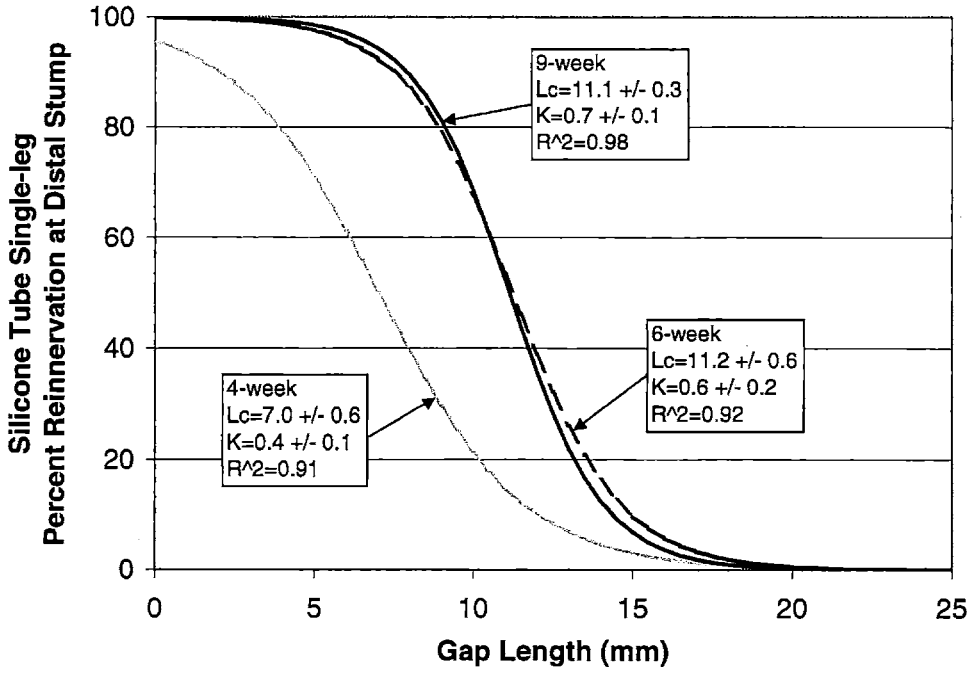

Figure 2.8 Chart showing the nonlinear regression sigmoidal curve fits to the experimental data for percent reinnervation at the distal stump versus gap length (silicone tube, single-leg model). Curve fitting was performed for the 4-, 6-, and 9-week data separately. For each curve, the values for the curve fit parameters (K and L_c) are

indicated along with their associated standard error. The correlation coefficient is also given for each curve.

Similar to the data at the gap midpoint (Figure 2.5), the experimental data at the distal stump (Figure 2.8) show a high degree of correlation with the sigmoidal model. The smallest correlation coefficient was observed for the 4-week data (R^2=0.91), and the highest correlation coefficient was observed for the 9-week data (R^2=0.98). Also similar to the midpoint reinnervation data, the curves and the curve fit parameters for the distal stump underwent substantial changes between 4 and 6 weeks, but relatively smaller changes between 6 and 9 weeks. Figure 2.9 below plots the changes in the values of L_c and K with time.

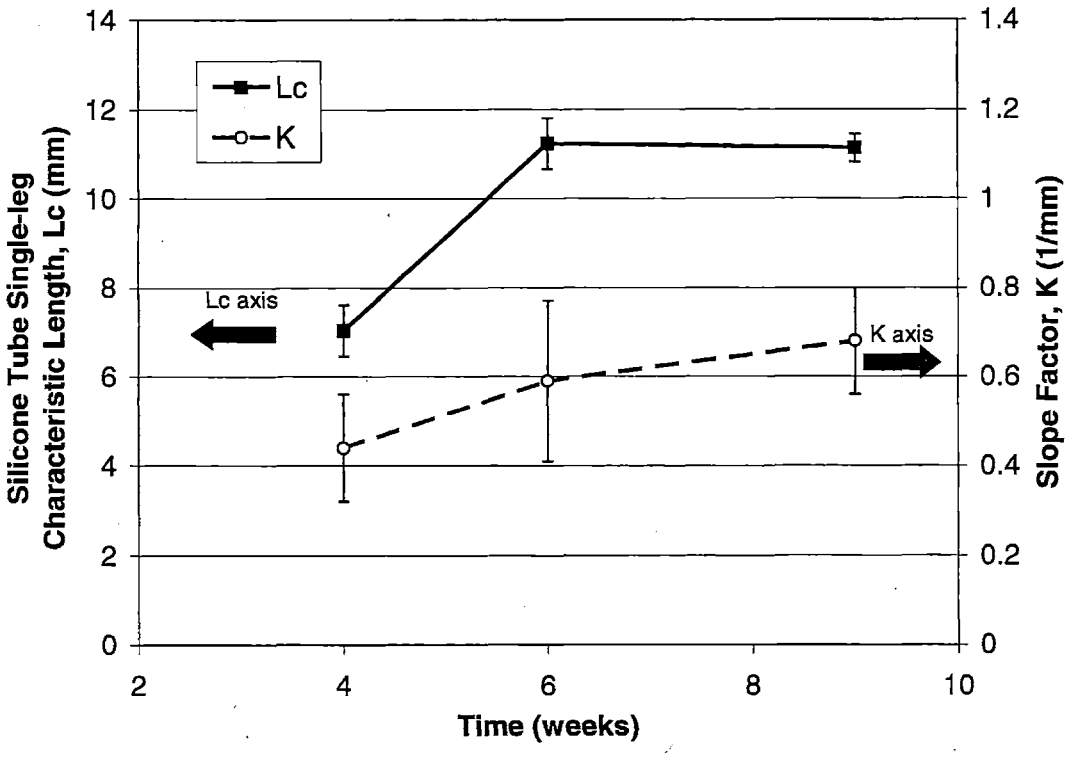

Figure 2.9 Chart showing the changes in characteristic length (L_c) and slope factor (K) between 4 and 9 weeks for the sigmoidal curve fit to data for reinnervation in the distal nerve stump (silicone tube, single-leg model). Data expressed as the resulting value from nonlinear least squares regression ± standard error.

Between 4 and 6 weeks, there was a 60% increase in L_c (statistically significant, $p<0.001$) and a 50% increase in K (not significant, $p>0.2$). Between 6 and 9 weeks, there was only a 1% decrease in L_c (not significant, $p>0.5$) and a 17% increase in K (not significant, $p>0.5$). Similar to L_c for the data at the gap midpoint, L_c for the distal stump reached an apparent plateau after 4 weeks. The values for K increased with time, but due to the large uncertainty, these differences were not statistically significant.

Figure 2.10 below shows the experimental data and the regression curve for the longest-time (including combined data from both 6 and 9 weeks) data at the distal stump. Similar to the data for the gap midpoint, these longest-time data include two data points from 6 weeks (6-7 mm and 8-9 mm gaps).

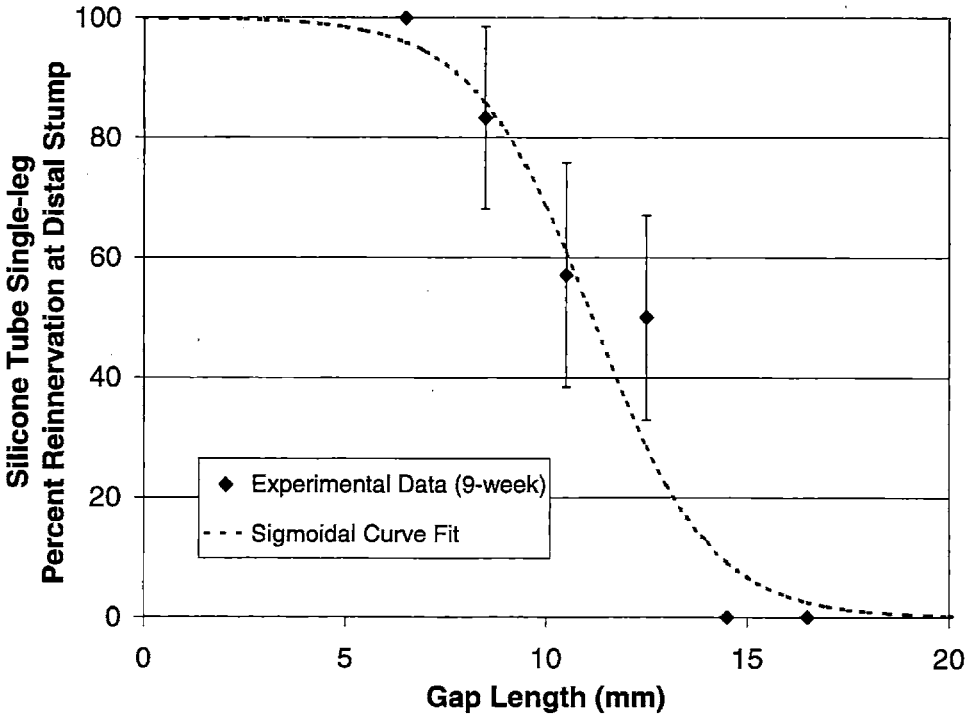

Figure 2.10 Chart showing the longest-time experimental data for percent reinnervation in the distal stump versus gap length and the sigmoidal curve fit (silicone tube, single-leg model). Experimental data expressed as value ± standard error.

The data in Figure 2.10 represent the longest-term data available from this study for reinnervation at the distal stump for silicone tube nerve repair in the single-leg model. The parameters of the sigmoidal equation that describes the relationship between percent reinnervation and gap length were L_c=11.1 ± 0.3 mm and K=0.7 ± 0.1 mm^{-1}. When compared to the curve fit parameters for the data from the gap midpoint, the L_c for the distal stump was 5% smaller, and K was unchanged. The difference in L_c between the midpoint data and the distal stump data was not statistically significant ($p>0.5$).

2.3.4 Assay #3: Number of Myelinated Axons at Gap Midpoint

The previous sections (sections 2.3.2 and 2.3.3) described assays of nerve regeneration based on the percent of animals in a given group in which myelinated axons had reached the gap midpoint or the distal stump (percent reinnervation assay). As an alternative to the percent reinnervation assay, the total number of myelinated axons was also measured at the midpoint (section 2.3.4) and the distal stump (section 2.3.5). The data for the number of myelinated axons at the gap midpoint were expressed as the arithmetic mean ± standard error of mean for all animals in a given experimental group. Figure 2.11 below shows the data for all experimental groups included in this chapter.

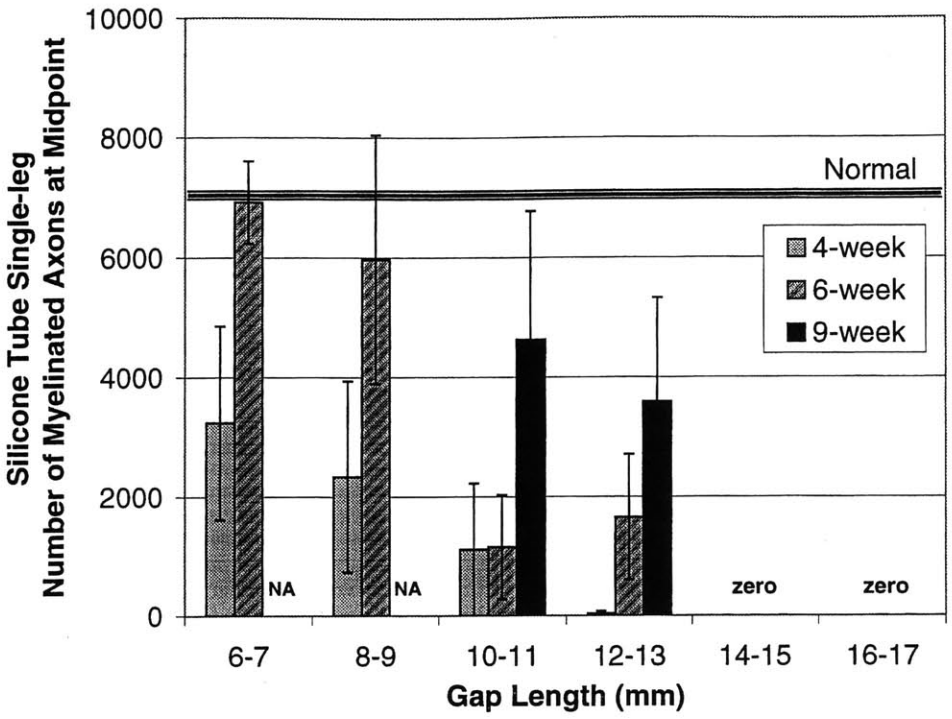

Figure 2.11 Data for number of myelinated axons at the gap midpoint for gap lengths between 6 and 17 mm and time points of 4, 6, and 9 weeks (silicone tube, single-leg model). Data were not available (NA) for the 9-week time point for gap lengths of 6-7 or 8-9 mm. Mean ± SEM.

The number of myelinated axons at the gap midpoint showed a general decreasing trend with increasing gap length for all three time points studied. For large gaps, greater than 13 mm, no axons were identified at the gap midpoint even after 9 weeks. None of the groups exhibited a greater number of myelinated axons than the normal nerve. The number of myelinated axons at the gap midpoint appeared to increase between 4 and 6 weeks as well as between 6 and 9 weeks. In contrast to the percent reinnervation data, the data for axon number did not appear to reach a plateau with time during 9 weeks. Two-factor ANOVA revealed that the number of myelinated axons at the gap midpoint was significantly affected by gap length ($p<0.01$) and time ($p<0.05$).

2.3.5 Assay #4: Number of Myelinated Axons in Distal Nerve Stump

In addition to the counting the number of myelinated axons at the gap midpoint, the number of myelinated axons in the distal nerve stump was also determined for each experimental group. The data for the number of myelinated axons in the distal nerve stump were expressed as the arithmetic mean value ± standard error of mean for all experimental groups. Figure 2.12 below shows the data for myelinated axons in the distal stump.

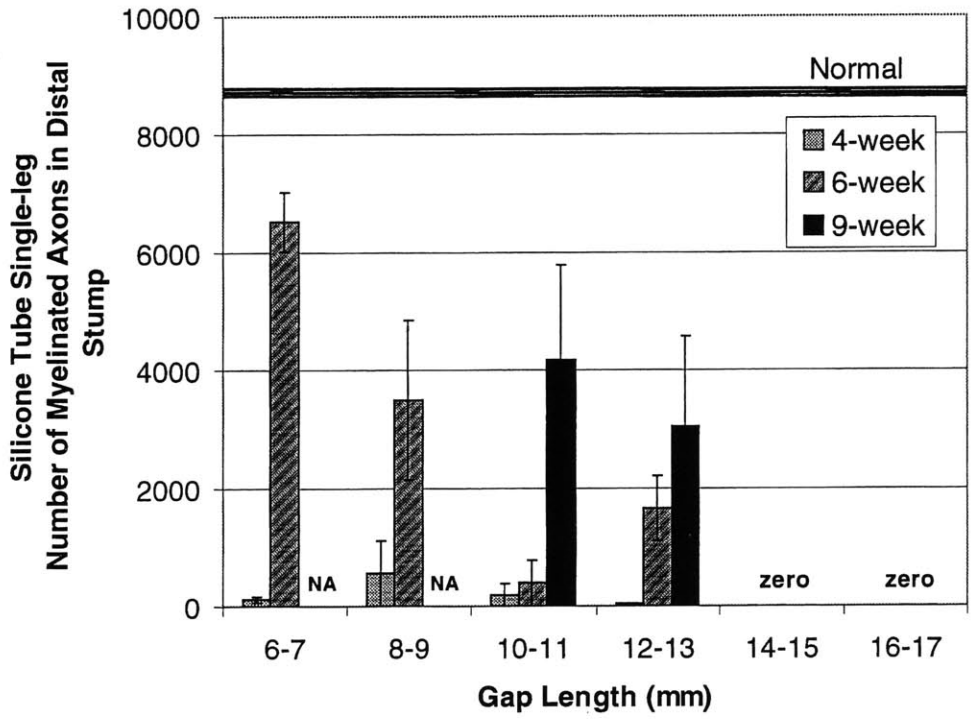

Figure 2.12 Data for number of myelinated axons in the distal nerve stump for gap lengths between 6 and 17 mm and time points of 4, 6, and 9 weeks (silicone tube, single-leg model). Data were not available (NA) for the 9-week time point for gap lengths of 6-7 or 8-9 mm. Mean ± SEM.

The data for myelinated axons in the distal nerve stump showed similar general trends to the data at the gap midpoint in which axon number tended to decrease

with increasing gap length, and axon number tended to increase with increasing time. For each experimental group, the mean number of myelinated axons in the distal stump was smaller than the mean number of myelinated axons at the gap midpoint. The number of myelinated axons in the distal stump tended to be very small (less than 1,000) for all gap lengths at the 4-week time point. This may be due to the fact that many axons may have not been able to traverse the entire length of the gap by four weeks. None of the groups contained a number of myelinated axons at the gap midpoint that was greater than that of the normal uninjured nerve. ANOVA revealed that the number of myelinated axons at the gap midpoint was significantly affected by gap length ($p<0.05$) and time ($p<0.01$).

2.4 Discussion

The study by Lundborg et al. (Lundborg et al., 1982) provided an initial description of the relationship between nerve regeneration and gap length for the silicone tube device in the cross-anastomosis model. Although the experiments in this chapter were performed using the single-leg nerve repair model, it was expected that our results would be similar to those of the Lundborg group. It was expected that regeneration would decrease with increasing gap length, and that a characteristic length would exist above which regeneration was not likely to occur. In the Lundborg study, regeneration was studied only at 4 weeks after injury. The experiments in this chapter examined regeneration at 4, 6, and 9 weeks. An additional goal of this study was to compare a number of different nerve regeneration assays with the purpose of identifying a preferred assay to rank-order nerve repair devices. Each of these topics is addressed below.

2.4.1 Relationship between Regeneration and Gap Length: Sigmoidal Equation

For the percent reinnervation data, the relationship between regeneration and gap length was described using the sigmoidal equation. The percent reinnervation data were well suited for analysis using the sigmoidal equation, being bounded between 100% and 0%. One benefit of fitting the experimental data with the sigmoidal equation is a well-defined mathematical description of the relationship between regeneration and gap length. The sigmoidal equation accurately fit the experimental data at both the gap midpoint and in the distal stump. The correlation coefficients for the nonlinear regression curve fits ranged between 0.89 and 0.98. The highest correlation coefficients were observed for the 9-week data at the gap midpoint (R^2=0.94) and in the distal stump (R^2=0.98).

An additional benefit of using the sigmoidal equation is the determination of the characteristic length by the least squares regression analysis. The data in this chapter were used to determine L_c for the silicone tube device. A similar procedure may be used to determine L_c for any given nerve repair device. The characteristic length has potential use as a single quantitative parameter that describes the effectiveness of a given device for peripheral nerve repair.

2.4.2 Alternative to the Sigmoidal Equation: Step Function

As described in section 2.2.7, the step function was examined as an alternative mathematical model to describe the relationship between reinnervation and gap length. This model was chosen since it would provide a quantitative measure of regeneration similar to the characteristic gap length. It was considered possible that the step function

might provide a more accurate fit than the sigmoidal equation to the experimental data. However, when applied to actual data resulting from the experiments in this chapter, it was apparent that the exact placement of the step along the gap length axis was not uniquely defined by the data (see Figure 2.4). The step function was therefore not suitable for the purposes of defining an assay and obtaining a single parameter to describe device effectiveness.

It is interesting to speculate that the nature of the relationship between nerve regeneration and gap length may reflect the nature of the physiological processes responsible for regeneration. For example, a set of experimental reinnervation data that closely resemble the form of a step function may suggest that nerve regeneration may be described as an "all or nothing" process. Step-shaped data would indicate that regeneration occurs when the nerve gap length is smaller than a strict cutoff and does not occur when the gap length is larger than the cutoff. The cutoff gap length may reflect a maximum distance across which bridging support cells and axons are able to successfully migrate. An alternative explanation of the step function shape is the possibility that nerve regeneration is inhibited by contraction and encapsulation of the nerve stumps. Above the cutoff gap length, each of the cut nerve stumps may heal separately, undergoing contraction and encapsulation without any contact with the opposite nerve stump. The result of this process would be neuroma formation without forming a tissue bridge between the stumps. This contraction theory is supported by previous findings in this laboratory in which contractile cells were identified in healing peripheral nerves (Chamberlain, 1998, Chamberlain et al., 1998, Chamberlain et al., 2000).

In contrast, experimental data for reinnervation versus gap length that exhibit a more gradual transition between 100 and 0 percent success may hypothetically suggest that a different subset of physiological processes may be important. A gradual decrease in reinnervation with gap length may reflect the possibility that regeneration is influenced by diffusion of growth factors or soluble agents that are chemo-attractant for axons or support cells. The concentration of soluble factors in the nerve gap would be expected to decrease with increasing gap length. The shape of the reinnervation curve may reflect the gradient in concentration of such factors.

2.4.3 Changes with Time: Time Independence

The results of this chapter revealed that changes in the regenerative outcome occurred between 4 and 9 weeks as indicated by all four assays of regeneration. In general, the percent reinnervation and axon number increased with time at both the gap midpoint and the distal stump. Increases in percent reinnervation and axon number were expected since axon sprouting and elongation have been shown to continue up to 30 weeks after injury (Chamberlain, 1998).

The assays based on continuous data (number of myelinated axons) tended to increase in both time periods, between 4 and 6 weeks and between 6 and 9 weeks (Figures 2.11 and 2.12), while the assays based on proportional data (percent reinnervation) tended to increase between 4 and 6 weeks but showed little or no change between 6 and 9 weeks (tables 2.2 and 2.3). Significant changes in the shapes of the sigmoidal curves were also apparent between 4 and 6 weeks, but not between 6 and 9 weeks (Figures 2.5 and 2.8). Changes were also evident in the curve fit parameters. Values of the L_c exhibited statistically significant changes between 4 and 6 weeks at the

gap midpoint ($p<0.001$) and also in the distal stump ($p<0.001$). However, changes in L_c between 6 and 9 weeks were not statistically significant ($p>0.2$). The value of K did not significantly change between 6 and 9 weeks for either the midpoint or distal stump data ($p>0.05$). Together, these data suggest that the proportional data have reached a plateau with time by 6 weeks. Being bounded by a maximum of 100% and a minimum of 0%, the values for percent reinnervation can only vary over a confined range. It is therefore not surprising that a plateau has been reached for these data by 6 weeks. In contrast, the continuous data for axon number at the gap midpoint and in the distal stump did not reach a plateau with time, increasing between 4 and 6 weeks and between 6 and 9 weeks (Figures 2.11 and 2.12). It was not expected that axon number would reach a plateau since previous studies in this laboratory indicated that the number of axons at the gap midpoint and distal stump increased up to 30 weeks following injury (Chamberlain, 1998).

One goal of the experiments in this chapter was to describe the relationship between regeneration and gap length using time-independent data. It appears that a plateau had been reached by 6 weeks in percent reinnervation at the gap midpoint and in the distal stump. The 9-week values for L_c and K can be considered to be time-independent. As parameters of the 9-week sigmoidal curve, L_c and K describe the ability of the silicone tube device to promote regeneration across nerve gaps of various lengths.

2.4.4 The Characteristic Gap Length

The Lundborg study of silicone tube nerve repair indicated that a decrease in reinnervation at the gap midpoint occurred at a gap length between 10 and 15 mm. The Lundborg data were gathered 4 weeks after injury using the cross-anastomosis model. It

can be concluded that the characteristic gap length for the Lundborg data would lie between 10 and 15 mm. Analysis of the 4-week data in this chapter identified the characteristic gap length for silicone tube nerve repair (single-leg model) as $L_c = 8.5 \pm 0.6$ mm for reinnervation at the gap midpoint. This value is somewhat smaller than what would be expected based on Lundborg's results. The difference between the results in this chapter and those of Lundborg may be due to differences between the single-leg and the cross-anastomosis models. The differences between models will be addressed in detail in chapter 3. Although the 4-week characteristic gap length from this chapter does not agree with the findings of Lundborg et al., the characteristic gap lengths for the 6- and 9-week data are within the range predicted by Lundborg, having values of 12.5 ± 0.5 mm and 11.7 ± 0.5 mm respectively.

2.4.5 Comparison of Assays

The four assays of nerve regeneration used in this chapter were: 1. percent reinnervation at the gap midpoint, 2. percent reinnervation in the distal stump, 3. number of myelinated axons at the gap midpoint, and 4. number of myelinated axons in the distal stump. Since all 4 assays depended on the presence of myelinated axons, it is not surprising that the assays yielded somewhat similar results. In this chapter, the four assays were compared with the purpose of identifying a single assay that can be used in short-term studies to quantify the effectiveness of a given nerve repair device.

For both assays in which percent reinnervation and axon number were measured, there were differences between data at the gap midpoint and the data from the distal stump. Percent reinnervation at the gap midpoint tended to be slightly higher than percent reinnervation in the distal stump (6.5% higher, averaged over all gap lengths and times).

Similarly, the number of myelinated axons tended to be higher at the gap midpoint than in the distal stump (33% higher averaged over all gap lengths and times). These differences are likely explained by the possibility that many axons that have elongated to the gap midpoint have not reached the distal stump. In the context of selecting a short-term assay to measure device effectiveness, the assays at the gap midpoint would be preferable since elongating axons reach the gap midpoint earlier than the distal stump. Percent reinnervation data could therefore be gathered earlier at the gap midpoint than in the distal stump.

As discussed in section 2.4.3 the percent reinnervation data and the associated sigmoidal curve parameters reached an apparent time-independent state by 6 weeks. However, the data for axon number increased without a plateau up to 9 weeks. Time independent data would be preferred for an assay for device effectiveness. For this reason the assays based on percent reinnervation would be favorable above of the assays based on axon number. On the basis of the discussion above, it is apparent that the assay based on percent reinnervation at the gap midpoint is best suited for evaluating device effectiveness in short-term studies.

2.4.6 Significance of Findings

The study by Lundborg et al. provided the initial description of the effect of gap length on peripheral nerve regeneration (Lundborg et al., 1982). In the Lundborg study, nerve regeneration was assessed across gap lengths of 6, 10, 15, and 20 mm at 4 weeks after injury. The data in this chapter expanded upon the Lundborg data in the following ways: 1. using nerve gap lengths in 2-mm increments to more accurately describe the relationship between regeneration and gap length, 2. fitting the experimental data to a

mathematical equation that describes this relationship, 3. determining the change in the relationship with time, and 4. defining the relationship in a time-independent state. Based on the time-independent data for percent reinnervation versus gap length at the gap midpoint, the characteristic length was determined for the silicone tube (L_c=11.7 ± 0.5 mm).

The value of the characteristic gap length for the silicone tube indicates that myelinated axons would hypothetically grow to the gap midpoint in approximately 50 percent of animals with 11.7-mm gaps repaired with silicone tubes. It is important to note that the value of characteristic gap length does not suggest that the silicone tube is appropriate for repairing nerve gaps of the characteristic length. In fact, reinnervation would not occur in 50 percent of animals with nerve gaps equal to the characteristic length, a result that would be unacceptable in the clinic. However, the value of the characteristic gap length represents a quantitative parameter by which the silicone tube may be compared with other nerve repair devices.

In terms of selecting a short-term assay for the evaluation of nerve repair devices, the data presented in this chapter suggest that an assay based on percent reinnervation at the gap midpoint is most useful. Reinnervation at the midpoint was chosen in preference to reinnervation at the distal stump on the assumption that elongating axons would reach the midpoint at earlier times than the distal stump, and thus the midpoint data would reach a time-independent state before the distal stump data. The midpoint data reached an apparent time-independent state after 6 weeks, and when fitted to the sigmoidal equation, they yield the characteristic length (L_c). The characteristic length can be considered to be a single quantitative parameter that describes the effectiveness of a given nerve repair

device in promoting nerve regeneration across gaps of various lengths. The characteristic length therefore has potential use for comparing various nerve repair devices based on effectiveness.

Chapter 3: Comparison of Single-leg and Cross-anastomosis Models

3.1 Introduction

3.1.1 Single-leg and Cross-anastomosis Models of Nerve Repair

The experiments in chapter 2 described the regeneration of sciatic nerves repaired with silicone tubes in the single-leg nerve repair model. The single-leg model in the rat is the most commonly used model for experimental research and is an accepted standard. However, as described in section 1.4.3, the single-leg model is limited in the length of nerve gaps that can be accommodated by the size of the animal. The length of the femur of the adult Lewis rat limits the length of a nerve gap in the single-leg model to a maximum of 15 mm. For this reason, the cross-anastomosis model is necessary if an investigator wishes to study nerve regeneration across gaps larger than 15 mm using an experimental model with animal subjects (rats) of the same species, strain, and age. The study of larger gap lengths may be desirable in the study of nerve repair devices for two reasons. First, nerve gaps in the clinic are often larger than 15 mm. Second, larger gap lengths represent a more stringent test of a nerve repair. Differences in effectiveness among competing devices may become apparent when the devices are tested in longer gap lengths as opposed to shorter lengths. Only a small number of investigators have employed the cross-anastomosis model (Lundborg et al., 1982, Yannas et al., 1985, Yannas et al., 1987), and there is a need to characterize this model. One purpose of the studies described in this chapter was to compare nerve regeneration outcomes in the single-leg model with those in the cross-anastomosis model.

3.1.2 Specific Aims

In chapter 2, four assays of nerve regeneration were compared. The results suggest that an assay based on time-independent percent reinnervation data at the gap midpoint can be used to evaluate the effectiveness of a nerve repair device in a short-term (9-week) study. Nonlinear regression fitting of the experimental data to the sigmoidal equation yielded a single quantitative parameter (the characteristic length) that can be used to quantify device effectiveness. The end-result of these experiments was the determination of the characteristic length for the silicone tube device in the single-leg model.

For the experiments described in chapter 3, four assays of regeneration (identical to those used in chapter 2) were used to evaluate nerve regeneration through silicone tubes in the cross-anastomosis model. The assays included: 1. percent reinnervation at midpoint, 2. percent reinnervation at distal stump, 3. the numbers of myelinated axons at the gap midpoint, and 4. the number of myelinated axons in the distal stump One goal of these experiments was to determine if an assay based on the sigmoidal curve could be applied to nerve regeneration data from the cross-anastomosis model.

The specific aims of the experiments in chapter 3 were: 1. to investigate the use of the sigmoidal equation to describe the relationship between regeneration and gap length in the cross-anastomosis model, 2. to use the sigmoidal equation to determine the characteristic length for the silicone tube in the cross-anastomosis model, 3. to compare regeneration in the single-leg and cross-anastomosis models with the same device (the silicone tube).

To accomplish the specific aims, the experimental design of chapter 3 was similar to that for the experiments in chapter 2. Groups of animals were implanted with saline-filled silicone tubes connecting the proximal sciatic nerve stump from the left hind leg to the distal sciatic nerve stump from the right hind limb (cross-anastomosis model, see Figure 1.3). At 4, 6, and 9 weeks after injury, nerve regeneration for each gap length was evaluated based on the four metrics described previously (sections 2.1.1 and 2.2.6). Similar to chapter 2, nerve regeneration, as measured by each of the four assays, was compared with the purpose of establishing an assay that could be used in short-term experiments to quantitatively measure device effectiveness. The data from the experiment were interpreted based on the predictions and hypotheses below.

It was expected that the results would be similar to those of chapter 2. The comparison of assays would lead to the conclusion that the data based on percent reinnervation would be reach a time-independent state before 9 weeks, and would be best choice for a short-term assay. It was expected that the data based on the number of myelinated axons would not reach a plateau with time. Based on sigmoidal curve fit analysis of the percent reinnervation data, we also expected that the characteristic length for the silicone tube in the cross-anastomosis model would be similar to the characteristic length for the silicone tube in the single-leg model.

3.2 Materials and Methods

The materials and methods for the experiments described in this chapter were similar to those for chapter 2, as described in section 2.2. Detailed protocols for many procedures can be found in Appendix A.

3.2.1 Experimental Configuration

The purpose of work described in this chapter was to examine silicone tube nerve repair using the cross-anastomosis model and to compare the results to the single-leg model (chapter 2). In this chapter, four assays were used to assess nerve regeneration across various gap lengths in rat sciatic nerves repaired with silicone tubes using the cross-anastomosis model. Table 3.1 below shows the various gap lengths and time points that were studied. Each cell of the table indicates the number of animals that were included in each experimental group.

Gap Length (mm)	4 weeks	6 weeks	9 weeks
4-5 mm	n=1	n=4	n=6
6-7 mm	n=2	n=5	n=6
8-9 mm	n=4	n=3	n=4
10-11 mm	n=1		n=3
14-15 mm			n=3

Table 3.1 Experimental groups for silicone tube nerve repair in the cross-anastomosis model

It is recognized that the number of animals was small for certain groups, especially at the early 4-week time point. One reason for the smaller number of animals was an unexpectedly high mortality rate following the cross-anastomosis repair procedure. The post-operative mortality rate for the cross-anastomosis procedure was 20 percent compared with only 2 percent for the single-leg procedure (see also section 3.3.1). The cross-anastomosis surgical procedure involves significantly greater trauma than the single-leg procedure, and the increase in mortality was not surprising. Attempts were made to compensate for the animal deaths by increasing the number of animals in

the 9-week groups. Based on the results of chapter 2, the 9-week data were most likely to be time-independent, and in this chapter emphasis was placed on gathering high quality data at the 9-week time point.

The range of gap lengths was initially chosen based both on the results of the experiments in chapter 2 and on the results of previous studies by Lundborg et al. (Lundborg et al., 1982). The original experimental design included gap lengths ranging between 6 and 16 mm in length, similar to the single leg model in chapter 2 (Table 2.1). However, it was apparent from results of the first animals with 6-mm nerve gaps in the cross-anastomosis model that 100 percent reinnervation was not reached. It was necessary to add additional animal groups in the 4-5 mm gap length range in order to achieve data at 100 percent reinnervation. These groups are shown in Table 3.1. Consistent with chapter 2, time periods of 4, 6, and 9 weeks were chosen in this chapter.

3.2.2 Animal Model: Cross-anastomosis Repair

For the experiments in this chapter, the implant devices (silicone tubes) as well as the size and strain of the experimental rats were identical to those described in section 2.2.2. The surgical procedure for the cross-anastomosis model differed significantly from that for the single-leg model as described below.

For the cross-anastomosis nerve repair procedures, all surgeries were performed to bridge the proximal stump of the left sciatic nerve over the back of the animal to connect with the distal stump of the right sciatic nerve. A detailed description of the surgical procedure can be found in Appendix A. A single incision was made through the skin starting near the left ankle, continuing over the back of the animal, and ending near the right ankle. The left sciatic nerve was exposed first by separating the *biceps femoris*

muscle. The left nerve was transected just proximal to the bifurcation of the tibial and peroneal branches using the procedure described in section 2.2.3. The right sciatic nerve was similarly exposed, but transected as far proximal as possible, just distal to the sciatic notch. Thus, the left sciatic nerve was transected as far distal as possible, and the right sciatic nerve was transected as far proximal as possible. This was done in order to provide the greatest possible length of nerve tissue for routing the bridged nerve over the back of the animal.

Following transection of both left and right nerves, the muscle and connective tissue overlying the lumbar spine were separated using a scalpel blade. The dorsal portion (spinous process) of the sixth lumbar vertebra was removed using bone rongeurs. Using a scalpel blade and scissors, a continuous trough was created in the muscle and connective tissue across the back of the animal connecting the surgical wound in the left hind limb to the surgical wound in the right hind limb. The proximal stump of the left sciatic nerve was gently elevated using fine forceps and placed in the trough over the back until the left nerve stump was located the desired distance away from the distal right nerve stump.

The silicone tube was placed in the gap and the proximal left and distal right nerve stumps inserted 4 mm into opposing ends, with a gap between the stumps of the desired length. For the experiments in this chapter, gap lengths between 4 mm and 14 mm were studied. Similar to the single-leg repair procedure, the error in the gap length at the time of surgery for the cross-anastomosis procedure was estimated to be approximately ± 1 mm. Each nerve stump was secured in the tube using two 10-0 sutures (Ethicon, Sommerville, NJ) at each end as described in section 2.2.3. The wound was

closed in layers, and the animals given post-operative care and housing as described previously.

3.2.3 Tissue Allocation, Histological Processing, and Morphometric Evaluation

Nerve tissue was harvested and processed for histology according to the procedures described in chapter 2. Morphometric data were gathered from Epon-embedded sections as previously described. Detailed protocols for experimental procedures can be found in
Appendix A.

3.2.4 Statistical Analysis and Sigmoidal Curve Fit

Statistical analysis of the data was performed as described in section section 2.2.6. The proportional data (percent reinnervation at the gap midpoint and at the distal stump) were fit to the sigmoidal equation as described in section 2.2.7.

3.3 Results

3.3.1 General Observations

For the experiments examining silicone tube nerve repair in the cross-anastomosis model (chapter 3), a total of 56 rats were implanted with silicone tubes. Eleven animals died from unknown causes before the scheduled sacrifice, resulting in a mortality rate of 20 percent. This mortality was substantially higher than the 2 percent mortality rate for the single-leg nerve repair model (section 2.3.1). It was likely that the additional trauma associated with the cross-anastomosis procedure was responsible for the increase in

mortality. Pullout of the nerve stump from the tube end was observed in only one animal with the cross-anastomosis procedure. One rat exhibited signs of infection at the wound site. At time of sacrifice, the tissue surrounding the implanted tube appeared necrotic. The tube itself was filled with opaque purulent fluid. This animal was excluded from the study.

Excluding the 11 animals with premature death, the single animal with nerve pullout, and the single animal with infection, the total number of animals included in the experiments in this chapter was 43 (see Table 3.1). The rats generally remained in good condition following surgery and throughout the duration of the experiment. The animals maintained the ability to move about the cage and access food and water. Since both the left and right sciatic nerves were transected during the cross-anastomosis procedure, the impairment for the animals was slightly greater than the single-leg model in chapter 2.

3.3.2 Assay #1: Percent Reinnervation at Gap Midpoint

The data for reinnervation at the gap midpoint for the cross-anastomosis model were expressed as the percent of animals in any group in which myelinated axons were identified at the midpoint of the gap. Table 3.2 below shows the data for percent reinnervation at the gap midpoint for all gap lengths and time points included in this chapter.

Gap Length (mm)	4 weeks	6 weeks	9 weeks
4-5 mm	100 ± 0% (1/1)	100 ± 0% (4/4)	100 ± 0% (6/6)
6-7 mm	50 ± 35% (1/2)	80 ± 18% (4/5)	83± 15% (5/6)
8-9 mm	25 ± 22% (1/4)	33 ± 27% (1/3)	25 ± 22% (1/4)
10-11 mm	0 ± 0% (0/1)		0 ± 0% (0/3)
14-15 mm			0 ± 0% (0/4)

Table 3.2 Percent of animals in which myelinated axons successfully reached the gap midpoint (silicone tube, cross-anastomosis model). Data are given for groups of animals with gap lengths between 4 and 15 mm and time points of 4, 6, and 9 weeks following tube implantation. Data expressed as percent ± standard error. Actual proportion for each group is given in parentheses.

The nature of data for the silicone tube in the cross-anastomosis model (table 3.2) was similar to that of the silicone tube data in the single-leg model (table 2.2). The same general trend of decreasing percent reinnervation with increasing gap length was observed. For the cross-anastomosis data, 100% reinnervation was observed at all three time points for the shortest gaps (4-5 mm), but not for any of the larger gaps (6-7 mm or larger). This differed slightly from the data for the single-leg model in which 100% reinnervation was observed at somewhat larger gap lengths (6-7 mm and 8-9 mm). In general, percent reinnervation for the cross-anastomosis model tended to be lower than percent reinnervation for the single-leg model for equivalent gap lengths and times.

Similar to the procedures used in chapter 2 (section 2.2.6), the experimental data for percent reinnervation were fit to the sigmoidal equation. Figure 3.1 below shows the results of nonlinear regression fitting of the 4-, 6-, and 9-week experimental data to the sigmoidal equation.

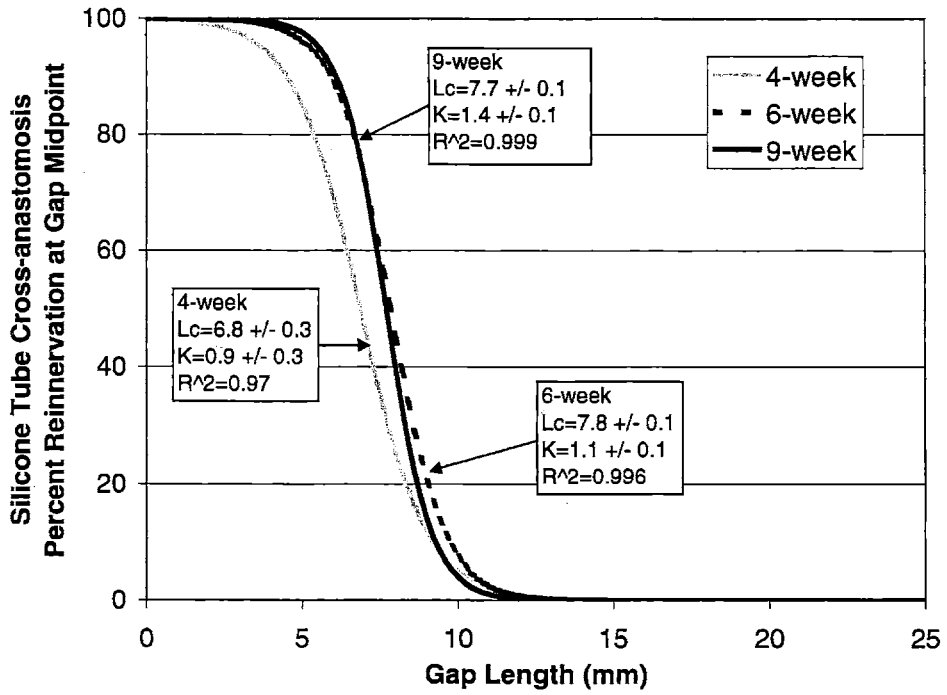

Figure 3.1 Chart showing the nonlinear regression sigmoidal curve fits to the experimental data for percent reinnervation at gap midpoint versus gap length (silicone tube, cross-anastomosis model). Curve fitting was performed for the 4-, 6-, and 9-week data separately. For each curve, the values for the curve fit parameters (K and L_c) are indicated along with their associated standard error. The correlation coefficient is also given for each curve.

Similar to the data for the single-leg model (Figure 2.5), the experimental data for the cross-anastomosis model showed a high degree of correlation with the sigmoidal equation. The correlation coefficients ranged between R^2=0.97 for the 4-week data and R^2=0.999 for the 9-week data. Also similar to the single-leg data, the curves exhibited a subtle transition in shape and location along the gap length axis with time between 4 and 9 weeks. The steepness of the curves increased with increasing time, and the position of the curve along length axis tended to shift toward larger gap lengths with increasing time. Figure 3.2 below plots the changes in the values of the characteristic length (L_c) and the slope factor (K) with time.

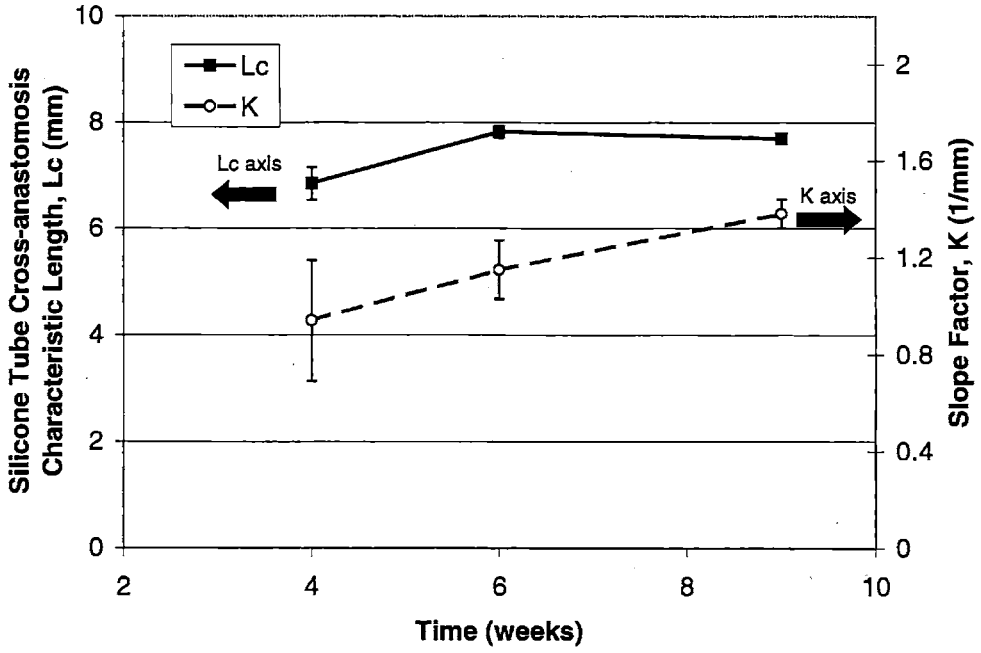

Figure 3.2 Chart showing the changes in characteristic length (L_c) and slope factor (K) between 4, 6, and 9 weeks for the sigmoidal curve fit to data for percent reinnervation at the gap midpoint (silicone tube, cross-anastomosis model). Data expressed as the resulting value from nonlinear least squares regression ± standard error.

As illustrated in Figure 3.2, the value of the characteristic length, L_c, increased 14 percent (statistically significant, $p<0.01$, student's t-test) between 4 and 6 weeks, but decreased 2 percent (not statistically significant, $p>0.2$, student's t-test) between 6 and 9 weeks. Similar to the trend observed with the the single-leg model (Figure 2.6), the data for the cross-anastomosis model suggest that the value of L_c has reached a time plateau by 6 weeks, showing no significant additional changes between 6 and 9 weeks. The value of the slope factor, K, increased 22% (not significant, $p>0.1$) between 4 and 6 weeks, and increased an additional 20% (statistically significant, $p<0.05$) between 6 and 9 weeks. These data suggest that although the value of L_c may have reached a plateau, the value of K may continue to increase beyond 9 weeks.

Figure 3.3 below shows the experimental data and the regression curve for the 9-week data for the cross-anastomosis model. The 9-week data represent the longest-term data collected during this experiment. The 9-week data were chosen since it is likely that a plateau in percent reinnervation has been reached before 9 weeks.

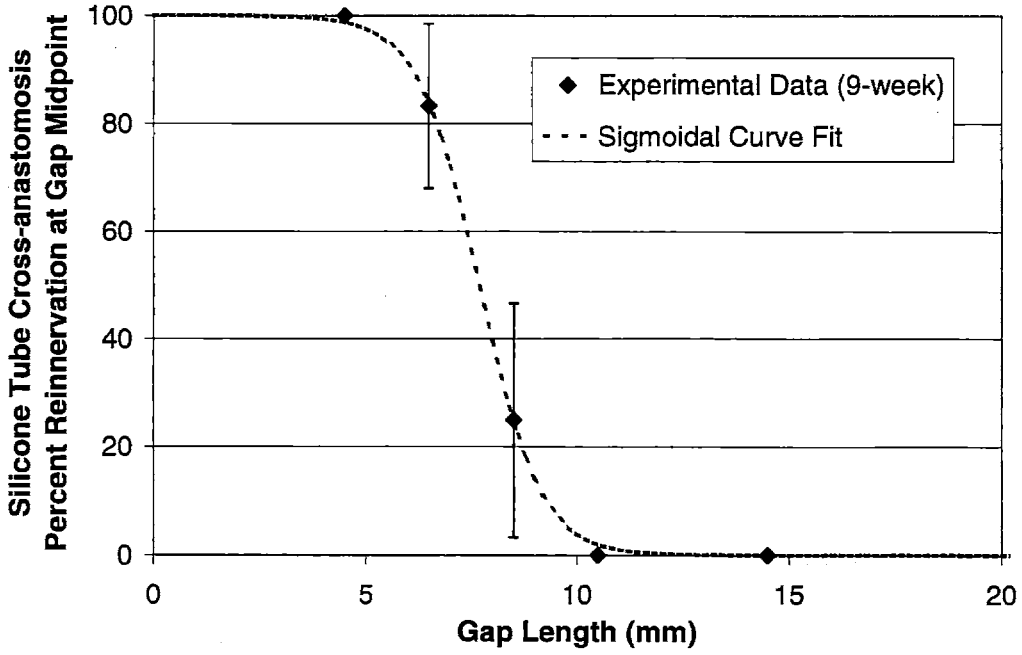

Figure 3.3 Chart showing the 9-week experimental data points for percent reinnervation at the gap midpoint versus gap length and the sigmoidal curve fit (silicone tube, cross-anastomosis model). Experimental data expressed as value ± standard error.

The sigmoidal equation approximates the 9-week experimental data quite well, with a high correlation coefficient, R^2=0.999. The parameters of the sigmoidal equation that describes the 9-week data were L_c=7.7 ± 0.04 mm and K=1.4 ± 0.06 mm^{-1}. In comparison to the sigmoidal parameters for the gap midpoint data for the single-leg model (section 2.3.2, Figure 2.5), L_c for the cross-anastomosis model was 34 percent smaller (statistically significant, $p<0.001$, student's t-test), and K was 47 percent larger (not significant, $p>0.05$, student's t-test). The difference in L_c indicates that, in the cross-

anastomosis model, the transition between 100% and 0% occurs at a smaller gap length. The difference in K indicates that the transition region of the curve is steeper in the cross-anastomosis model.

3.3.3 Assay #2: Reinnervation at the Distal Nerve Stump

Table 3.3 below contains the data for percent reinnervation at the distal stump for sciatic nerves repaired with silicone tubes in the cross-anastomosis model. These data were identical to the reinnervation data collected at the gap midpoint (table 3.2). The fact that the midpoint and distal stump data are identical indicates that myelinated axons were found in the distal stump in every animal in which myelinated axons were found at the gap midpoint.

Gap Length (mm)	4 weeks	6 weeks	9 weeks
4-5 mm	100 ± 0% (1/1)	100 ± 0% (4/4)	100 ± 0% (6/6)
6-7 mm	50 ± 35% (1/2)	80 ± 18% (4/5)	83± 15% (5/6)
8-9 mm	25 ± 22% (1/4)	33 ± 27% (1/3)	25 ± 22% (1/4)
10-11 mm	0 ± 0% (0/1)		0 ± 0% (0/3)
14-15 mm			0 ± 0% (0/4)

Table 3.3 Percent of animals in which myelinated axons successfully reached the distal nerve stump (silicone tube, cross-anastomosis model). Data are given for groups of animals with gap lengths between 4 and 15 mm and time points of 4, 6, and 9 weeks following tube implantation. Data expressed as percent ± standard error. Actual proportion for each group is given in parentheses.

Since the data for percent reinnervation at the gap midpoint were identical to the percent reinnervation at the distal stump, it follows that the results of the sigmoidal curve fits (see Figure 3.1) and the corresponding characteristic length and slope factor would also be identical (see Figures 3.2 and 3.3). Therefore, the data for assay #2 (percent

reinnervation at the distal stump) for the cross-anastomosis model can be summarized by the characteristic length (L_c=7.7 ± 0.04 mm) and the slope factor (K=1.4 ± 0.06 mm^{-1}).

3.3.4 Assay #3: Number of Myelinated Axons at Gap Midpoint

The data for the number of myelinated axons at the gap midpoint were expressed as the arithmetic mean ± standard error of mean for all animals in a given experimental group. Figure 3.4 below shows the data for all experimental groups for silicone tube nerve repair with the cross-anastomosis model.

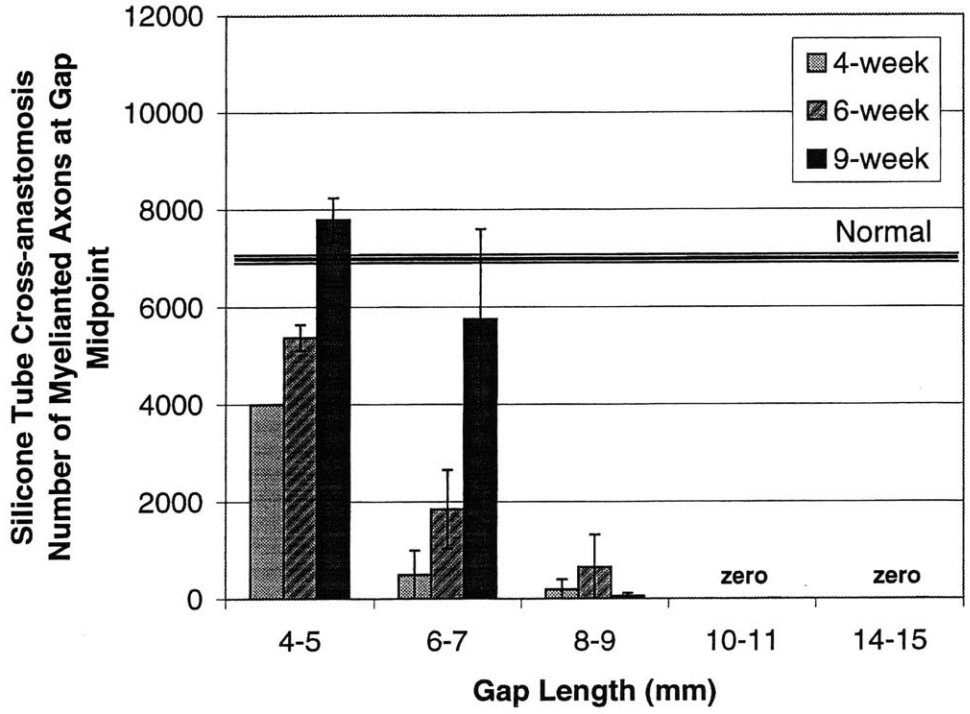

Figure 3.4 Data for number of myelinated axons at the gap midpoint for gap lengths between 4 and 15 mm and time points of 4, 6, and 9 weeks (silicone tube, cross-anastomosis model). Mean ± SEM.

Similar to the corresponding data for the single-leg model (Figure 2.11), the number of myelinated axons at the gap midpoint for the cross-anastomosis model showed

a general decreasing trend with increasing gap length for all three time points studied. The number of myelinated axons tended to increase with time between 4 and 9 weeks. For large gaps, greater than 9 mm, no myelinated axons were identified at the gap midpoint even after 9 weeks. The experimental group with a 4-mm gap length at the 9-week time point exhibited a number of myelinated axons at the gap midpoint larger than the number of myelinated axons in the normal sciatic nerve. This is not surprising since, during regeneration, it is well established that a severed axon may extend multiple sprouts, each of which may elongate into the wound. In previous experiments in this laboratory, the total numbers of myelinated axons in tubulated wounds were typically greater than the number in the normal nerve at 30 and 60 weeks after injury (Chamberlain, 1998).

When compared to the data for the single-leg model, axon number for the cross-anastomosis model tended to be smaller for equivalent gap lengths and times. Data for axon number at the gap midpoint did not appear to reach a plateau with time during the 9-week study. Significant increases in axons number were observed between 4 and 6 weeks as well as between 6 and 9 weeks in the 4-5 mm and 6-7 mm gap length groups. ANOVA revealed that the number of myelinated axons at the gap midpoint was significantly affected by both gap length ($p<0.01$) and time ($p<0.01$).

3.3.5 Assay #4: Number of Myelinated Axons in Distal Nerve Stump

The number of myelinated axons in the distal nerve stump was determined for each experimental group and recorded as the arithmetic mean ± standard error of mean. Figure 3.5 below shows the data for myelinated axons in the distal stump.

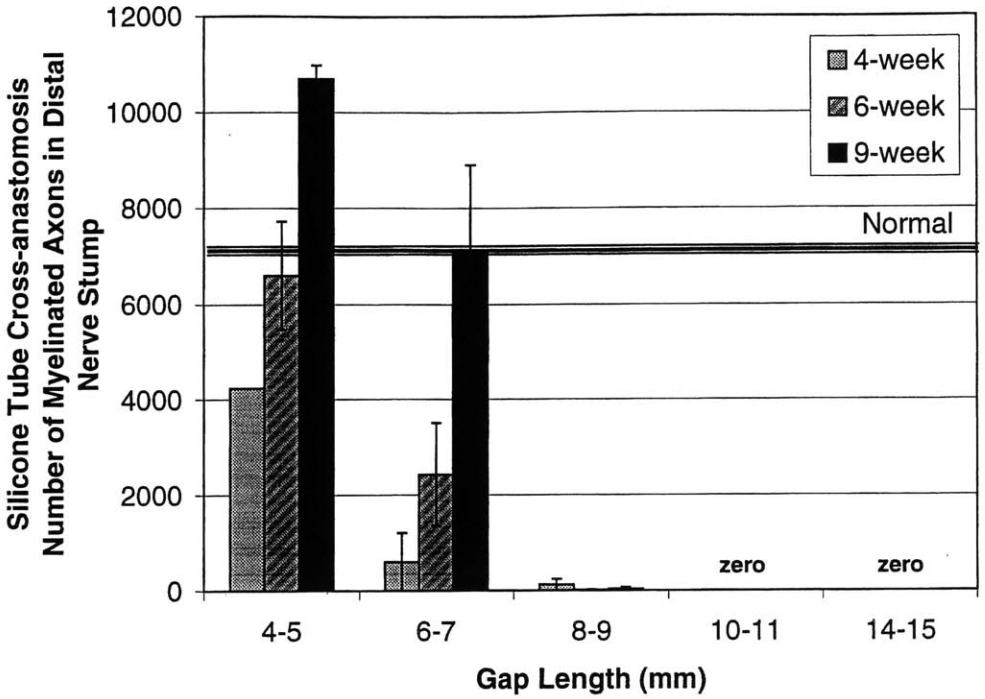

Figure 3.5 Data for number of myelinated axons in the distal nerve stump for gap lengths between 4 and 15 mm and time points of 4, 6, and 9 weeks (silicone tube, cross-anastomosis model). Mean ± SEM.

The data for myelinated axons in the distal nerve stump showed similar general trends to the data at the gap midpoint (Figure 3.4) with decreasing axon number with increasing gap length and increasing axon number with increasing time. No myelinated axons were observed in the distal stump at gap lengths greater than 9 mm, and very few axons were observed with 8-9 mm gap length.

In comparing the data from the distal stump (Figure 3.5) to the data from the gap midpoint (Figure 3.5), it was observed that the number of myelinated axons at the distal stump tended to be larger than the number of myelinated axons at the gap midpoint, especially in the smaller gap length groups (4-5 and 6-7 mm). This result is somewhat unexpected since axon elongation is usually assumed to progress with time from the

proximal stump through the gap midpoint toward the distal stump. We would therefore expect to see a larger number of axons at the midpoint.

3.4 Discussion

The data in chapter 2 described the relationship between regeneration and gap length for the silicone tube in the single-leg model. Four assays were compared, and an assay of device effectiveness was established that yielded a characteristic length parameter that represents a quantitative measure of regeneration. Experiments in chapter 2 were performed using the single-leg model of nerve repair. In the present chapter, the same four assays were used to measure nerve regeneration through silicone tube implants in the cross-anastomosis model. The goals of the experiments in chapter 3 were: 1. to demonstrate that the relationship between regeneration and gap length can be described by the sigmoidal equation in the cross-anastomosis model, 2. to verify that the analysis of the data using the sigmoidal equation (characteristic gap length assay) was appropriate in the cross-anastomosis model, and 3. to compare the cross-anastomosis and single-leg models based on the characteristic length assay for an identical device (the silicone tube). Each of these topics is discussed below.

3.4.1 Comparison of Assays: Validation of the Characteristic Gap Length Assay

The assays based on the number of myelinated axons at the gap midpoint and at the distal stump (assays #3 and #4) were not well suited for a short-term assay. First, the data for number of myelinated axons showed a high degree of variability within a given experimental group. For example, the data for axon number at the gap midpoint (Figure

3.4) exhibited values of the standard error that were approximately 50 percent of the value of the mean, when averaged across all experimental groups. Such large variability within experimental groups may preclude the statistical detection of differences among devices. In previous studies in this laboratory, statistically significant differences among devices in axon number were not detected in short-term studies due to the large variability in the data (Landstrom, 1993).

The data for axon number were also not well suited for a short-term assay since they failed to reach a plateau with time over 9-weeks. Time-independent data would be preferred for an experimental assay of device effectiveness. Previous studies in this laboratory have shown that axon number may not reach a plateau until 30 weeks after injury (Chamberlain, 1998). In summary, assays based on axon number were not well suited for detecting differences among nerve repair devices in short-term studies.

Similar to the observations in the single-leg model, the sigmoidal equation showed a high degree of correlation with the cross-anastomosis experimental data at all time points (Figure 3.1). The 9-week data showed a high degree of correlation with the sigmoidal equation (R^2=0.999). It was also apparent that the data for percent reinnervation had reached a plateau with time before 9 weeks (Figures 3.1 and 3.2). In chapter 2, it was suggested that reinnervation data gathered at the gap midpoint were preferable to data from the distal stump for a short-term assay since elongating axons would reach the gap midpoint at an earlier time. It also followed that the midpoint data would reach a plateau earlier than the distal stump data. The current data for the cross-anastomosis model do not directly support this hypothesis since the data at the gap midpoint were identical to those from the distal stump.

3.4.2 Comparison of Single-leg and Cross-anastomosis Models

In general, nerve regeneration in the cross-anastomosis model tended to be inferior to nerve regeneration in the single-leg model, based on the results of all four assays. For a given gap length and time, the values of both percent reinnervation and axon number at the gap midpoint or the distal stump were lower for the cross-anastomosis model than for the single-leg model, but the differences were generally not statistically significant ($p>0.1$ based on the student's t-test). Most importantly, the characteristic length for the cross-anastomosis model was significantly lower than the characteristic length for the single-leg model ($p<0.001$, student's t-test)). However, the slope factor (K) was not significantly different ($p>0.05$).

There are a number of plausible explanations for the differences in results between the single-leg and cross-anastomosis models. The cross-anastomosis surgical procedure involves much more severe trauma than the single-leg procedure. The difference in post-operative mortality rate (20 percent for cross-anastomosis versus 2 percent for single-leg) indicates the difference in overall effect on the condition of the animals. Also, the increased amount of trauma in the cross-anastomosis procedure may have lead to a cascade of wound healing processes in the surrounding tissue including increased inflammation and increased scar formation. Formation of connective tissue scar is one of the inhibitory influences responsible for preventing axon regeneration following nerve injury (Fu and Gordon, 1997).

During the surgical procedure for the single-leg model, the sciatic nerve was transected roughly mid-way between the sciatic notch and the bifurcation point of the tibial and peroneal branches. In the cross-anastomosis model, the proximal (left leg)

nerve stump was transected as far distal as possible, near the bifurcation point, and the distal (right leg) nerve was transected as far proximal as possible near the sciatic notch. It is possible that the differences in nerve transection site (proximal versus middle) may affect the ability of the axons to regenerate and may have been responsible for the differences in outcome that were observed between the two models.

3.4.4 Significance of Findings

Previously, Lundborg et al. examined peripheral nerve regeneration across nerve gaps of different lengths (6, 10, 15, and 20 mm) (Lundborg et al., 1982). The Lundborg studies were performed using a silicone tube in the cross-anastomosis model, and the resulting regeneration was measured at only one time point, 4 weeks after injury. The experiments described in the present chapter were similar to those of Lundborg and colleagues, with gap lengths ranging between 4 and 15 mm in in the cross-anastomosis model. Regeneration was measured at 4, 6, and 9 weeks after injury. The data gathered in chapter 3 were, therefore, directly comparable to the data from the Lundborg study.

The results of this chapter were similar to those of Lundborg et al. in that they define the relationship between regeneration and gap length for the silicone tube in the cross-anastomosis model. The current results improve on Lundborg's findings in two ways: first, the current data more accurately define the relationship between regeneration and gap length, and second, the dependence of this relationship on time was determined. In the current study, gap lengths between 4 and 15 mm were used in 2-mm increments to more precisely define the gap length at which the silicone tube is no longer effective (the characteristic gap length). The relationship between regeneration and gap length was also fit to a mathematical model in order to accurately define the relationship. Lastly, the

experiments in this chapter determined that changes in the relationship occur beyond the 4-week time point studied by the Lundborg group. The data in this chapter also suggest that the relationship reached an apparent plateau before 9 weeks.

The results in chapter 3 differed somewhat from Lundborg's results in the respect that the characteristic length was different. Lundborg's data suggest that the characteristic length for the silicone tube in the cross-anastomosis model would be located between 10 and 15 mm. The data in this chapter determined a smaller characteristic length value, L_c=7.7 ± 0.04 mm. Although many of the experimental techniques in this chapter were similar to those of the Lundborg study, it is possible that differences may be responsible for the differences in the results. These include the strain of the rat Lundborg used Sprague-Dawley outbred rats and we used Lewis inbred rats. Surgical technique may be different. The success of a nerve repair surgical procedue is dependent upon surgical technique (Archibald and Fisher, 1987), and it is quite possible that subtle differences in technique between the present study and Lundborg's may be responsible for the differences in results.

The data in this chapter demonstrated that the relationship between regeneration (as measured by percent reinnervation at the gap midpoint) and gap length can be described by the sigmoidal equation. The sigmoidal equation yielded a single parameter (the characteristic gap length) that can be used to describe the effectiveness of the silicone tube device in the cross-anastomosis model. The characteristic length was useful in quantitatively comparing the single-leg and cross-anastomosis models. The data in this chapter improved upon the study by Lundborg et al. by showing that the shape of the

relationship between regeneration and gap length changes with time, but apparently reach a time-independent state before 9 weeks.

When taken together, the experiments in chapters 2 and 3 demonstrate that significant differences in regeneration exist between the single-leg and cross-anastomosis models of nerve repair as indicated by the results of the characteristic gap length assay. The characteristic gap length for the silicone tube in the cross-anastomosis model (7.7 ± 0.04 mm) was significantly smaller than that for the single-leg model (11.7 ± 0.5 mm). The experiments in the following chapter (chapter 4) were designed to examine the possibility that the characteristic length assay may be used to compare nerve regeneration following implantation of two different nerve repair devices in the same model.

Chapter 4: Comparison of the Silicone Tube and the CG Device

4.1 Introduction

4.1.1 Previous studies of the Silicone Tube and the CG Device

Silicone tubes were among the first implanted devices used to facilitate peripheral nerve regeneration. Over nearly forty years, the silicone tube has been used by a large number of researchers and has become an experimental standard for nerve repair. Although recent experiments suggest that tubes composed of alternative materials may be superior to silicone tubes in terms of repair effectiveness (Archibald et al., 1991, Li et al., 1992, Chamberlain, 1998), silicone tube implants remain useful as well-characterized tools for the study of mechanisms of nerve regeneration (Lundborg et al., 1982, Williams et al., 1983, Williams and Varon, 1985, Williams, 1987) or as experimental standards for the comparison of competing devices (Landstrom, 1993, Chamberlain, 1996, Chamberlain, 1998). In chapters 2 and 3 of this thesis, the silicone tube was used to establish a new assay of nerve regeneration, the characteristic gap length assay. The silicone tube was used since it is a commonly accepted nerve repair device, and there exists a large pool of data from other investigators for comparison and validation of the experimental data.

Previous experiments in this laboratory have utilized the silicone tube as a baseline device against which the effectiveness of alternative nerve repair devices can be compared (Landstrom, 1993, Chamberlain, 1996, Chamberlain, 1998). The first of these studies (Landstrom, 1993) was performed with the goal of demonstrating superior effectiveness of matrix-filled collagen tubes (the CG device) over silicone tubes in short-

term (6-week) studies. Statistically significant differences between the CG device and the silicone tube were not detected after 6 weeks based on the total number of regenerated myelinated axons at the gap midpoint. However, subsequent studies have determined that the CG device was superior to the silicone tube based on total number of myelinated axons at the gap midpoint at 30 weeks (Chamberlain, 1996) and also at 60 weeks (Chamberlain, 1998). The 60-week study also demonstrated that the CG device was statistically superior to the silicone tube based on a functional electrophysiological assay and based on the number of large-diameter nerve fibers at the termini of the tibial and peroneal nerve branches (Chamberlain et al., (in press)).

One hypothesis of the experiments in chapter 4 was that statistically significant differences between the CG device and the silicone tube would be detectable in short-term (9-week) studies on the basis of the characteristic gap length assay.

4.1.2 Specific Aims

In chapter 2, the characteristic gap length assay was established for the silicone tube in the single-leg model. The characteristic gap length assay was selected based on a comparison of four assays. In chapter 3, the same four assays were compared using the silicone tube in the cross-anastomosis model, and the characteristic gap length assay was validated. The combined data from chapters 2 and 3 also represent a comparison between the single-leg and cross-anastomosis models using an identical device (the silicone tube). The goals of the experiments described in chapter 4 were to validate the characteristic gap length assay using a new device (the CG device) and to compare the characteristic length for the CG device with that for the silicone tube in the cross-anastomosis model.

The specific aims of the experiments in chapter 4 were: 1. to validate the use of the sigmoidal equation to describe the relationship between regeneration and gap length for the CG device in the cross-anastomosis model, 2. to use the sigmoidal equation to determine the characteristic gap length for the CG device, 3. to compare regeneration promoted by the CG device to that promoted by the silicone tube on the basis of the characteristic gap length assay.

To accomplish the specific aims, the experimental design of chapter 4 was similar to that of chapters 2 and 3. Groups of animals were implanted with CG devices using the cross-anastomosis model (Figure 1.3). At 9 and 12 weeks after injury, nerve regeneration for each gap length was evaluated based on the four assays described previously (sections 2.1.1 and 2.2.6). Nerve regeneration, as measured by each of the four assays, was compared with the purpose of validating the characteristic gap length assay for use in short-term experiments to quantitatively measure device effectiveness. The data in chapter 4 were interpreted based on the predictions and hypotheses below.

It was expected that the results would be similar to those of chapters 2 and 3. The comparison of assays would lead to the conclusion that data based on percent reinnervation would reach a time-independent state before 9 weeks, and thus would be suitable for a short-term assay. We also hypothesized that the experimental reinnervation data for the CG device would show a high degree of correlation with the sigmoidal equation, and that the sigmoidal analysis would yield a quantitative measure of device effectiveness (L_c). It was also expected that the assays based on myelinated axon number would not reach a plateau during the duration of the experiment and would not be well suited for a short-term assay. Since the CG device has been shown to be superior to the

silicone tube in previous long-term studies in this laboratory (Chamberlain, 1998), it was hypothesized that the CG device would also be superior to the silicone tube in the current short-term studies based on the value of the characteristic gap length.

4.2 Materials and Methods

The materials and methods for the experiments described in this chapter were similar to those for chapter 2, as described in section 2.2. The animal model was identical to that described in chapter 3 (section 3.2.2). Detailed protocols for many procedures can be found in Appendix A.

4.2.1 Experimental Configuration

The purpose of work described in this chapter was to validate the use of the characteristic gap length assay to evaluate nerve regeneration promoted by the CG device. Table 3.1 below shows the various gap lengths and time points that were studied. Each cell of the table indicates the number of animals that were included in each experimental group.

Gap Length (mm)	9 weeks	12 weeks
12 mm	n=5	
14 mm	n=5	
16 mm	n=6	n=6
18 mm	n=4	n=5
20 mm	n=4	n=5
22 mm		n=4

Table 4.1 Experimental groups for nerve repair using the CG device in the cross-anastomosis model

The experimental groups for the studies in chapter 4 differed significantly from those of chapter 3 (table 3.1). In chapter 3, the gap lengths ranged between 4 and 15 mm. This gap length range was chosen primarily on the basis of findings of previous experiments by Lundborg et al. that suggested that the characteristic gap length for the silicone tube was located between 10 and 15 mm (Lundborg et al., 1982). Previous studies with the CG device in this laboratory indicated that reinnervation at the gap midpoint was observed in 100 percent of animals with 10-mm gaps at 30 and 60 weeks after injury (Chamberlain, 1998). Based on these findings, it was expected that the characteristic gap length for the CG device would be 12 mm or greater, and gap lengths between 12 and 22 mm were chosen for the studies in chapter 4.

The time points for chapter 4 also differed from those for chapters 2 and 3. Since the CG device was assumed capable of bridging much larger gap lengths than the silicone tube, it was anticipated that more time would be required for axons to elongate to the gap midpoint and to the distal stump. Therefore time points of 9 and 12 weeks were chosen. Only two time periods were chosen due to the availability of only a finite number of collagen tubes provided by the commercial supplier. It was hypothesized that the reinnervation data for the CG device would reach a plateau before 9 weeks and no differences would be observed between 9 and 12 weeks.

4.2.2 Preparation of the collagen-GAG (CG) Devices

The CG device comprises a collagen tube filled with a highly porous scaffold composed of a copolymer of type I collagen and chondroitin 6-sulfate. The tube component of the devices was provided by Integra LifeScience Corporation (Dr. Simon Archibald, Plainsboro, NJ). Unfilled collagen tubes have been used for peripheral nerve

repair in previous studies in this lab (Landstrom, 1993, Chamberlain, 1996, Chamberlain, 1998) and others (Li et al., 1990, Archibald et al., 1991, Li et al., 1992, Archibald et al., 1995). Collagen tubes were composed of type I bovine tendon collagen and had an inside diameter of 1.5 mm. Details of the procedure for molding the collagen tubes have been described previously (Li et al., 1990, Archibald et al., 1991, Li et al., 1992, Archibald et al., 1995). The collagen tubes are manufactured such that the pore walls are semi-permeable to the passage of certain molecules. The collagen tube walls contain pores with a maximum diameter of 22 nm, a size which excludes transfer of proteins with molecular weight higher than 540 kD (Li et al., 1990, Li et al., 1992). The walls of the collagen tubes were approximately 650 μm thick and were comprised of loosely packed collagen layers, arranged in a laminar fashion (Figure 4.1). The collagen tubes were crosslinked by treatment with gaseous formaldehyde in order to increase mechanical stiffness and to decrease the degradation rate following implantation (Archibald et al., 1995). Tubes were sterilized by ethylene oxide treatment by Integra LifeSciences prior to shipment.

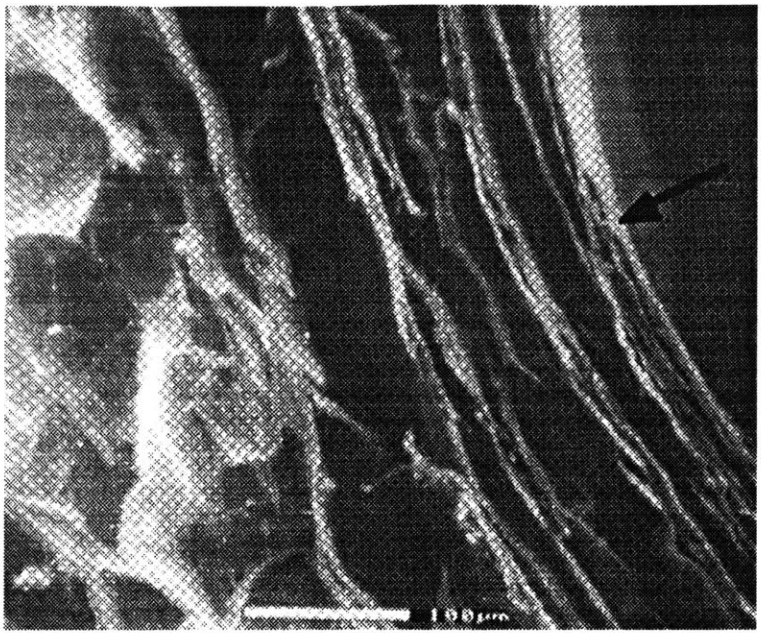

Figure 4.1 Scanning electron micrographs of the collagen tube. The tube walls are comprised of concentric layers of collagen in a laminar arrangement. The tube wall thickness, measured from the luminal surface (black arrow) to the outer surface (not visible), is approximately 650 μm. Scale bar = 100 μm.

The CG device comprises a collagen tube filled with a specifically synthesized collagen-glycosaminoglycan (CG) matrix. The family of CG matrices was developed in the Yannas laboratory and has been shown to favorably alter the wound healing process following injury to several tissue types. CG matrix has been shown capable of facilitating partial regeneration of the injured dermis in the guinea pig (Yannas et al., 1980, Yannas et al., 1987, Yannas, 1989) and human (Burke et al., 1981, Heimbach et al., 1988, Stern et al., 1990). Regeneration of the knee meniscus of the greyhound was achieved following 80 percent transection and implantation of CG matrix (Stone et al., 1990). The CG matrix has also been used to promote regeneration of the rabbit conjunctiva after full-thickness injury (Hsu et al., (in press)).

The CG matrix has been used in previous studies in this laboratory for the repair of peripheral nerves (Chang et al., 1990, Chang and Yannas, 1992, Landstrom, 1993,

Chamberlain, 1996, Chamberlain, 1998, Chamberlain et al., 1998) and spinal cord (Spilker, 1997, Spilker et al., 1997). The CG matrix used for nerve repair was identical in chemical composition to the matrix used for dermal and meniscal regeneration but differs in average pore diameter and pore orientation.

The CG matrix used in the current study comprises fibrous, type I bovine tendon collagen (Integra LifeSciences, Plainsboro, NJ) and chondroitin 6-sulfate (Sigma Chemical Company, St. Louis, MO) in a 98/2 wt./wt. ratio, with a pore void volume fraction of approximately 95 percent. The CG matrix was prepared using procedures that have been well established in this laboratory (Loree et al., 1989, Yannas et al., 1989, Chang et al., 1990). A detailed protocol for matrix production can be found in Appendix A. Briefly, the matrix was manufactured in this laboratory by a freeze-drying process comprising multiple steps: 1) a copolymer of type I collagen and chondroitin 6-sulfate is formed as a suspension in dilute (0.05M) acetic acid; 2) the suspension is injected into a silicone tube and frozen, forming ice dendrites; 3) sublimation of ice dendrites by freeze-drying yields a cylinder of highly porous matrix with axially oriented pore channels, about 35 μm in diameter (Figure 4.2); and 4) dehydrothermal treating the collagen-GAG network to form covalent crosslinks between polymer chains. The dehydrothermal treatment serves both to cross-link the matrix and to achieve sterilization. The exposure to elevated temperatures does not denature the collagen, provided that the moisture content of collagen prior to heat treatment is less than 1 wt. % (Yannas, 1972, Loree et al., 1989, Yannas et al., 1989, Chang et al., 1990). Following this cross-linking procedure, the matrix has a half-life of bioresorption of approximately 4-6 weeks in the rat sciatic nerve. The CG matrix synthesized in this study differed in degradation rate,

average pore diameter, and orientation of pore channel axes, but not in chemical composition, from a CG matrix which has induced partial regeneration of dermis in adult mammals (Yannas et al., 1989).

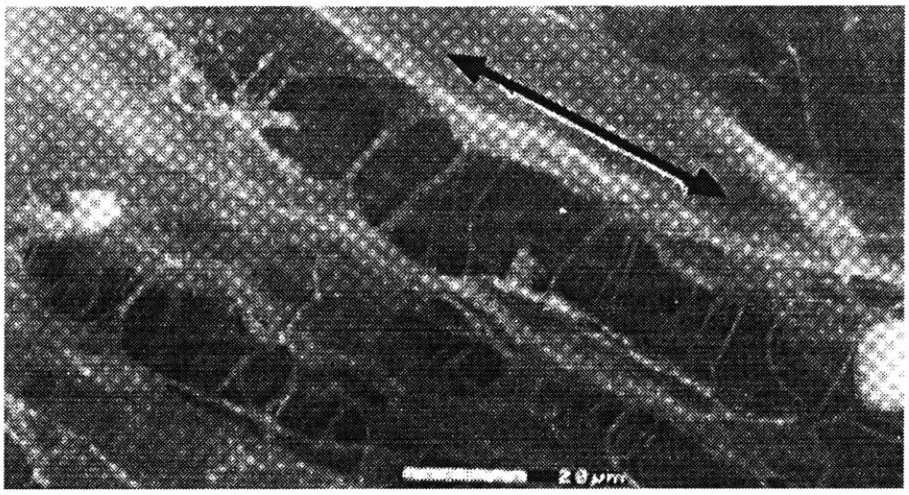

Figure 4.2 Scanning electron micrograph (SEM) of the CG matrix in a longitudinal orientation. The matrix has pore channels, approximately 35 μm in diameter, oriented parallel to the nerve axis (arrow). Each 35-μm pore channel contains a network of fine collagen-GAG fibers. Scale bar = 20 μm.

In a sterile hood, the collagen tubes were trimmed to a length 8 mm longer than the desired gap length (4 mm extra length at each end for insertion of the nerve stumps). A segment of CG matrix was cut to a length equal to the desired gap length and inserted into the midpoint of the tube, taking care not to collapse the pore structure of the matrix. Each implant was placed in a sterile glass vial filled with sterile-filtered phosphate buffered saline (Sigma Chemical Company, St. Louis, MO) prior to implantation. Implants in PBS were stored no more than 48 hours at 4°C prior to implantation.

4.2.3 Animal Model: Cross-anastomosis Repair

For the experiments in this chapter, the cross-anastomosis surgical procedure and the size and species of the experimental rats were identical to those described in chapter 3. The present experiments primarily differed from those of chapter 3 in the implant device (CG device as opposed to the silicone tube) and the gap lengths and time points being studied. All surgical procedures have been described previously (section 3.2.2). A detailed protocol can be found in Appendix A.

4.2.4 Tissue Allocation, Histological Processing, and Morphometric Evaluation

Nerve tissue was harvested and processed for histology using procedures identical to those used in chapters 2 and 3. Morphometric data were gathered from Epon-embedded sections as previously described (sections 2.2.4 and 2.2.5). Detailed protocols for experimental procedures can be found in Appendix A.

4.2.5 Statistical Analysis and Sigmoidal Curve Fit

Statistical analysis of the data was performed as described in section section 2.2.6. The proportional data (percent reinnervation at the gap midpoint and at the distal stump) were fit to the sigmoidal equation as described in section 2.2.7.

4.3 Results

4.3.1 General Observations

A total of 53 rats were implanted with CG devices for the experiments described in this chapter. Nine animals died from unknown causes before the scheduled sacrifice,

resulting in a mortality rate of 17 percent. This mortality was substantially higher than the 2 percent mortality rate for silicone tube repair in the single-leg model (section 2.3.1) but similar to the mortality rate for silicone tube repair in the cross-anastomosis model (section 3.3.1). Pullout of the nerve stumps from the tube ends was not observed in any animals in this chapter.

Excluding the 9 animals with premature death, the total number of animals included in the experiments in this chapter was 44 (see Table 4.1). The rats generally remained in good condition following surgery and throughout the duration of the experiment. The animals maintained the ability to move about the cage and access food and water. Since both the left and right sciatic nerves were transected during the cross-anastomosis procedure, the impairment for the animals was slightly greater than the single-leg model in chapter 2.

4.3.2 Assay #1: Percent Reinnervation at Gap Midpoint

The data for reinnervation at the gap midpoint for the cross-anastomosis model were expressed as the percent of animals in a given group in which myelinated axons were identified at the midpoint of the gap. Table 4.2 below shows the data for percent reinnervation at the gap midpoint for all gap lengths and time points included in this chapter.

Gap Length (mm)	9 weeks	12 weeks
12 mm	100 ± 0% (5/5)	
14 mm	100 ± 0% (5/5)	
16 mm	100 ± 0% (6/6)	100 ± 0% (6/6)
18 mm	75 ± 22% (3/4)	100 ± 0% (5/5)
20 mm	100 ± 0% (4/4)	100 ± 0% (5/5)
22 mm		100 ± 0% (4/4)

Table 4.2 Percent of animals in which myelinated axons successfully reached the gap midpoint (CG device, cross-anastomosis model). Data are given for groups of animals with gap lengths between 12 and 22 mm and time points of 9 and 12 weeks following device implantation. Data expressed as percent ± standard error. Actual proportion for each group is given in parentheses.

The data in table 4.2 indicate that successful reinnervation at the gap midpoint occurred in nearly every animal implanted with the CG device. The exception was a single animal with an 18-mm nerve gap at 9 weeks. The high rate of successful reinnervation, especially at the larger gap lengths (up to 22 mm), was unexpected since reinnervation following implantation of silicone tubes was mostly unsuccessful at gap lengths greater than 8 mm (section 3.3.2). The data in the current chapter indicate that the CG device was clearly capable of promoting axon growth across gap lengths significantly larger than the silicone tube.

Since nearly all of the midpoint data were saturated at the 100 percent level at both 9 and 12 weeks, the data were not well suited for mathematical analysis using the sigmoidal equation. Therefore, quantitative statistical information concerning the characteristic gap length could not be obtained. However, it can be inferred from the 9-week data that the characteristic length is greater then or equal to 20 mm. It can similarly

be inferred from the 12-week data that the characteristic gap length is greater than or equal to 22 mm.

Since the reinnervation data have already reached 100 percent by 9 weeks, it is reasonable to conclude that the data have reached a time-independent state. The data for nearly all gap lengths (with the exception of 18 mm) had reached saturation by 9 weeks, and all gap lengths were saturated by 12 weeks.

To summarize, although analysis of the midpoint data with the sigmoidal curve was not possible, the data define a lower bound for the characteristic gap length ($L_c \geq 22$ mm based on the 12-week data). No conclusions can be reached concerning the value of the slope factor (K) for the midpoint data. Although the data yielded a lower bound for the characteristic length for the CG device, they do not contribute to the specific aim of determining if the sigmoidal model is well-suited to describe regeneration in the CG device since they were not suitable for curve fitting.

4.3.3 Assay #2: Reinnervation at the Distal Nerve Stump

The data for reinnervation at the distal sump for the CG device were expressed as the percent of animals in any group in which myelinated axons were identified in the distal nerve stump. Table 4.3 below shows the data for percent reinnervation at the distal stump for all gap lengths and time points included in this chapter.

Gap Length (mm)	9 weeks	12 weeks
12 mm	100 ± 0% (5/5)	
14 mm	80 ± 18% (4/5)	
16 mm	83 ± 15% (5/6)	100 ± 0% (6/6)
18 mm	0 ± 0% (0/4)	60 ± 22% (3/5)
20 mm	25 ± 22% (1/4)	100 ± 0% (5/5)
22 mm		50 ± 25% (2/4)

Table 4.3 Percent of animals in which myelinated axons successfully reached the distal nerve stump (CG device, cross-anastomosis model). Data are given for groups of animals with gap lengths between 12 and 22 mm and time points of 9 and 12 weeks following tube implantation. Data expressed as percent ± standard error. Actual proportion for each group is given in parentheses.

The 9-week distal stump data exhibited the general trends that would be expected based on the reinnervation data from the silicone tubes, including steadily decreasing reinnervation with increasing gap length. The 12-week data also show a decreasing trend with gap length but with a higher degree of fluctuation between gap lengths.

For data from the gap midpoint (table 4.2) all gap length groups had reached 100 percent reinnervation by 12 weeks. In contrast, only two groups of data at the distal stump showed 100 percent reinnervation. This finding has two implications: first, axons that have elongated to the gap midpoint have not necessarily reached the distal stump, and second, the data from the gap midpoint have reached a plateau (saturation at 100 percent) earlier than the data from the distal stump.

Based on the finding that reinnervation in silicone tubes reached an apparent plateau before 9 weeks, it was expected that the reinnervation data for the CG device would also reach a plateau prior to 9 weeks and would therefore undergo no significant

changes between 9 and 12 weeks. However, the distal stump reinnervation data exhibited consistent increases in reinnervation between 9 and 12 weeks (table 4.3). It remains unknown if the reinnervation values at the distal stump would continue to increase up to saturation if a time beyond 12 weeks had been studied. Based on the data available in this chapter, it appears that the distal stump data had not reached a plateau before 12 weeks.

The data for reinnervation at the gap midpoint (table 4.2) were not suitable for analysis using the sigmoidal equation since most of the data points at both 9 and 12 weeks were saturated at the 100 percent level. The same difficulty was encountered with the 12-week reinnervation data from the distal stump (table 4.3) in which data for two of four gap length groups were saturated at 100 percent. For the CG device, only the 9-week data at the distal stump were appropriate for analysis with the sigmoidal equation. Figure 4.3 below shows the experimental data and the regression curve for the 9-week data. The sigmoidal equation approximates the 9-week experimental data reasonably well, with a correlation coefficient of R^2=0.86. The parameters of the sigmoidal equation that describes the 9-week data were L_c=16.5 ± 1.7 mm and K=3.1 ± 10.0 mm^{-1}. The unusually large standard error on the value of K is a result of the both the exponential nature of the sigmoidal equation and the mathematical methods of the curve fit.

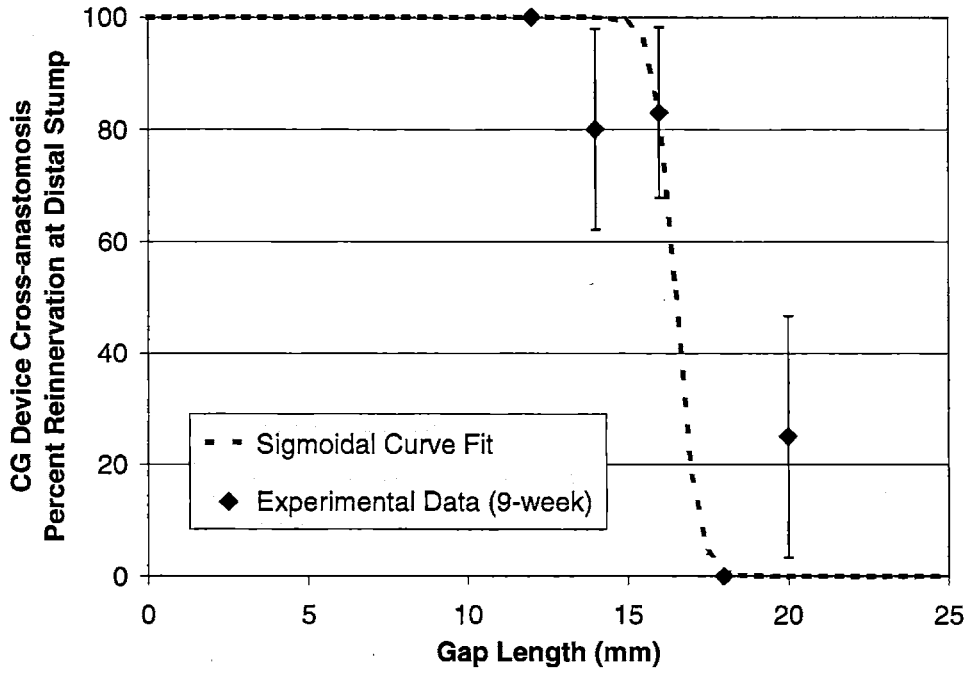

Figure 4.3 Chart showing the 9-week experimental data points for percent reinnervation at the distal stump versus gap length and the sigmoidal curve fit (CG device, cross-anastomosis model). Experimental data expressed as value ± standard error.

In comparison to the sigmoidal parameters for the equivalent 9-week distal stump data for the silicone tube in the cross-anastomosis model (section 3.3.3, Figure 3.3), L_c for the CG device was 114 percent larger (statistically significant, $p<0.001$), and K was 121 percent larger (not significant, $p>0.5$). The difference in L_c indicates that, for the CG device, the transition between 100% and 0% occurred at a much larger gap length. The difference in K indicates that the transition region of the curve was steeper for the CG device than for the silicone tube.

Although the 9-week distal stump data were suitable for analysis with the sigmoidal equation, these data had clearly not reached a time-independent state as indicated by the increase in percent reinnervation between 9 and 12 weeks. These data were therefore not suitable for use as a short-term assay.

4.3.4 Assay #3: Number of Myelinated Axons at Gap Midpoint

The data for the number of myelinated axons at the gap midpoint were expressed as the arithmetic mean ± standard error of mean for all animals in a given experimental group. Figure 4.4 below shows the data for all experimental groups for nerve repair with the CG device using the cross-anastomosis model.

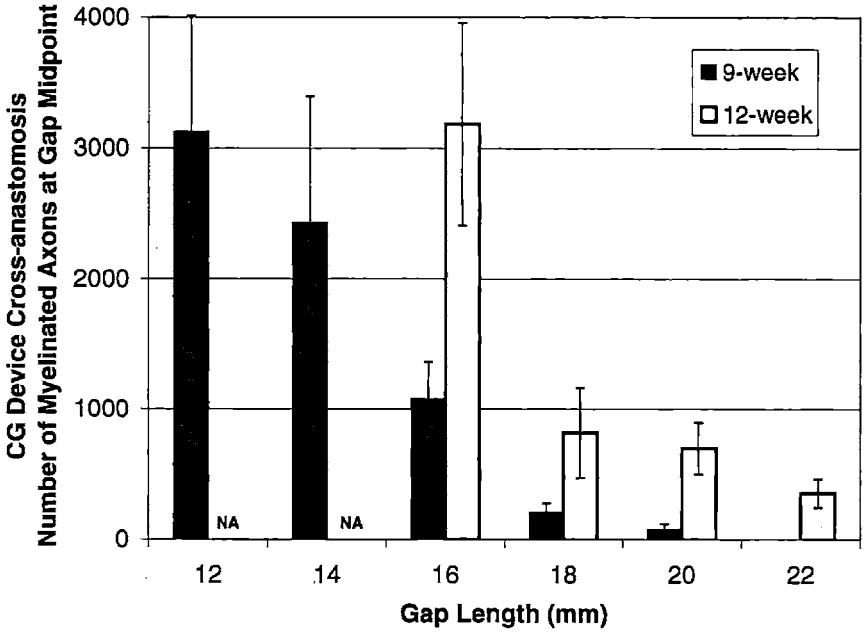

Figure 4.4 Data for number of myelinated axons at the gap midpoint for gap lengths between 12 and 22 mm and time points of 9 and 12 weeks (CG device, cross-anastomosis model). Mean ± SEM.

For the silicone tube in both the single-leg and cross-anastomosis models, it was observed that axon number tended to decrease with increasing gap length and increase with increasing time. These general trends were also observed for the midpoint data for the CG device. The data for the CG device were different from those for the silicone tube (section 3.3.4, Figure 3.4) in that the number of myelinated axons at the gap midpoint for the CG device tended to be higher than the number of axons for the silicone tube at

comparable gap lengths and times. For the silicone tube after 9 weeks, axons were not observed in any gap lengths 14 mm or greater for either the single-leg or cross-anastomosis models. For the CG device, more than 2,000 axons were observed after 9 weeks at the gap midpoint for the 14-mm gap, and more than 1,000 axons were observed for the 16-mm gap. It appears that the CG device is capable of promoting axon regrowth into larger nerve gaps than the silicone tube.

None of the experimental groups for the CG device exhibited a number of myelinated axons greater than that of the normal sciatic nerve (approximately 7,000). Data for axon number at the gap midpoint did not appear to reach a plateau with time during the 12-week study. Significant increases in axon number were observed between 9 and 12 weeks in the 16- and 20-mm gap length groups.

One unexpected finding was that myelinated axons had regenerated to the gap midpoint in all gap lengths studied, up to 22 mm. The discovery that the CG device promoted axon regrowth to the midpoint of a 22-mm gap in the cross-anastomosis model is unprecedented and may represent evidence of the longest nerve gap successfully bridged by an implant device in the rat model.

4.3.5 Assay #4: Number of Myelinated Axons in Distal Nerve Stump

The number of myelinated axons in the distal nerve stump was determined for each experimental group and recorded as the arithmetic mean ± standard error of mean. Figure 4.5 below shows the data for number of myelinated axons in the distal stump for the CG device in the cross-anastomosis model.

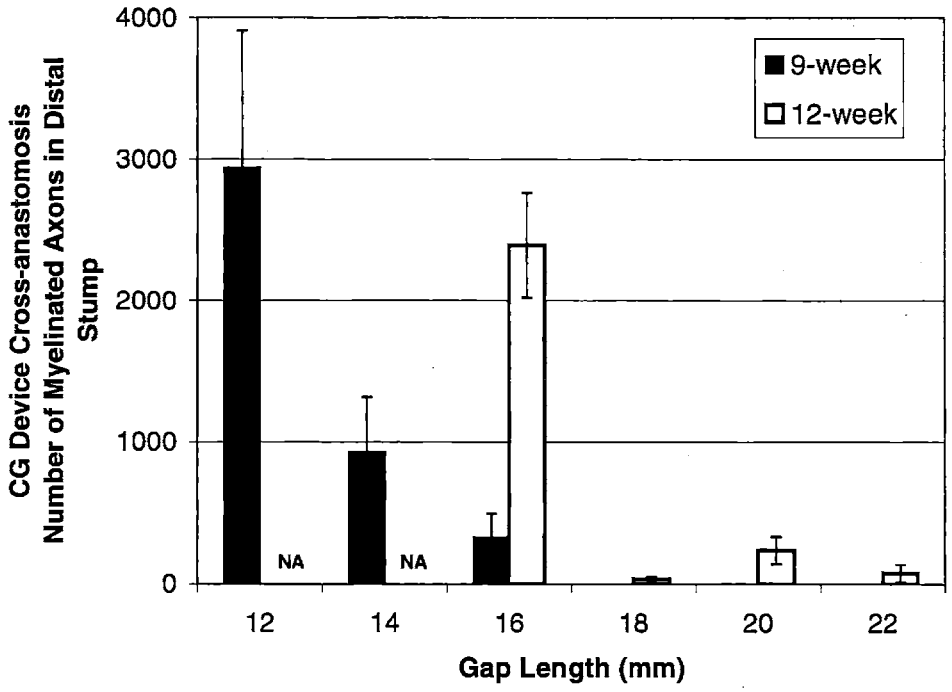

Figure 4.5 Data for number of myelinated axons in the distal nerve stump for gap lengths between 12 and 22 mm and time points of 9 and 12 weeks (CG device, cross-anastomosis model). Mean ± SEM.

The data for myelinated axons in the distal nerve stump showed similar general trends to the data at the gap midpoint. In comparing the data from the distal stump (Figure 4.5) to the data from the gap midpoint (Figure 4.4), it was observed that the number of myelinated axons at the distal stump tended to be smaller than the number of myelinated axons at the gap midpoint. This was especially evident at gap lengths greater than 18 mm at which very few axons were observed in the distal stump even after 12 weeks.

The data in section 4.4.4 and Figure 4.4 demonstrated that the CG device was capable of promoting axon regeneration to the midpoint of a 22-mm nerve gap at 12 weeks after implantation. The data from the distal stump (Figure 4.5) verify that

myelinated axons not only reached the gap midpoint, but completely traversed the gap and entered the distal stump. The mean number of myelinated axons for the 22-mm gap group (76 ± 56 myelinated axons) was small relative to normal (approximately 7,000 myelinated axons), but the result is nevertheless encouraging. The data from 9 and 12 weeks exhibited a general increase in axon number with time, and it is possible that the axon number for the 22-mm gap group may increase to a functional level if allowed sufficient time.

4.4 Discussion

The experiments in chapters 2 and 3 used the silicone tube implant to establish the characteristic gap length assay for one device (the silicone tube) in two different models (single-leg and cross-anastomosis). The goals of the experiments described in chapter 4 were to investigate the use of the characteristic gap length assay for application with a new device (the CG device) and to use the characteristic gap length assay to identify statistically relevant differences between the silicone tube and the CG device in a short-term study.

4.4.1 Comparison of Assays

One specific aim of the experiments in this chapter was to compare the four regeneration assays in order to identify an assay that would be suitable for evaluating the effectiveness of nerve repair devices (the CG device in this case) in short-term studies. The data from previous chapters for the silicone tube indicated that assays based on myelinated axon number at the gap midpoint and distal stump did not reach a plateau during the 9-week duration of the experiments. A similar conclusion can be reached

concerning the axon number assays for the CG device in the present chapter. The number of myelinated axons increased significantly between 9 and 12 weeks at the gap midpoint and at the distal stump. It was also evident that the data for axon number exhibited a fairly large degree of variability within experimental groups as evidenced by the large standard error values (Figures 4.4 and 4.5). Large variability within experimental groups may preclude the ability of the axon number assays to be used for comparisons among devices.

The data for percent reinnervation at the gap midpoint had reached an apparent plateau by 9 weeks (section 4.3.2) with nearly all of the experimental groups being saturated at 100 percent at both 9 and 12 weeks. It appears that the gap lengths chosen during the initial experimental design for the CG device (Table 4.1) did not include sufficiently long gap lengths to yield data suitable for curve fitting with the sigmoidal equation. The data from the gap midpoint were nearly all saturated at 100 percent and were not suitable for curve fitting and therefore did not yield quantitative data for the characteristic gap length. However, since 100 percent reinnervation was achieved even at gap lengths up to 22 mm, the midpoint data suggest that the characteristic gap length is greater than or equal to 22 mm. Due to the high success rate of reinnervation with the CG device, it is apparent that additional experiments performed at larger gap lengths would be required to gather data suitable for sigmoidal analysis and specific determination of the characteristic gap length.

The 9-week data for percent reinnervation at the distal stump were suitable for analysis using the sigmoidal equation and yielded curve fit parameters L_c=16.5 ± 1.7 mm and K=3.1 ± 10.0 mm^{-1}. However, when compared with the 12-week data, it was

apparent that the 9-week data had not reached a plateau. The 9-week data would therefore not be acceptable for use as a short-term assay. The fact that these data showed a reasonable correlation with the sigmoidal equation (R^2=0.86) suggests that percent reinnervation data for the CG device would be suitable for sigmoidal analysis provided that all of the data points were not saturated at the 100 percent level.

In summary, the data in chapter 4 did not suffice to achieve the specific aim of validating the characteristic gap length assay for the CG device. The midpoint reinnervation data (Table 4.2) were saturated at 100 percent and the distal stump reinnervation data (Table 4.3) had not reached a plateau with time before 12 weeks. It is important to note that the data in the present chapter do not indicate that curve fitting with the sigmoidal equation is inappropriate for the CG device. In fact, the 9-week data from the distal stump suggest that sigmoidal analysis would indeed be appropriate. It is also encouraging that the reinnervation data from the gap midpoint had reached an apparent plateau by 9 weeks and also possible that a short-term experiment that included gap lengths longer than 22 mm may yield data suitable for the characteristic gap length assay. Although the present data did not precisely define the value of L_c, they suggest that $L_c \geq 22$ mm.

4.4.2 Comparison of the Silicone Tube and the CG Device

Table 4.4 below lists the descriptive parameters (characteristic lengths and slope

factors) for the silicone tube (single-leg and cross-anastomosis models) and the CG device (cross-anastomosis model).

Device: Model	Characteristic Length (L_c, mm)	Slope Factor (K, mm^{-1})
Silicone Tube: Single-Leg	11.7 ± 0.5	0.7 ± 0.2
Silicone Tube: Cross-anastomosis	7.7 ± 0.04	1.4 ± 0.06
CG Device: Cross-anastomosis	≥ 22.0	No information

Table 4.4 Comparison of the characteristic lengths and slope factors for the silicone tube and the CG device. Values for the silicone tube were derived from nonlinear fitting of reinnervation data at the gap midpoint with the sigmoidal equation (chapters 2 and 3). The lower bound value for the CG device was based on the 100 percent successful reinnervation at the gap midpoint observed in all animals with nerve gap lengths up to and including 22 mm. Since curve fitting was not performed for the CG device, the slope factor was not determined.

A comparison of the values of L_c for the silicone tube and the CG device in the cross-anastomosis model (Table 4.4) indicates that the CG device is indeed superior to the silicone tube. Although a statistical comparison was not possible due to the nature of the L_c value for the CG device, the nearly three-fold difference in L_c strongly suggests a difference between devices. This finding was expected based on previous studies in which the CG device was more effective than the silicone tube in repairing a standard 10-mm gap in the rat sciatic nerve in long-term tests (Chamberlain, 1998, Chamberlain et al., 1998, Chamberlain et al., (in press)).

4.4.3 Significance of Findings

The data in chapter 4 were not able to definitively validate the use of the characteristic gap length assay for the CG device. The reason for this was the fact that the CG device yielded 100 percent reinnervation for most gap lengths for data gathered at both the gap midpoint and at the distal stump. With the exception of the reinnervation data gathered at 9 weeks in the distal stump (section 4.3.3), the data were not suitable for sigmoidal analysis. It is important to recognize that the present findings do not indicate that the data for the CG device are in general not suitable for analysis with the sigmoidal equation. In fact, the 9-week reinnervation data from the distal stump showed a reasonable correlation with the sigmoidal equation. Rather, it is apparent that the range of gap lengths included in this study was not sufficiently large to produce data suitable for the sigmoidal analysis.

The data in this chapter also indicate that the CG device exhibited superior performance to that of the silicone tube based on the values of the characteristic gap length. As indicated in section 4.4.2 and Table 4.4, L_c for the CG device in the cross-anastomosis model was greater than or equal to 22 mm whereas L_c for the silicone tube in the same model was 7.7 ± 0.04 mm. A statistical comparison was not possible due to the nature of L_c for the CG device, but the values of L_c strongly suggest a large difference in effectiveness between the two devices with the CG device identified as superior.

An unexpected, but perhaps the most significant, finding of these experiments was the successful repair of gap lengths up to 22 mm with the CG device. Previous studies in this laboratory have demonstrated that the CG device was more effective than all other tubular devices, including a silicone tube and an unfilled collagen tube, in long-

term studies (Chamberlain, 1998). The CG device exhibited performance equivalent to or superior to the autograft as measured by both morphological and electrophysiological assays after 60 weeks (Chamberlain, 1998, Chamberlain et al., 1998, Chamberlain et al., 2000). Based on a survey of the literature, the 22-mm gap may be the largest reported gap successfully repaired by a tubular device in the rat model.

Chapter 5: Conclusions

5.1 The Characteristic Gap Length Assay

Previous studies in this laboratory have focussed on comparing the effectiveness of various tubular devices in repairing a standard experimental nerve injury (10-mm gap) in the rat animal model. The devices were rank-ordered based on clinically relevant assays of regeneration such as the number regenerated nerve fibers and the values of the electrophysiological conduction properties of the regenerated nerves. Such assays provided a useful estimate of the clinical efficacy of devices but required long-term (up to 60-week) studies in order to statistically distinguish among different devices. There exists a need for a short-term (less than 12-week) assay with which nerve repair devices can be compared. The overall goal of this thesis was to establish an experimental assay that can be used to detect statistically significant differences among nerve repair devices in short-term studies.

In this thesis, four different assays of nerve regeneration were compared on the basis of the ability to compare the extent of regeneration following implantation of nerve repair devices in studies less than 12 weeks in duration. An acceptable assay must reach a plateau with time during short-term studies and must yield a quantitative measure of device effectiveness with relatively small variability within experimental groups. The results of this thesis suggest that the "characteristic gap length assay" based on the ability of a nerve repair device to successfully repair nerve gaps of various lengths meets the criteria for an acceptable assay. The characteristic gap length quantity (L_c) was derived from experimental data for the relationship between percent reinnervation versus gap length for a given device. The experimental data indicate that for the silicone tube device,

the value of L_c reached a plateau with time before 9 weeks, and the standard error in L_c was less than 5 percent of the value in two different nerve repair models. The data also suggest that statistically significant differences between the silicone tube device and a collagen-based device (the CG device) are obtainable during short-term (12-week) studies. An additional significant finding of this thesis was the ability of the CG device to promote regeneration of myelinated axons across a 22-mm gap in the rat sciatic nerve.

5.2 Future Work

The most immediately useful future experiment would be to conclusively determine the characteristic gap length for the CG device. In chapter 4 of this thesis the experimental data were not sufficiently complete to determine L_c for the CG device, although it was suggested that $L_c \geq 22$ mm. An additional useful experiment would involve animal experiments in which nerve gaps larger than 22 mm would be repaired with the CG device. It is suggested that nerve gaps in 2-mm length increments be used. The regeneration outcome should be quantified at time points of 9 and 12 weeks. Assuming that the data would be suitable for analysis with the sigmoidal equation, the characteristic gap length could be determined for the CG device. In this thesis, it was also not conclusively determined for the CG device whether the reinnervation data had reached a plateau before 9 weeks. If the data have not reached a plateau by 9 or 12 weeks, additional longer-term experiments may be necessary, perhaps 15 weeks in duration.

The encouraging results with the CG device in promoting regeneration across large gap lengths suggest that additional studies be performed to more accurately characterize the extent of regeneration that may be achieved with the CG device. Possible studies include long-term investigations that quantify the recovery of sensory and motor

function as well as the recovery of electrophysiological conduction properties of regenerated nerves at larger gap lengths (greater than 10 mm). It would also be necessary to compare nerve regeneration following implantation of the CG device with that following autograft repair at gap lengths in excess of 10 mm.

The focus of this thesis was not to examine physiological mechanisms of nerve regeneration, but rather to establish tools that can be used by scientists to evaluate and compare the effectiveness of nerve repair devices. The assays established in this thesis revealed striking differences in nerve regeneration promoted by the silicone tube and the CG device. The differences in regeneration between these devices suggest that characteristics of the device fundamentally affect the regenerative process. Future experiments should include basic studies of the mechanisms by which device parameters such as tube material, tube wall permeability and porosity, and the presence of the CG matrix in the tube lumen modify the physiologic processes of regeneration.

Appendix A: Protocols

A.1 Collagen-Glycosaminoglycan (CG) Slurry Protocol

(adapted from Chamberlain 1998)

1. Turn on cooling system for blender (Granco overhead blender, Granco Co., Kansas City, MO) and allow to cool to 4 °C (Brinkman cooler model RC-2T, Brinkman Co., Westbury, NY).

2. Prepare 0.05M acetic acid (HOAc) solution: add 8.7 ml HOAc (glacial acetic acid, Mallinckrodt Chemical Co., Paris, KY) to 3 liters distilled water. (This solution has a shelf life of approximately 1 week).

3. Blend 3.6 g of dry microfibrillar bovine tendon collagen with 600ml of 0.05 M acetic acid on HIGH speed setting for 90 mintues at 4 °C.

4. Prepare chondroitin 6-sulfate solution: dissolve 0.32 g chondroitin 6-sulfate (from shark cartilage: no. C-4384, Sigma Chemical Co., St. Louis, MO) in 120 ml acetic acid.

5. Calibrate peristaltic pump (Manostat Cassette Pump, Catalog no. 75-500-0.00, Manostat, NY, NY) to 40 ml/5 min.

6. Add 120 ml of chondroitin 6-sulfate solution dropwise to the blending collagen dispersion over 15 minutes using the peristaltic pump (maintain blender at 4°C).

7. Blend 90 additional minutes on HIGH speed at 4°C.

8. Degas in a vacuum flask for 15 minutes until bubbles are no longer present.

9. Store in a capped centrifuge bottle at 4°C (will keep for up to about four months, re-blend 15 minutes on LOW speed, 4°C, and degas before using if stored more than four weeks).

A.2 CG Matrix Manufacture Protocol

(adapted from Chamberlain 1998)

ONE TO TWO DAYS BEFORE FREEZING:

1. Prepare PVC jackets by cutting off 12-cm sections of flexible PVC tubing (0.125 inches ID, 0.25 inches OD) and straighten at 105°C for 2 hours. Puncture the tube with a needle at 90° intervals around the tube and spaced 1 cm apart for the length of the tube. (See Loree, 1988, for more details).

2. Flush silicone prostheses tubing (Dow-Corning model 602-235 medical grade Silastic 0.058 inch ID, 0.077 inch OD, Dow-Corning Co., Midland, MI) with deionized water (Deionizing Organic Adsorption System, Hydro Services and Supplies, Inc., Durham, NC) and cut off 15-cm lengths.

3. Seal one end of the silicone prosthesis tubes with silicone adhesive (Silastic, Dow-Corning, medical grade Silastic). Inject approximately 5 mm into the tube and allow the excess to stay on the outside of the tube. (The excess is important for adhesion and can be cut away later) Let cure for 24 hours at room temperature. Make plenty of tubes, approximately three times the number you plan to freeze, because some will not be usable.

4. Order a 160-liter liquid nitrogen tank from the MIT Cryogenic lab.

THE DAY OF FREEZING:

5. Dearate CG suspension in a 1500 ml Erlenmeyer flask at -30mmHg for 10 minutes with agitation or until large bubbles are no longer visible.

6. Turn on the uniaxial freezing bath (Loree, 1988) and set the temperature to -80°C. It will take approximately 45 minutes for the bath to reach this temperature.

7. Insert each silicone tube into a prepared PVC jacket. Draw 10 cc of CG suspension into a 10 cc syringe (model 5604, Becton Dickinson Co., Rutherford, NH). Expel air bubbles. Attach a 25 gauge needle (model 25G5/8, Becton Dickinson Co., Rutherford, NH) to the syringe and insert carefully into the plugged end of the silicone tube. The needle should be inserted far enough so that 3-5 mm of needle is beyond the silicone plug (Figure A.1a).

8. Inject CG suspension until a few drops come out the free end. Plug the end of the PVC tube opposite the needle with a pipette tip. Insert another pipette tip into the needle end of the tube. The tip at this end should be secure, but not too tight (Figure A.1a). Inject additional slurry until the silicone tube is pressurized and expands to fill the entire PVC jacket. The end of the needle should be inside the PVC jacket to help prevent a pressure build up at the needle tip. When the tube is pressurized, **carefully** remove the needle and simultaneously press the pipette tip into the end of the tube.

Pressure should be kept on the syringe plunger until the needle is completely out of the tube. Check to make sure the tube is still pressurized (Figure A.1b).

9. Attach the large gear to either motor on the freezing apparatus. Tape four prepared PVC jackets to the PVC hanger and place it on the gear train. Lower manually until the pipette tips are just touching the bath. Start the appropriate motor and let the tubes lower into the bath at a velocity of 10^{-4} m/s (Figure A.2a). Watch to make sure the tubes are lowering and that they do not stick to any of the parts of the freezing apparatus.

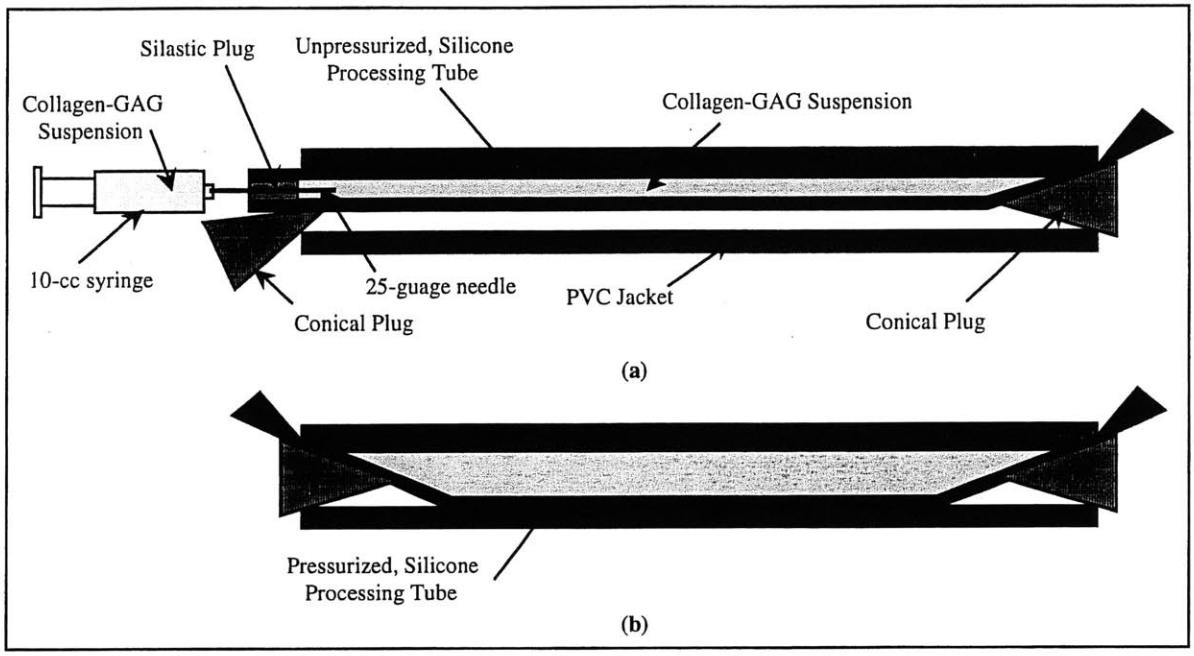

Figure A.1 Schematic detailing the procedure for injecting the silicone processing tube with CG slurry. (a) Configuration of the processing tube prior to pressurization. (b) Final configuration of the tube assembly prior to lowering into the freezing bath.

10. Turn on the freeze drier (VirTis Gènesis). Follow the manual freeze-dryer steps below. Place the freeze drier tray in the freezer to cool.

11. When PVC jackets are fully immersed in the bath, turn off the motor and remove the tubes from the bath. Quickly separate the tubes and remove the pipette tips. Cut off the plugged end of the silicone tube and cut each PVC jacket approximately in half with an extremely sharp razor blade (Be sure to have plenty of new blades handy). Place the tubes on the cooled freeze drier tray (Figure A.2b) and put the tray either in the freezer, or in the freeze drier if it has reached -20°C. This step must be done as quickly as possible to ensure that the tubes stay completely frozen.

12. Place the tray containing the frozen tubes in the freeze-drier. Seal the chambers on the freeze drier and close the vacuum outlet tube. Check that the door is sealed shut when the vacuum comes on. After the program is finished, clear the chamber and

allow the vacuum to totally release before opening the chamber door. Turn off the unit and remove the tray.

13. Prepare aluminum foil packets for the matrices and place each PVC tube along with the matrix in a packet. Leave one end of the packet open. Place the packets in the dehydrothermal treatment (DHT) oven at 105°C. Seal the chamber and turn on the vacuum pump. DHT the matrices for 24 hours. Remove the packets and quickly close them. The matrices are now sterile and must be handled using sterile procedure from this point forward.

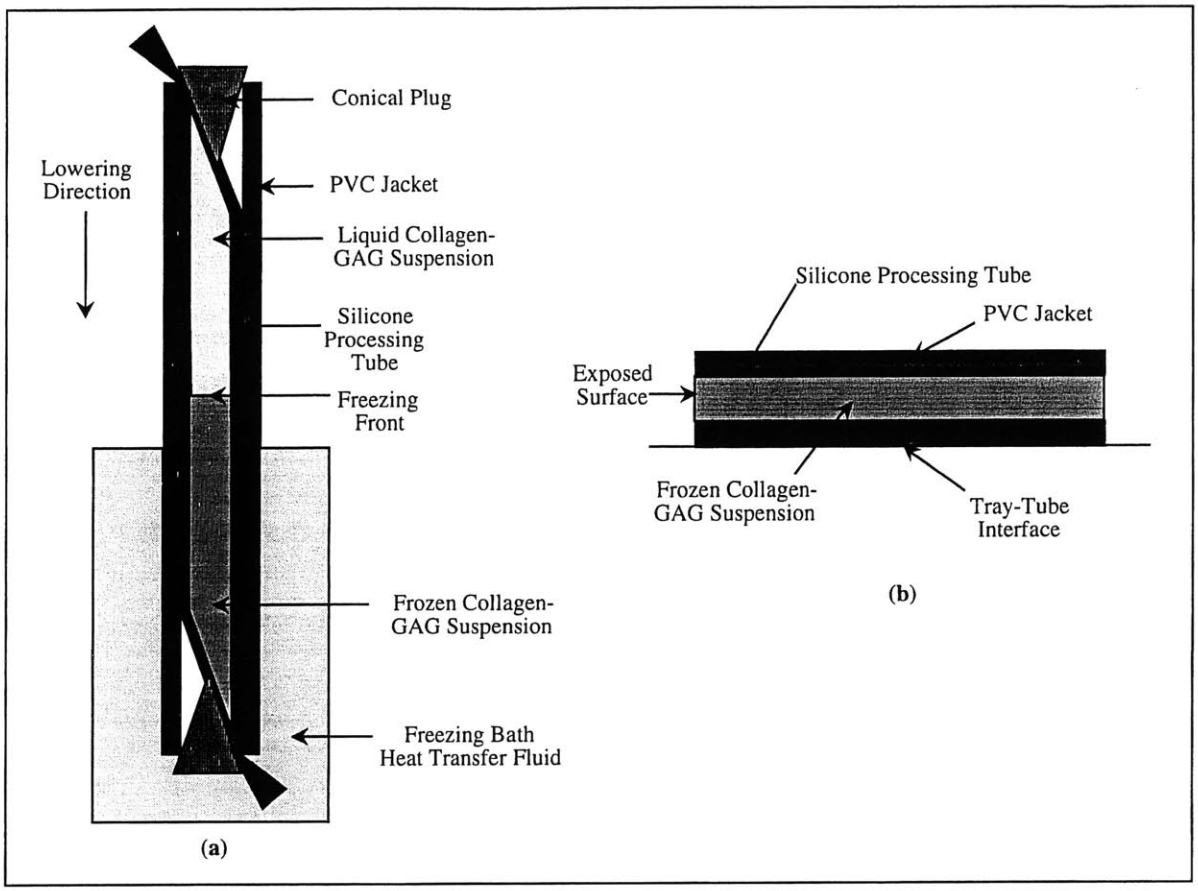

Figure A.2 Schematic detailing the tube assembly orientation during (a) freezing and (b) sublimation.

MANUAL FREEZE DRIER STEPS:

1. Turn on the freeze switch and set the shelf temperature to -20°C.

2. Turn on the condenser (at the same time as step 1) and let it cool until it reaches -45°C.

3. When the shelf reaches -20°C, insert the tray containing the frozen tubes.

4. If the condenser is already below -45°C, turn on the vacuum switch and wait for the vacuum to reach 100mTorr. Make sure that the chamber door seals. It sometimes requires assistance in sealing.

5. Once the vacuum reaches 100 mTorr, turn on the heat switch and set the temperature to 0°C. Leave the product in the freeze drier for 17 hours at this temperature and pressure.

6. Set the temperature to 25°C and remove the product when the chamber has reached room temperature. Turn off the freeze drier.

A.3 Sterile Procedure and Implant Assembly Protocols

(adapted from Chamberlain 1998)

ONE TO TWO DAYS BEFORE GRAFT PREPARATION:

1. Sterilize the necessary implements:

In Autoclave Bags:

Tool Pack:
- 1 jewelers forceps
- 2 regular forceps
- 1 large forceps
- 1 surgical blade holder
- 1 needle holder

1 glass specimen jar for each prosthesis (Put a small piece of autoclave tape on each jar for labeling purposes later)

1 500 ml glass bottle

(Always keep an extra tool pack and an extra set of specimen jars sterile in case of an emergency. It's easiest to rotate the packs so that they don't sit unused for too long)

Wrap in Autoclave Paper:

1 Teflon sheet for working area (Tape a ruler to the sheet with autoclave tape. This makes cutting easier in the sterile environment)

Dehydrothemally Treat (DHT):

Appropriate tubes for graft preparation. Procedure is the same as with the matrix (see section A.2 for details).

Sterilize Liquid Using ZapCap and autoclaved 500-ml bottle:

Phosphate Buffered Saline Solution (PBS)

2. Turn on the HEPA hood, at least 1 hour before working, preferably 24 hours prior.

GRAFT PREPARATION:

3. Bring necessary sterile implements to workbench:

All items sterilized in step 1.
Envelopes with CG matrices
Envelopes with tubes
1 ring stand

4 #10 surgical blades
1 sterile pipette
1 sterile pen
Whirl-Pak bags (1 per prosthesis plus 3; 1 for extra tubes, 1 for extra matrix, 1 for the pen)

4. Put on latex gloves, a cap, a mask and a clean, disposable lab coat. Wipe bench, metal frames and ring stand with 70% ethanol.

5. Using sterile technique, set up sterile field with Teflon pad. Open all tool packs and pour onto sterile field, including prostheses, scalpel blades, etc. Fill each jar with sterile PBS using the sterile pipette (if the prostheses are not going to be implanted for a week or two, fill jar with 70% ethanol for storage. Before surgery, rinse in two rinses of sterile saline solution immediately before surgery). Carefully open Whirl-Pak bags and stand on metal frames in hood.

6. Trim prosthesis tubes to the desired length using scalpel. Remove the matrix from the silicone processing tube by making a careful slit with the scalpel down the length of the silicone and gently pulling out the matrix with the forceps. Trim off any crushed or otherwise damaged matrix and cut remaining portion to the desired length to be inserted into the center of the trimmed tubes. The length of the matrix is 8-mm shorter than the length of the tube.

7. Place prostheses into specimen jars with PBS, close jars tightly, label, place in Whirl-Pak bags, and close bags. Label each prosthesis by type: silicone tube or CG device.

A.4 Surgical Protocol

(adapted from Chamberlain 1998)

SUPPLIES

1. Order animals: Adult, female Lewis rats, 150 - 175 grams, from Charles River Laboratories. Animals must arrive at least one week in advance of surgery to reduce the stress placed on the animal due to travel.

2. Sterilize the necessary items:

1 metal bowl	1 large scissors
gauze	1 surgical (tenotomy) scissors
1 surgical blade holder	2 paper clip retractors
1 micro-needle holder	2 forceps
1 micro-scissors	1 needle holder
2 jewelers forceps	animal skin staples
1 large forceps	wooden rods (cotton swabs)

3. Ready other sterile items:

sterile table covering	sterile pen
scalpel blades (4 #15 blade, 1 #11 blade)	10-0 sutures
1 bottle of PBS	4-0 sutures
iodine sponge	1 ml syringes
sterile draping	1 bottle Lidocaine, 1%

Implants (sterilized and prepared as in section A.3)
1 bottle pentobarbital (Nembutal Sodium Solution), 50mg/ml

4. Ready other non-sterile items:

surgical board	numbered ear tags
4 rubber bands	microsurgery glasses (loops)
rat ear tagging tool	hair clippers

SURGICAL PROCEDURE

1. Weigh animal on an appropriately sized balance. Record the weight and determine anesthetic dosage based on the pre-operative weight.

2. Anesthetize animal with injection of sodium pentobarbital (50 mg of solution per kg of animal). Allow 10-15 minutes for anesthesia to take effect. Each animal reacts differently to the anesthetic and in some cases, more time may be required.

3. Meanwhile, arrange the surgical area so that the table is at a comfortable level for the surgeon, and the tools are conveniently located.

4. The surgeon should be sterilely dressed in scrub shirt and pants, hat and mask.

5. When ready, shave the animal using the animal hair clippers from the base of the tail up to the middle of the back. The leg receiving the prosthesis should be shaved carefully and completely.

6. Place the animal on the surgical board in the prone position and secure the arms and legs to the board using rubber bands. The legs should be in 30° abduction. Place a piece of gauze under the appropriate thigh to elevate the leg slightly.

7. Clean the shaved portion of the animal vigorously with the iodine sponge to disinfect the area. At this point, the surgeon should put on the sterile gloves and remain sterile for the rest of the procedure. Cut a hole in the sterile draping small enough so that only the leg is exposed. Place the draping over the animal.

8. Using the #15 scalpel, make a 4 cm incision along the leg of the animal. Separate the skin from the muscle along the incision by cutting through the connective tissue with the surgical scissors.

9. Using the surgical scissors, separate the muscles until the sciatic nerve is visible. Carefully cut back the muscle along the skin incision line exposing the sciatic nerve.

10. Place the paper clip retractors inside the muscle to separate the wound edges. Anesthetize the nerve by placing a few drops of Lidocaine directly on the area. Cut away the fascia surrounding the sciatic nerve carefully so that the nerve is free from constraint.

11. Transect the nerve midway between the proximal nerve trunk and the distal bifurcation using microscissors. Measure the prosthesis and make a mark 5 mm in on each end. Place the tube in the gap and insert the proximal nerve stump 5 mm into the tube end, as marked. Secure the nerve in place by using two 10-0 sutures which travel through the epineurium and then through the tube. Tie the sutures with four single knots. Insert the distal nerve end 5 mm into the other end of the tube and secure in the same manner.

12. In the case of the cross-anastomosis procedure, the sciatic nerve in the opposite hind limb is similarly exposed and transected. The two skin incisions are then joined across the rat's back using a scalpel blade.

13. The dorsal spinous processes are removed using bone rongeurs to create a trough to make space for the tube implant to be routed over the back.

14. The proximal left sciatic nerve stump is bridged to the distal right nerve stump with a tube implant over the back.

15. For both single-leg and cross-anastomosis procedures, the paper clip retractors are removed. Close the muscle using three 4-0 sutures. Close the skin using two 4-0 sutures and three skin staples.

16. Place the animals back in the cage and observe frequently until they are awake.

A.5 Animal Sacrifice and Tissue Processing Protocols

(adapted from Chamberlain 1998)

EQUIPMENT

surgical instruments
15-ml Falcon tubes (1 for each animal)
camera to take gross photographs
container with ice

SOLUTIONS

Yanoff's Fixative

Stock Solutions

Stock A: 1.67 grams Monobasic Sodium Phosphate NaH_2PO_4
8.95 grams Dibasic Sodium Phosphate Na_2HPO_4
960 ml Distilled H_2O
40 ml 25% Glutaraldehyde

Stock B: 4.0 grams Monobasic Sodium Phosphate NaH_2PO_4
8.95 grams Dibasic Sodium Phosphate Na_2HPO_4
900 ml Distilled H_2O
100 ml 38-40% Formaldehyde

Yanoff's fixative is 1:1 mixture of stock A and stock B

10% Neutral Buffered Formalin

Stock B of Yanoff's Fixative is 10% Neutral Buffered Formalin.

70% EtOH

SACRIFICE PROCEDURE

1. Sacrifice animals by placing in carbon dioxide chaber for 3-5 mintues.

2. Open the original wound with a #15 salpel blade The wound can be located by identifying the dermal scar or original suture marks.

3. Open the fascia and muscle to locate the tube implant and the adjacent nerve stumps.

4. Remove the entire tube implant as well as at least 10 mm of proximal and distal nerve tissue including the nerve branches at the distal end.

TISSUE PROCESSING PROCEDURE

1. Place tissue into Yanoff's fixative for 24 hours at 4°C.
2. Transfer tissue into 10% neutral buffered formalin solution for 24 hours at 4°C.
3. Remove tissue from formalin and rinse 1X in 70% EtOH.
4. Photograph the nerve to capture the gross morphology of the tissue.
5. Section the nerve into segments according to Figure 2.3.
6. Place each small nerve segment into an individual vial containing 70% EtOH. Each tissue segment will be either embedded in Epon or stored in 70 EtOH for future use.

A.6 Epon Embedding Protocol

SOLUTIONS

Cacodylate Buffer (pH 7.4)
Stock Solutions
Stock A (0.2 M Sodium Cacodylate (mw 214)): 4.28 grams sodium cacodylate
100 ml of distilled water

Stock B (0.2 M HCl (mw 36.46)): 1.7 ml HCl
100 ml of distilled water

Composition of Buffer
25 ml of Stock A + 1.4 ml of Stock B (for pH 7.4)* + 73.6 ml of distilled water
*Volume of Stock B changes for different pH levels

Cacodylate Buffered Glutaraldehyde
2% Solution: 8 ml, 25% Glutaraldehyde
92ml, Cacodylate Buffer (made as described above)

Cacodylate Buffered Sucrose Solution
0.2 M Solution: 6.846 grams, Sucrose (mw 342.3)
100 ml, Cacodylate Buffer (made as described above)

Osmium Tetroxide (Catalog #0972A, Polysciences, Inc., Warrington, PA)
1% Solution: 2 ml, 4% Osmium Tetroxide
6 ml, Distilled Water

Poly/Bed 812 Embedding Kit (Catalog #08792, Polysciences, Inc., Warrington, PA)

EMBEDDING PROCEDURE

1. Soak nerves in 2% cacodylate buffered glutaraldehyde overnight at 4°C.
2. Soak nerves in 0.2 M cacodylate buffered sucrose solution overnight at 4°C.
3. Rinse nerves 1 time in cacodylate buffer for 10 minutes at 4°C.
4. Fix in 1% osmium tetroxide for 2 hours at room temperature (in the hood).

5. Dehydrate nerves in EtOH:	30%	5 minutes
	50%	5 minutes
	70%	5 minutes
	80%	5 minutes
	90%	5 minutes
	95%	5 minutes
	100%	5 minutes
	100%	5 minutes
	100%	5 minutes

6. Clear nerves in acetone 2 times for 5 minutes each.

7. Infiltrate in 1:1 acetone/Epon* mixture overnight at room temperature.

8. Infiltrate in 1:3 acetone/Epon* mixture for 5 hours at room temperature.

9. Infiltrate in 100% Epon with hardener overnight at room temperature.

10. Embed with fresh 100% Epon with hardener in TEM molds. (Make well labels with pencil or on computer)

11. Let cure 24 hours at 60°C.

*During infiltration, the Epon mixture should NOT contain the hardener.

A.7 Toluidine Blue Staining Protocol

SOLUTIONS

Toluidine Blue Solution (Catalog #BP107-10, Fisher Biotech, Boston, MA)
1% Toluidine Blue Solution: 1 gram, Toluidine Blue Powder
1 gram, Sodium Borate Powder
100 ml, Distilled Water
Solution should be filtered and stored in a stopped bottle.

Cytoseal 60 Mounting Medium (Catalog #8310-16, Stephens Scientific).

STAINING PROCEDURE

1. Heat slides on hot plate to 60 - 80°C (setting about 4.5 on blue VWR 320 plates).

2. Stain with Toluidine Blue Solution for 30 - 60 seconds. Thicker sections will take less time.

3. Rinse in distilled water and allow to dry on hot plate for 2 - 3 minutes.

4. Mount with mounting medium.

A.8 Image Capture and Analysis Protocol

(adapted from Chamberlain 1998)

COMPUTER SETUP

1. Turn on the Power Macintosh computer. Open the ORL Microscope hard drive. Open the Applications folder. Open the Microscope Stuff folder. Open the Scion Image folder.

2. Open the application Scion Image.

MICROSCOPE SETUP

1. Turn the microscope on (green button on the right side). Microscope (Olympus Vanox-T, Olympus, Japan) should have video camera (Hamamatsu CCD Video Camera Module, Model XC-77, Hamamatsu, Japan) attached.

2. Select the white button (max) for light level (on right side, there are 3 light choices)

3. Locate the two knobs on the top portion of the microscope, one on the left and one on the right. Pull out both knobs to the TV position.

4. Insert a microscope slide into the scope and focus on the selected sample you want to image. Adjust to the appropriate magnification.

VIDEO BOX SETUP

1. Turn the Gain and Offset knobs completely to the left. This is essentially the off position.

2. Turn the video box on (Hamamatsu CCD Camera Control, Hamamatsu, Japan).

3. Watch the video level on the box at all times to make sure the "Normal" indicator light is on. If the "Over" light is on, there is too much light and it can damage the computer screen. If the "Over" light comes on, adjust the light on the microscope or the gain and offset knobs on the video box accordingly.

IMAGE CAPTURING PROCEDURE

1. Select *Start Capturing* from the *Special* menu (keystroke: apple-G).

2. Turn the Gain and Offset knobs up to approximately the midpoint. Turn the offset knob up even more until the image is visible. Watch the light indicator on the video box for the over signal. The light can also be adjusted on the microscope to make the image visible on the screen. Again, watch the light indicator.

3. Position the image you want to capture on the screen. Focus the image and adjust the light to the appropriate level.

4. Select *Stop Capturing* from the *Special* menu (keystroke: apple-G).

5. Save the image onto a Zip Disk (keystroke: apple-S).

6. Repeat procedure to capture the next image.

IMAGE SELECTION PROCEDURE

1. Capture one low magnification image of the nerve trunk (as described above).

2. Measure the cross-sectional area of the nerve trunk (follow the Analysis Procedure outlined below). If there are multiple fascicles, measure each area separately and then sum the areas to get a total area.

3. Determine how many images are necessary to adequately sample the nerve (Table A.1).

4. Position the nerve so that the long axis of the nerve is on the Y axis (Figure A.6).

5. Divide the nerve into 4 quadrants (Figure A.3). Count the number of images from the top center of the cross-section to the bottom center of the cross-section (**Y**), and the number of images from the left center to the right center (**X**).

3. Begin imaging. Refer to Figure A.6 to see image placement. I find it easiest to start with image 5, the geometric center. Then move to quadrant 1 and capture all images in that quadrant. Then all images in quadrant 2, and so on. Use the values of **X** and **Y** counted in Step 5 to locate the images. For example, image 11 is 1/4 **Y** down from the top center of the cross-section and 1/4 **X** to the left.

4. Capture the appropriate number of images. If only 3 images are needed capture: **11, 41, & 5.** If 5 images are needed capture: **11, 21, 31, 41, & 5.** If 9 images are needed: **11, 12, 21, 22, 31, 32, 41, 42, & 5;** and so on. Refer to Figure A.6 to see image placement.

Fascicle Area Range (mm^2)	Number of Images Necessary	Image Area Divided by Total Fascicle Area
A<0.25	3	≥10%
0.25<A<0.4167	5	10% - 16%
0.4167<A<0.75	9	10% - 18%
0.75<A<1.08	13	10% - 14%
1.08<A<1.417	17	10% - 13%
1.417<A<1.75	21	10% - 12%
A>1.75	21	<10%

Table A.1 Number of images necessary to describe nerve trunks of different cross-sectional area. Capturing the appropriate number of images results in sampling of at least 10% of the total tissue area, except when the area is larger than 1.75 mm^2. If tissue filled the entire inside diameter of the implant tubes, the area would be 1.77 mm^2; therefore, in the majority of cases sampling is greater than 10%.

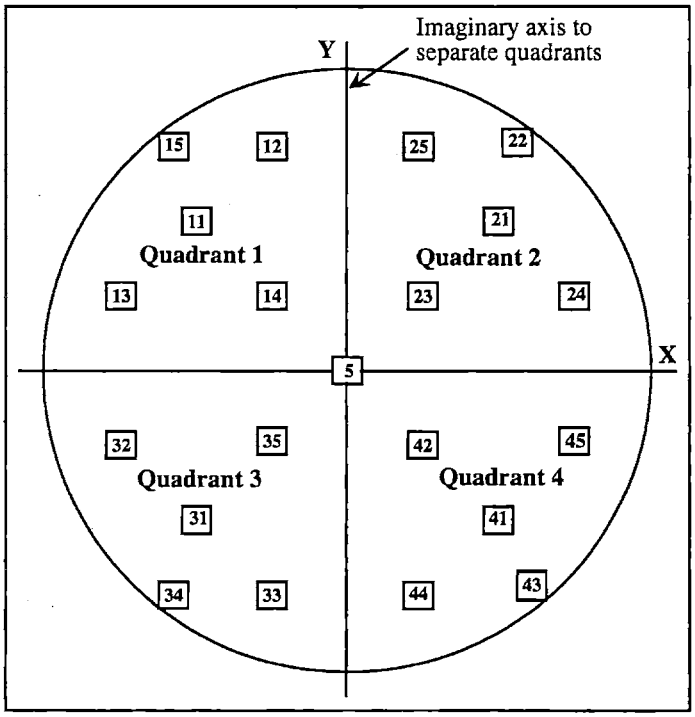

Figure A.3. Schematic showing the location of images around the nerve section.

IMAGE ANALYSIS PROCEDURE

1. Open Scion Image.

2. Open image file.

3. Go to the *Analyze* menu and select *Set Scale*. Select the appropriate unit of measure for the magnification of the image (*i.e.*, millimeters for low magnification images and micrometers for high magnification images). Use Table A.2 to fill in the *Known Distance* and the *Pixels* entries. Table A.2 is calibrated for the microscope at the Brigham, with images captured in Scion Image. When the scale is set a diamond appears next to the file name on the top bar of the window.

4. Use *Smooth* and/or *Sharpen* from the *Enhance* menu to improve the quality of the image if needed. If you do not like the effect of these, choose *Undo* from the *Edit* menu before doing anything else.

5. From the *Enhance* menu, choose *Arithmetic, Subtract*. Subtract 3.

6. From the *Options* menu, select *Density Slice*. Threshold all the way to black so that no red should be showing in the image.

7. Select the pencil from the toolbar. Move the cursor over the red portion of the color scale and choose red as the color. (The paintbrush will appear red when the appropriate color has been selected).

Magnification Power	Known Distance	Pixels
1	1 mm	61
4	1 mm	243
10	0.9 mm	543
20	0.44 mm	539
40	220 μm	526
100	80 μm	485.5

Table A.2 Calibration values to set the scale for the appropriate magnifications on NIH Image. The magnification power refers to the objective that was used on the microscope at the Brigham & Women's Hospital, Orthopedic Research Lab (Olympus Vanox-T, Olympus, Japan).

8. Circle the axons with the pencil on the OUTSIDE perimeter of the myelin sheath.

9. When all axons have been circled, go to the *Analyze* menu and select *Options*. Choose Area, Perimeter/Length and Headings.

10. Choose SAVE AS from the *File* menu and save the image as an edited file. Don't forget to save at this point!!

11. Again in the *Analyze* menu choose *Analyze Particles* Enter the following:

Minimum particle size:	5 pixels
Maximum particle size	30000 pixels
Label	
Outline	
Include	
Reset	

12. Each axon will become filled and numbered as it is counted. Make sure that all axons are filled in. If an axon is not darkened, part of the perimeter is not complete, therefore, it has been measured inappropriately. Fix and repeat step 11.

12. Choose *Show Results* from the *Analyze* menu. Copy the results (keystroke: apple-C) and paste them into Excel for analysis (keystroke: apple-V).

14. Close the image. Do not save the changes to your edited file!

A.9 Sample Input Code and Output from Mathematica Software

Samples included on following pages for reinnervation a the gap midpoint for the silicone tube implant in the single-leg model for 4-week, 6-week,. and 9-week data

Silicone Tube : Single - leg, reinnervation at midpoint, 4 - week

```
<< Statistics`NonlinearFit`

data = {{6.5, 66.7}, {8.5, 57.1}, {10.5, 20.0}, {12.5, 20.0}, {14.5, 16.7}};

NonlinearRegress[data, 100 / (Exp[(x - L) * K] + 1), {x}, {{K, 0.37}, {L, 8.5}}]
```

```
{BestFitParameters → {K → 0.372723, L → 8.46182},
                          Estimate      Asymptotic SE      CI
 ParameterCITable → K     0.372723      0.0960385          {0.067086, 0.678361},
                    L     8.46182       0.599112           {6.55518, 10.3685}
 EstimatedVariance → 83.9823,
                                  DF      SumOfSq      MeanSq
             Model                2       8536.24      4268.12
 ANOVATable → Error               3       251.947      83.9823,
             Uncorrected Total    5       8788.19
             Corrected Total      4       2272.14
 AsymptoticCorrelationMatrix → ( 1.        0.317401 ),
                                ( 0.317401  1.       )
                                                    Curvature
 FitCurvatureTable → Max Intrinsic                  0.211609 }
                     Max Parameter-Effects          0.499557
                     95. % Confidence Region        0.323557
```

Silicone Tube, Single - leg, reinnervation at midpoint, 6 - week

```
<< Statistics`NonlinearFit`

data = {{6.5, 100.0}, {8.5, 100.0}, {10.5, 66.7}, {12.5, 66.7}, {14.5, 0.0}, {16.5, 0.0}};

NonlinearRegress[data, 100 / (Exp[(x - L) * K] + 1), {x}, {{K, 0.747}, {L, 12.3}}]
```

```
{BestFitParameters → {K → 0.856364, L → 12.4837},

                                 Estimate      Asymptotic SE      CI
 ParameterCITable → K            0.856364      0.360233           {-0.143804, 1.85653},
                    L            12.4837       0.546263           {10.9671, 14.0004}

 EstimatedVariance → 214.275,

                                      DF      SumOfSq      MeanSq
              Model                   2       28040.7      14020.3
 ANOVATable → Error                   4       857.099      214.275,
              Uncorrected Total       6       28897.8
              Corrected Total         5       10371.9

 AsymptoticCorrelationMatrix → ( 1.           -0.000834115 ),
                               ( -0.000834115  1.          )

                                                    Curvature
 FitCurvatureTable → Max Intrinsic                  0.500153 }
                     Max Parameter-Effects          0.941632
                     95. % Confidence Region        0.379478
```

Silicone Tube, Single - leg, reinnervation at midpoint, longest - time (6 & 9 week)

```
<< Statistics`NonlinearFit`

data = {{6.5, 100.0}, {8.5, 100.0}, {10.5, 57.1}, {12.5, 50.0}, {14.5, 0.0}, {16.5, 0.0}};

NonlinearRegress[data, 100 / (Exp[(x - L) * K] + 1), {x}, {{K, 0.7}, {L, 11.9}}]
```

```
{BestFitParameters → {K → 0.734879, L → 11.6972},
                              Estimate      Asymptotic SE      CI
 ParameterCITable → K         0.734879      0.237505           {0.0754597, 1.3943},
                    L         11.6972       0.497982           {10.3146, 13.0798}
 EstimatedVariance → 151.58,
                                    DF      SumOfSq      MeanSq
              Model                 2       25154.1      12577.
 ANOVATable → Error                 4       606.32       151.58,
              Uncorrected Total     6       25760.4
              Corrected Total       5       10042.
 AsymptoticCorrelationMatrix → ( 1.          0.00117686 ),
 AsymptoticCorrelationMatrix →   0.00117686  1.         )
                                                  Curvature
 FitCurvatureTable → Max Intrinsic                0.454963 }
                     Max Parameter-Effects        0.64959
                     95. % Confidence Region      0.379478
```

References

1. Madison RD, Archibald SJ, and Krarup C (1992) Peripheral nerve injury. In: Cohen IK, Diegelmann RF, Lindblad WJ, eds. *Wound Healing: Biochemical and Clinical Aspects*. Philadelphia. W.B. Saunders:450-487.
2. Janecka IP, Sen LN, Sekhar LN, and Arriaga M (1990) Facial translocation: A new approach to the cranial base. *Otolaryngol Head Neck Surg*. 103:413-419.
3. Mackinnon SE, and Dellon AL (1988) Surgery of the Peripheral Nerve. New York. Thieme Medical Publishers.
4. Kim DH, Connolly SE, Kline DG, et al. (1994) Labeled Schwann cell transplants versus sural nerve grafts in nerve repair. *J. Neurosurg*. 80:254-260.
5. Chamberlain LJ (1998) Influence of implant parameters on the mechanisms of peripheral nerve regeneration. *Mechanical Engineering*. Cambridge. Massachusetts Institute of Technology.
6. Chamberlain LJ, Yannas IV, Hsu H-P, Strichartz G, and Spector M (1998) Collagen-GAG substrate enhancesthe quality of nerve regeneration through collagen tubes up to level of autograft. *Exp. Neurol.* 154:315-329.
7. Buti M, Verdu E, Labrador RO, Vilches JJ, Fores J, and Navarro X (1996) Influence of physical parameters of nerve chambers on peripheral nerve regeneration and reinnervation. *Exp. Neurol.* 137:26-33.
8. Lundborg G, Dahlin LB, Danielsen N, et al. (1982) Nerve regeneration in silicone chambers: Inlfuence of gap length and of distal stump components. *Exp Neurol.* 76:361-375.
9. Fields RD, LeBeau JM, Longo FM, and Ellisman MH (1989) Nerve regeneration through artificial tubular implants. *Prog. Neurobiol.* 33:87-134.
10. Fawcett JW, and Keynes RJ (1990) Peripheral nerve regeneration. *Ann. Rev. Neurosci.* 13:43-60.
11. Fu SY, and Gordon T (1997) The cellular and molecular basis of peripheral nerve regeneration. *Mol Neurobiol.* 14:67-116.
12. Ramon y Cajal S (1928) Degeneration and Regeneration in the Nervous System. London. Oxford University Press.
13. Williams LR, Longo FM, Powell HC, Lundborg G, and Varon S (1983) Spatial-temporal progress of peripheral nerve regeneration within a silicone chamber: parameters for a bioassay. *J. Comp. Neurol.* 218:460-470.
14. Scaravilli F (1984) Regeneration of the perineurium across a surgically induced gap in a nerve encased in a plastic tube. *J. Anat.* 139:411-424.
15. Chang A, Yannas IV, Perutz S, et al. (1990) Electrophysiological study of recovery of peripheral nerves regenerated by a collagen-glycosaminoglycan

copolymer matrix. In: Gebelin CG, Dunn RL, eds. *Progress in Biomedical Polymers*. New York. Plenum Press:107-119.

16. Fawcett JW, and Keynes RJ (1986) Muscle basal lamina: a new graft material for peripheral nerve repair. *J. Neurosurg.* 65:354-363.

17. Whitworth IH, Brown RA, Dore C, Green CJ, and Terenghi G (1995) Orientated mats of fibronectin as a conduit material for use in peripheral nerve repair. *J. Hand Surg.* 20B:429-436.

18. Noback CR, Husby J, Girardo JM, Andrew C, Bassett L, and Campbell JB (1958) Neural regeneration across long gaps in mammalian peripheral nerves: early morphological findings. *Anat. Rec.* 131:633-647.

19. Rosen JM, Hentz VR, and Kaplan EN (1983) Fascicular tubulization: A cellular approach to peripheral nerve repair. *Ann. Plast. Surg.* 11:397-411.

20. Dellon AL, and Mackinnon SE (1988) An alternative to the classical nerve graft for the management of the short nerve gap. *Plast Reconstr Surg.* 82:849-56.

21. Archibald SJ, Shefner J, Krarup C, and Madison RD (1995) Monkey median nerve repaired by nerve graft or collagen nerve guide tube. *J. Neurosci.* 15:4109-4123.

22. Navarro X, Verdu E, Wendelschafer-Crabb G, and Kennedy WR (1995) Innervation of cutaneous structures in the mouse hind paw: A confocal microscopy immunohistochemical study. *J. Neurosci. Res.* 41:111-120.

23. Carr MM, Best TJ, Mackinnon SE, and Evans PJ (1992) Strain differences in autotomy in rats undergoing sciatic nerve transection or repair. *Ann. Plast. Surg.* 28:538-544.

24. Wall PD, Devor M, Inbal R, et al. (1979) Autotomy following peripheral nerve lesions: Experimental anaesthesia dolorosa. *Pain.* 7:103-113.

25. Landstrom A (1993) Nerve regeneration induced by collagen-GAG matrix in collagen tubes. *Mechanical Engineering*. Cambridge. Massacusetts Institute of Technology.

26. Haftek J, and Thomas PK (1968) Electron-microscope observations on the effects of localized crush injuries on the connective tissues of peripheral nerve. *J. Anat.* 103:233-243.

27. Devor M, and Govrin-Lippman R (1979) Maturation of axonal sprouts after nerve crush. *Exp. Neurol.* 64:260-270.

28. Walker JL, Evans JM, Resig P, Guarnieri S, Meade P, and Sisken BS (1994) Enhancement of functional recovery following a crush lesion to the rat sciatic nerve by exposure to pulsed electromagnetic fields. *Exp. Neurol.* 125:302-305.

29. Danielsson P, Dahlin L, and Povlsen B (1996) Tubulization increases axonal outgrowth of rat sciatic nerve after crush injury. *Exp. Neurol.* 139:238-243.

30. Hoffman JR, and O'Shea KS (1999) Thrombospondin expression in nerve regeneration I. Comparison of sciatic nerve crush, transection, and long-term denervation. *Brain Res Bull.* 48:413-420.

31. Korompilias AV, Chen LE, Seaber A, V,, and Urbaniak JR (1999) Interleukin-1 beta promotes functional recovery of crushed peripheral nerve. *J. Orthop. Res.* 17:714-719.

32. Yannas IV, Orgill DP, Silver J, Norregaard TV, Zervas NT, and Schoene WC (1987) Regeneration of sciatic nerve across 15 mm gap by use of a polymeric template. In: Gebelin CG, ed. *Advances in Biomedical Polymers.* New York. Plenum Publishing Corporation:1-9.

33. deMedinaceli L, Freed WJ, and Wyatt RJ (1982) An index of the functional condition of rat sciatic nerve based on measurements made from walking tracks. *Exp. Neurol.* 77:634-643.

34. Bain JR, Mackinnon SE, and Hunter DA (1989) Functional evaluation of complete sciatic, peroneal, and posterior tibial nerve lesions in the rat. *Plast. Reconstr. Surg.* 83:129-138.

35. deMedinaceli L (1990) Use of sicatic function index and walking track assessment. *Microsurgery.* 11:191-192.

36. Dellon AL, and Mackinnon SE (1989) Sciatic nerve regeneration in the rat. Validity of walking track assessment in the presence of chronic contractures. *Microsurgery.* 10:220-225.

37. Chamberlain LJ (1996) Long term functional and morphological evaluation of peripheral nerves regenerated through degradable collagen implants. Massachusetts Institute of Technology.

38. Frykman GK, McMillan PJ, and Yegge S (1988) A review of experimental methods measuring peripheral nerve regeneration in animals. *Orthop. Clin. North Am.* 19:209-219.

39. Cragg BG, and Thomas PK (1964) The conduction velocity of regenerated peripheral nerve fibres. *J. Physiol.* 171:164-175.

40. Dellon AL, and Mackinnon SE (1989) Selection of the appropriate parameter to measure neural regeneration. *Ann. Plast. Surg.* 23:197-202.

41. Seckel BR, Chiu TH, Nyilas E, and Sidman RL (1984) Nerve regeneration through synthetic biodegradable nerve guides: Regulation by the target organ. *Plast. Reconstr. Surg.* 74:173-181.

42. Williams LR, Powell HC, Lundborg G, and Varon S (1984) Competence of nerve tissue as distal insert promoting nerve regeneration in a silicone chamber. *Brain Res.* 293:201-211.

43. Williams LR (1987) Exogenous fibrin matrix precursors stimulate the temporal progress of nerve regeneration within a silicone chamber. *Neurochem Res.* 12:851-860.

44. Navarro X, Rodriguez FJ, Labrador RO, et al. (1996) Peripheral nerve regeneration through bioresorbable and durable nerve guides. *J. Peripher. Nerv. Sys.* 1:53-64.

45. Ducker TB, and Hayes GJ (1968) Experimental improvements in the use of silastic cuff for peripheral nerve repair. *J. Neurosurg.* 28:582-587.

46. Lundborg G, Gelberman RH, Longo FM, Powell HC, and Varon S (1982) *In vivo* regeneration of cut nerves encased in silicone tubes. *J. Neuropathol. Exp. Neurol.* 41:412-422.

47. Jenq C-B, and Coggeshall RE (1984) Effects of sciatic nerve regeneration on axonal popoulations in tributary nerves. *Brain Res.* 295:91-100.

48. Williams LR, and Varon S (1985) Modification of fibrin matrix formation in situ enhances nerve regeneration in silicone chambers. *J. Comp. Neurol.* 231:209-220.

49. Fields RD, and Ellisman MH (1986) Axons regenerated through silicone tube splices. I. Conduction properties. *Exp. Neurol.* 92:48-60.

50. Fields RD, and Ellisman MH (1986) Axons regenerated through silicone tube splices. II. Functional morphology. *Exp. Neurol.* 92:61-74.

51. LeBeau JM, Ellisman MH, and Powell HC (1988) Ultrastructural and morphometric analysis of long-term peripheral nerve regeneration through silicone tubes. *J. Neurocytol.* 17:161-172.

52. Williams LR, Azzam NA, Zalewski AA, and Azzam RN (1993) Regenerating axons are not required to induce the formation of a Schwann cell cable in a silicone chamber. *Exp. Neurol.* 120:49-59.

53. Lundborg G, Dahlin LB, and Danielsen N (1991) Ulnar nerve repair by the silicon chamber technique. *Scand. J. Plast. Reconstr. Hand Surg.* 25:79-82.

54. Janecka IP, Sekhar LN, and Sen CN (1993) Facial nerve management in cranial base surgery. *Laryngoscope.* 103:291-298.

55. Jenq C-B, and Coggeshall RE (1985) Numbers of regenerating axons in parent and tributary peripheral nerves in the rat. *Brain Res.* 326:27-40.

56. Colin W, and Donoff RB (1984) Nerve regeneration through collagen tubes. *J. Dent. Res.* 63:987-993.

57. Li S-T, Archibald SJ, Krarup C, and Madison R (1990) Semipermeable collagen nerve conduits for peripheral nerve regeneration. *Polym Mater Sci. Eng.* 62:575-582.

58. Archibald SJ, Krarup C, Shefner J, Li S-T, and Madison RD (1991) A collagen-based nerve guide conduit for peripheral nerve repair: An electrophysiological study of nerve regeneration in rodents and nonhuman primates. *J. Comp. Neurol.* 306:685-696.

59. Li ST, Archibald SJ, Krarup C, and Madison R (1992) Peripheral nerve repair with collagen conduits. *Clin Mater.* 9:195-200.

60. Chamberlain LJ, Yannas IV, Hsu H-P, and Spector M (2000) The connective tissue response to tubular implants for peripheral nerve regeneration: the role of myofibroblasts. *J. Comp. Neurol.* 417:415-430.

61. Madison R, da Silva CF, Dikkes P, Chiu T-H, and Sidman RL (1985) Increased rate of peripheral nerve regeneration using bioresorbable nerve guides and a laminin-containing gel. *Exp. Neurol.* 88:762-772.

62. Glasby MA, Gschmeissner SG, Hitchcock RJ, and Huang CL (1986) The dependence of nerve regeneration through muscel grafts in the rat on availability and orientation of basement membrane. *J. Neurocytol.* 15:497-510.

63. Yoshii S, Yamamuro T, Ito S, and Hayashi M (1987) In vivo guidance of regenerating nerve by laminin-coated filaments. *Exp. Neurol.* 95:469-473.

64. Gulati AK (1988) Evaluation of acellular and cellular nerve grafts in repair of rat peripheral nerve. *J. Neurosurg.* 68:117-123.

65. Madison RD, da Silva C, and Dikkes P (1988) Entubulation repair with protein additives increased the maximum nerve gap distance successfully bridged with tubular prostheses. *Brain Res.* 447:325-334.

66. Rosen JM, Padilla JA, Nguyen KD, Padilla MA, Sabelman EE, and Pham HN (1990) Artificial nerve graft using collagen as an extracellular matrix for nerve repair compared with sutured autograft in a rat model. *Ann. Plast. Surg.* 25:375-387.

67. Bailey SB, Eichler ME, Villadiego A, and Rich KM (1993) The influence of fibronectin and laminin during Schwann cell migration and peripheral nerve regeneration through silicon chambers. *J. Neurocytol.* 22:176-184.

68. Bryan DJ, Miller RA, Costas PD, Wang K-K, and Seckel BR (1993) Immunocytochemistry of skeletal muscle basal lamina grafts in nerve regeneration. *Plast. Reconstr. Surg.* 92:927-940.

69. Ohbayashi K, Inoue HK, Awaya A, et al. (1996) Peripheral nerve regeneration in a silicone tube: effect of collagen sponge prosthesis, laminin, and pyrimidine compound administration. *Neurol. Med. Chir.* 36:428-433.

70. Yannas IV, Orgill DP, Silver J, Norregaard TV, Zervas NT, and Schoene WC. Polymeric template facilitates regeneration of sciatic nerve across 15-mm gap, Society for Biomaterials Annual Meeting, 1985. Vol. 8.

71. Daniel WD (1995) Biostatistics. New York. John Wiley & Sons Inc.

72. Chamberlain LJ, Yannas IV, Arrizabalaga A, Hsu H-P, Norregaard TV, and Spector M (1998) Early peripheral nerve healing in collagen and silicone tube implants: myofibroblasts and the cellular response. *Biomaterials.* 19:1393-1403.

73. Archibald SJ, and Fisher TR (1987) Micro-surgical fascicular nerve repair: a morphological study of the endoneurial bulge. *J Hand Surg [Br].* 12:5-10.

74. Yannas IV, Burke JF, Gordon PL, Huang C, and Rubenstein RH (1980) Design of an artificial skin. Part II. Control of chemical composition. *J. Biomed. Mater. Res.* 14:107-131.

75. Yannas IV (1989) Regeneration of skin and nerves by use of collagen templates. In: Nimni M, ed. *Collagen Vol. III: Biotechnology*. Boca Raton, FL. CRC Press:87-115.

76. Burke JF, Yannas IV, Quinby WC, Bondoc CC, and Jung WK (1981) Successful use of a physiologically acceptable artificial skin in the treatment of extensive burn injury. *Ann. Surg.* 194:413-428.

77. Heimbach D, Luterman A, Burke J, et al. (1988) Artifical dermis for major burns: A multi-center randomized clinical trial. *Ann. Surg.* 208:313-320.

78. Stern R, McPherson M, and Longaker MT (1990) Histological study of artificial skin used in the treatment of full-thickness thermal injury. *J. Burn Care Rehab.* 11:7-13.

79. Stone KR, Rodkey WG, Webber RJ, McKinney L, and Steadman JR (1990) Future directions: collagen-based prostheses for meniscal regeneration. *Clin. Orthop.* 252:129-135.

80. Chang AS, and Yannas IV (1992) Peripheral nerve regeneration. In: Smith B, Adelman G, eds. *Encyclopedia of Neuroscience*. Boston. Birkhauser:125-126.

81. Spilker MH (1997) The effect of a porous collagen-glycosainoglycan matrix on healing of the injured rat spinal cord. Massachusetts Institute of Technology.

82. Spilker MH, Yannas IV, Hsu H-P, Norregaard TV, Kostyk S, and Spector M (1997) The effects of collagen-based implants on early healing of the adult rat spinal cord. *Tissue Eng.* 3:309-317.

83. Loree HM, Yannas IV, Mikic B, et al. (1989) A freeze-drying process for fabrication of polymeric bridges for peripheral nerve regeneration. *NE Bioeng. Conference Proc.* :53-54.

84. Yannas IV, Lee E, Orgill DP, Skrabut EM, and Murphy GF (1989) Synthesis and characterization of a model extracellular matrix that induces partial regeneration of adult mammalian skin. *Proc Natl Acad Sci USA*. 86:933-937.

85. Yannas IV (1972) Collagen and gelatin in the solid state. *J. Macromol. Sci. Rev. Macromol. Chem.* C7:49-104.

86. Chamberlain LJ, Yannas IV, Hsu H-P, Strichartz GR, and Spector M ((in press)) Near-terminus axonal structure and function following rat sciatic nerve regeneration through collagen-GAG matrix in a ten-millimeter gap. *J. Neurosci. Res.* .